CS-46

APPLICATION OF SHE MODEL TO HEMAVATI (UPTO SAKLESHPUR) BASIN

NATIONAL INSTITUTE OF HYDROLOGY
JAL VIGYAN BHAWAN
ROORKEE - 247 667 (U.P.)

1990-91

APPLICATION OF SHE MODEL TO HEMAVATI (UPTO SAKLESHPUR) BASIN

NATIONAL INSTITUTE OF HYDROLOGY
JAL VIGYAN BHAWAN
ROORKEE - 247 667 (U.P.)

1990-91

PREFACE

The increasing rate of water resources development activity and utilization of water for various uses has focused attention on development and application of physically based hydrological models to deal with constantly changing hydrological environment. When the hydrological system is subject to change or when a realistic physical representation of flow in space and time is required for studies of water quality or soil erosion,the conceptual representation of traditional rainfall runoff models with lumped approach are not suitable.

Due to its general formulation and physical basis, the SHE may be able to give a very detailed and to a large extent physically correct description of the water flow processes. Therefore,the SHE will be applicable to almost any kind of hydrological problem, although extensive further development and refinement is still needed to realise this vision. The flexible model structure combined with the distributed structure and the physical interpretation of the hydrological processes, is expected to provide significant advantages over existing hydrological models for a wide range of applications.

The present study is a part of the project concerned with the transfer of the Systeme Hydrologique Europeen (SHE) hydrological modelling system to the National Institute of Hydrology, Roorkee and is intended to increase India's capabilities for formulating water and land resources development strategies through numerical modelling. The project is financed by Agreement ALA 86/19, Hydrological Computerized Modelling System, signed between the Commission of the European Communities (CEC) and the Government of India. Under the project, six NIH scientists have been trained in theoretical and practical aspects of SHE, at Danish Hydraulic Institute, Denmark. Mr. Chandra Prakash Kumar, one of the trainees, has carried out a study on application of SHE model to Narmada (upto Manot) basin.

The Hemavati (upto Sakleshpur) basin is one of the sub-basins selected for model applications since this basin is undergoing large scale water resources development with complex environmental repercussions. The present study consists of data assembly and processing, evaluation of model parameters, assessment of uncertainty in input quantities, carrying out simulation runs, including formulating the approach to calibration, validation and sensitivity analysis and interpreting the results. The study has been carried out by Mr. Chandra Prakash Kumar, Scientist 'C' under the guidance of Mr. K.S. Ramasastri, Scientist 'F'.

Date: 21-11-91

SATISH CHANDRA

Director

CONTENTS

LIST OF FIGURES

LIST OF TABLES

ABSTRACT

The Systeme Hydrologique Europeen (SHE) is a deterministic distributed and physically-based hydrological modelling system developed from the partial differential equations describing the processes of subsurface, overland and channel flow solved by finite difference methods. The model is completed by the processes of interception, evapotranspiration and snowmelt. SHE has been developed in a joint effort by the Institute of Hydrology (UK), SOGREAH (France) and the Danish Hydraulic Institute (Denmark).

The description of the hydrological processes has been simplified by solving the unsaturated flow equation in independent one-dimensional vertical columns of variable depths. The columns link a two-dimensional surface flow component with a two-dimensional ground water flow component. The catchment is represented in the horizontal plane by grid squares and the river system is superimposed on the boundaries of the grid squares. In the SHE programme, each process is solved in separate model components. The coordination and parallel running of the individual components is controlled by a Frame component. This means that the process components can be applied independently and/or in combination. The processes in the various components can be modelled at different levels of complexity and, in its simplest form, a component can be replaced by a dummy component in which default boundary conditions (flows or levels) are prescribed and transferred to the other components. This allows for great flexibility and the applications with SHE may range from single sub-surface column simulations to runs on large complex catchments. The capacity of SHE to account for spatial variations

in meteorologic and hydrologic inputs represents an important advantage over traditional lumped catchment models.

The computational grid network and channel system was set up for the basin, forming the basis for the spatial distribution of topographic elevation, soil type, land use and rainfall stations in the data files. The basic network was composed of grid squares of 1 km x 1 km, but in view of the heavy computing requirements associated with such densely defined systems, this was converted to arrays with grid squares of 2 km x 2 km for the simulation work. Since direct measurements of soil and vegetation properties for the basin were not available, the model parameters were evaluated using information taken from the literature on neighbouring areas. Three land uses (forests, coffee plantations and unirrigated crop land) and two soil types (red loamy soils and red sandy soils) were identified. Three categories of soil depth were defined for low land, semi-hilly and hilly areas, the distributions obtained from the topographic maps. However, only one soil retention curve was used throughout.

The calibration and validation of the model was achieved on the basis of physical reasoning and through consideration of the variation of runoff response from the basin. The calibration was carried out for the period 1975-77 by varying only a few of the parameters and was then validated against hydrographs for the period 1978-80, on the basis of changes in the initial level of the phreatic surface. In general, there were good agreements between observed and simulated responses. Sensitivity analysis was also carried out for the basin to study the sensitivity to the simulated hydrological regime of model structural parameters, flow resistance, unsaturated flow parameters, saturated flow parameter and spatial distribution of rainfall.

1.0 INTRODUCTION

1.1 General

India is a vast country with a wide variety of climate and hydrological environments, snow clad mountains of the Himalayas in the north, a long coastline in the south, desert in the western part, alluvial plains to the north and hard rock regions to the south. The rainfall is seasonal in nature and most of it falls during the five monsoon months (June to October) with erratic patterns leading to floods as well as droughts in different parts of the country. To meet the increasing demands of the growing population, there has been considerable development of water resources in the country. The increasing rate of water resource development activity and utilization of water for various uses including domestic and industrial purposes, has focused attention on environmental aspects and more particularly water quality. The catchments of rivers are no longer virgin and the process of development and man's activities are continuously changing the hydrological regime of the river basins. The application of the science of hydrology is increasingly becoming necessary in all aspects and all stages of water resource development and management. Increasingly sophisticated hydrological models are in demand to address the increasingly severe problems arising from the adverse impacts of man's activities on the hydrological cycle and thence on water resources development and management, e.g. the effects of land use change related to agricultural and forestry practices, hazards of pollution and toxic waste disposal and general problems arising from conjunctive uses of water.

1.2 Classification of Hydrological Models

In simple terms, a hydrological model is a simplified description of (parts of) the hydrological cycle. However, the term hydrological model is often understood to be and is used more narrowly as a computer-based mathematical model. The development and application of such models have increased tremendously during the last two or three decades, so that engineering hydrology today usually involves consideration of some kind of hydrological model. With the current rapid developments within computer technology and hydrology, the application of computer-based hydrological models can only continue to increase in the near future.

A mathematical model provides a quantitative mathematical description of the processes or phenomena, i.e. a collection of mathematical equations (often partial differential equations), logical statements, boundary conditions and initial conditions, expressing relationships between inputs, variables and parameters. The usual aim is to model the interaction of an input (e.g. rainfall) with a system (e.g. a catchment) to produce an output (e.g. the outflow hydrograph). The hydrological cycle is represented mathematically to imitate the natural system. The mathematical functions employed, can be designed to simulate the natural hydrological processes as closely as present knowledge, mathematical constraints, data availability and user requirements allow. Depending on the required accuracy of results, available funds and efforts to be spent in data collection and modelling, the model can approximate the natural system more or less closely. In classifying mathematical models, the following terms are widely used:

A deterministic model is one in which no uncertainties in prediction are admitted, so that two equal sets of input always yield the same output if run through the model under identical conditions. The model has no component with stochastic behaviour, i.e. the variables are free from random variation and have no distribution in probability.

A stochastic model has some component of random character, having a distribution in probability through time. Identical inputs may result in different outputs if run through the model under identical conditions.

A lumped model is a model where the catchment is regarded as one unit. The inputs, variables and parameters represent average values for the entire catchment.

A distributed model includes spatial variations in all variables and parameters. A probability-distributed model describes spatial variability without reference to the geometrical configuration of the points in the network at which inputs, variables and parameters are determined. A geometrically-distributed model expresses spatial variability in terms of the orientation of the network points one to another and their distances apart.

A black box model is a model developed without any consideration of the physical processes in the catchment. The model is merely based on analyses of concurrent input and output time series.

A conceptual model is based on some consideration of the physical processes in the catchment. In a conceptual model, physically sound structures and equations are used together with semi-empirical ones. However, the physical significance is not so clear that the parameters can be assessed from direct measurements. Instead it is necessary to estimate the parameters from calibration, applying concurrent input and output time series. A conceptual model, which is usually a lumped type model, is often called a grey box model.

A fully physically based model describes the system using the basic equations governing the flows of energy and water. For catchment models, a fully physically based model in practice also has to be a fully distributed model. This type of model, also called a white box model,thus consists of a set of linked partial differentile equations together with parameters which,in principle, have direct physical significance and can be evaluated by independent measurements.

Development over recent decades has been in the form of a natural progression from black box models to grey box models (lumped, conceptual) and onward to increasingly sophisticated physically-based, distributed models (white box). This progression has taken place concurrently with and dependent on (a) the increasing understanding of the physics of the hydrological processes, (b) the increasing quality and quantity of hydrological data being collected, particularly in a large number of well-instrumented research catchments and (c) the explosive progress within computer technology.

Physically-based, distributed models are based on our understanding of the physics of the hydrological processes which control catchment response and use physically-based equations to describe these processes. From their physical basis, such models can simulate the complete runoff regime, providing multiple outputs (e.g. river discharge, phreatic surface level and evaporation loss) while black box models can offer only one output. Also, almost by definition, physically-based models are spatially distributed since the equations, from which they are formed, generally involve one or more space coordinates. They can therefore simulate the spatial variation in hydrological conditions within a catchment as well as simple outflows and bulk storage volumes. On the other hand, such models make huge demands in terms of computational time and data requirements and are costly to develop and operate.

1.3 Selection of Appropriate Model Type

A large number of hydrological models exist. However, many of the models function in fundamentally the same way. For some hydrological problems, the selection of model type is more or less obvious, e.g. probabilistic models for frequency analysis or stochastic time series models for generation of long (100-1000 years) synthetic streamflow series. Empirical (black box) models are mainly of interest as single event models or as sub-components of more complicated models. Lumped, conceptual models are especially well suited to simulation of the rainfall-runoff process when hydrological time series sufficiently long for a model calibration exists. Thus typical fields of application are (i) extension of short streamflow records based on long rainfall records and (ii) real time rainfall-runoff simulation for flood forecasting. Other fields of possible application, to which the lumped conceptual models are not especially well suited, but where they can be used if no better model or method is available, include (i) prediction of runoff from ungauged catchments and (ii) general water balance studies, availability of ground water resources, irrigation needs, analyses of variations in water availability due to climatic variability etc. Physically-based distributed models can in principle be applied to almost any kind of hydrological problem. Obviously, there are many problems for which the necessary solutions can be obtained using cheaper and less sophisticated empirical, lumped conceptual or statistical models. However, for the more complicated problems there may be little alternative, but to use a physically-based distributed model. Some examples of typical fields of application are:

Catchment changes

These include both natural and man-made changes in land use, such as the effects of forest fires, urbanisation and forest clearance for agricultural purposes. The parameters of a physically-based, distributed model have a direct physical interpretation, which means that they can be evaluated for the new state of the catchment before the change actually occurs. This enables the effects of changes to be examined in advance of such changes. In addition, the characteristically localized nature of catchment changes can easily be accounted for within the spatially distributed model structure.

Ungauged catchments

An application in a previously ungauged catchment requires the initiation of a programme of field work to provide data and parameters for calibration. Here, the physical significance of its model parameters enables e.g. the SHE to be applied on the basis of a much shorter, and therefore more cheaply obtained, hydrometeorological record than is necessary for more conventional models. Similarly, the catchment parameters can be estimated from intensive , short-term field investigations.

Evaluation of irrigation schemes

A detailed examination of the efficiency of irrigation schemes require a modelling of the surface water/ground water interaction at a field scale in the command area. The model e.g. the SHE can be used for prediction of crop and irrigation water requirements, water losses in canals and fields, return flow, water logging, effects of drainage etc. By also adding chemical and crop calculation modules, furthermore salinity and crop yield can be examined.

Movement of pollutants and sediments

In order to model the movement of pollutants and sediments, it is first necessary to model the water flows which provide the basic dispersion mechanism. Most water quality and sediment problems are distributed in nature, so distributed models are the most suitable for supplying the basic information on water flows.

The choice of model for a particular 'real-world' application is likely to be heavily influenced by non-hydrological criteria such as the time, manpower and money available to support the project, availability of data, desired accuracy of results and computer resources. Selecting a model requires balancing the degree to which the model represents the hydrological system against the general difficulty in obtaining a result. If a highly complex mathematical representation of a system is used, the risk of not representing the system is minimized but the difficulty of obtaining a useful result is maximized. Many data will be required, programming effort and computer time are large, the general mathematical complexity may even render the problem formulation intractable and the resource constraints of time, money and manpower may be exceeded.

Conversely, if a greatly simplified mathematical model is applied without a proper examination of its physical significance, the difficulties in obtaining a result may be reduced but the risk of not representing the physical system is increased.

1.4 The European Hydrological System (SHE)

The SHE (Systeme Hydrologique Europeen), developed jointly by the Danish Hydraulic Institute, the British Institute of Hydrology and SOGREAH (France), employs a physically-based distributed modelling approach in order to provide realistic representation of the hydrological processes viz. interception, evapotranspiration, overland and channel flows, subsurface flows in the soil root, unsaturated and saturated zones, snowmelt etc., and their complex interaction in space and time. It involves subdivision of the catchment in square grids and models the entire land-based part of the hydrological cycle, taking into consideration soil types and land use distribution. The model has the capability of predicting the effects of land use changes, runoff from ungauged watersheds and also for providing the hydrological basis for water quality and soil erosion modelling.

In view of the large scale water resources development activities in the Cauvery basin and the availability of data, the Hemavati (upto Sakleshpur) sub-basin of the Cauvery has been selected for application of the SHE. The climate , topography, vegetation, soil and rainfall in the basin have provided a good sample for application of the SHE, from data collection and processing to calibration, validation and sensitivity studies.

2.0 THE SHE

2.1 General

The Systeme Hydrologique Europeen (SHE) is an advanced, physically-based, distributed modelling system developed by DHI, the UK Institute of Hydrology and SOGREAH. Currently British responsibility for the SHE lies with the Natural Environmental Research Council's Water Resource Systems Research Unit at the University of Newcastle upon Tyne (UON). In France the responsibility has been transferred from SOGREAH to Laboratoire d' Hydraulique de France (LHF) in 1988.

Within the SHE, each of the major components of the land phase of the hydrological cycle (snowmelt, canopy interception, evapotranspiration, overland and channel flow, unsaturated and saturated subsurface flow) is modelled either by finite difference representations of the theoretical partial differential equations of mass, momentum and energy conservation or by empirical equations derived from independent experimental research. The spatial distribution of catchment parameters, rainfall input and hydrological response is achieved in the horizontal through the representation of the catchment by an orthogonal grid network and in the vertical by a column of horizontal layers at each grid square. River channels are superimposed on the grid element boundaries. Parameters must be evaluated as appropriate for each grid element, river link and subsurface layer.

The physical processes considered in the SHE are schematized in figure 1. The SHE software is structured so that each hydrological process is allocated its own component and the simultaneous operation of each component is controlled by a central frame component. For flexibility, the components can be

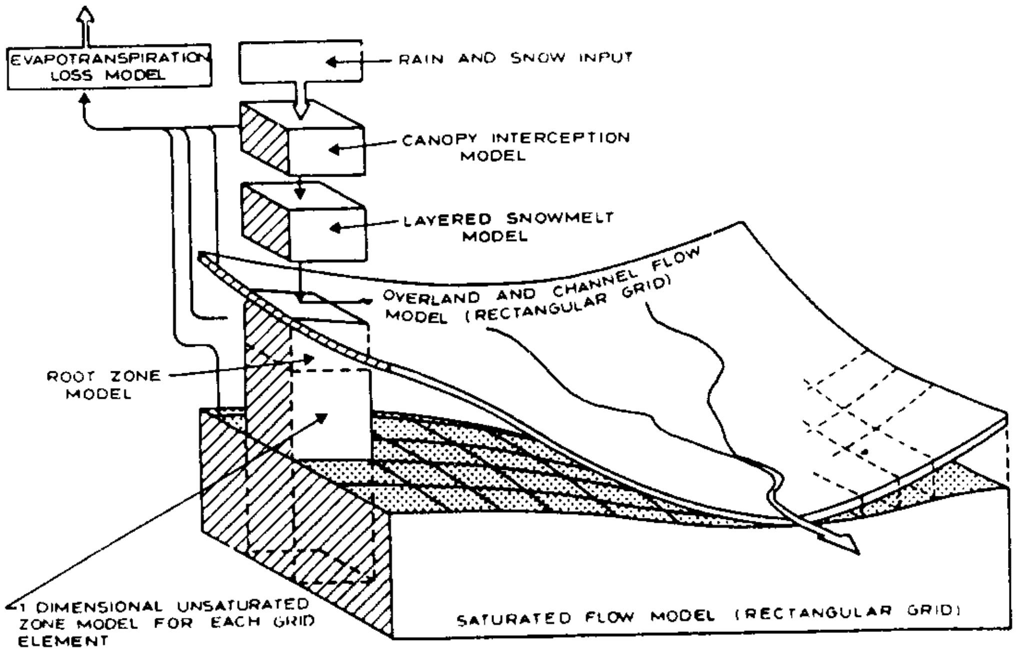

FIGURE 1 - STRUCTURE OF THE EUROPEAN HYDROLOGIC SYSTEM (SHE)

modified or omitted (to be replaced by dummy exchange components) in any given application, depending on the hydrological conditions and availability of data.

The SHE is designed as a practical system for application in a variety of water resource problems. In particular, its physical and spatially distributed basis gives it an advantage over simpler regression and lumped models in simulating land use change impact, ungauged basins, spatial variability in catchment inputs and outputs, ground water and soil moisture conditions, and the water flows controlling the movement of pollutants and sediments. It is therefore appropriate for use in the Hemavati basin where the assessment of land use change impacts, waterlogging risks from irrigation and other problems is hampered by the lack of extensive hydrometeorological records and can not easily be carried out by simpler models.

2.2 Model Structure and Process Description

The SHE has been developed as a fully modular system for mathematical description of the land phase of the hydrological cycle. The system comprises the following models for description of water flows:

- a one-dimensional interception and evapotranspiration model, called the ET component;
- a two-dimensional overland flow model and one-dimensional river/channel flow model, called the OC component;
- a one-dimensional unsaturated zone flow model, called the UZ component;
- a two-dimensional saturated flow (ground water) model, called the SZ component (a three-dimensional SZ component has recently been developed); and

- a one-dimensional snowmelt model, called the SM component.

The overall exchange of information between the SHE components is controlled by the FRAME component. The components are described in the following sections. In addition to these water flow components, add-on modules have been/are being developed for

- a two-dimensional irrigation model, called the IR component;
- a one-dimensional description of solute transport and chemical processes in the unsaturated zone;
- a three-dimensional description of solute transport and chemical processes in the saturated zone;
- a description of soil erosion and sediment transport;
- a description of the transport and fate of radio-nuclear isotopes; and
- a description of nitrogen transport and processes at a catchment scale.

2.2.1 FRAME (Central Control) component

The frame component of SHE provides the controlling function to ensure an orderly and consistent execution of the other components and transfer of data between them. In brief, it performs the following functions:

i) steers the reading of data for each component and the initialization of all computation variables.

ii) Controls the sequence in which each component is called to perform its computations and controls the time steps of the computations.

iii) Controls the data flow from one component to another i.e. processes the results of the computation in one component into the correct form for input to another component as internal boundary data.

iv) prints a summary of the results at specified intervals.

v) records the calculation results on permanent storage, for further processing by use of the SHE Output Retrieval and Graphical Display package.

vi) maintains a check on the water mass balance for the whole model except the river.

The order, in which the frame carries out its functions, is illustrated in figure 2. First, there is an initialization section which calls the initialization routines for each component, including its own. These routines read all the relevant data and initialize the multitude of variables and arrays. Then follows the section of the frame called the Chef d' Orchestre which gets its name from its task of directing the sequence of calculations and controlling the flow of data between components. Because of the close links between the evapotranspiration and interception (ET/IC), unsaturated zone (UZ) and snowmelt (SM) components, the frame calls only the UZ, which then calls the ET and SM.

2.2.2 Interception and evapotranspiration component

This component uses meteorological input data and vegetation parameters to simulate the total evapotranspiration and net rainfall amounts resulting from the processes of interception of rainfall by the vegetation canopy, drainage from the canopy, evaporation from the canopy surface, evaporation from the soil surface, and uptake of water by plant roots and its transpiration. Net rainfall, transpiration and soil evaporation

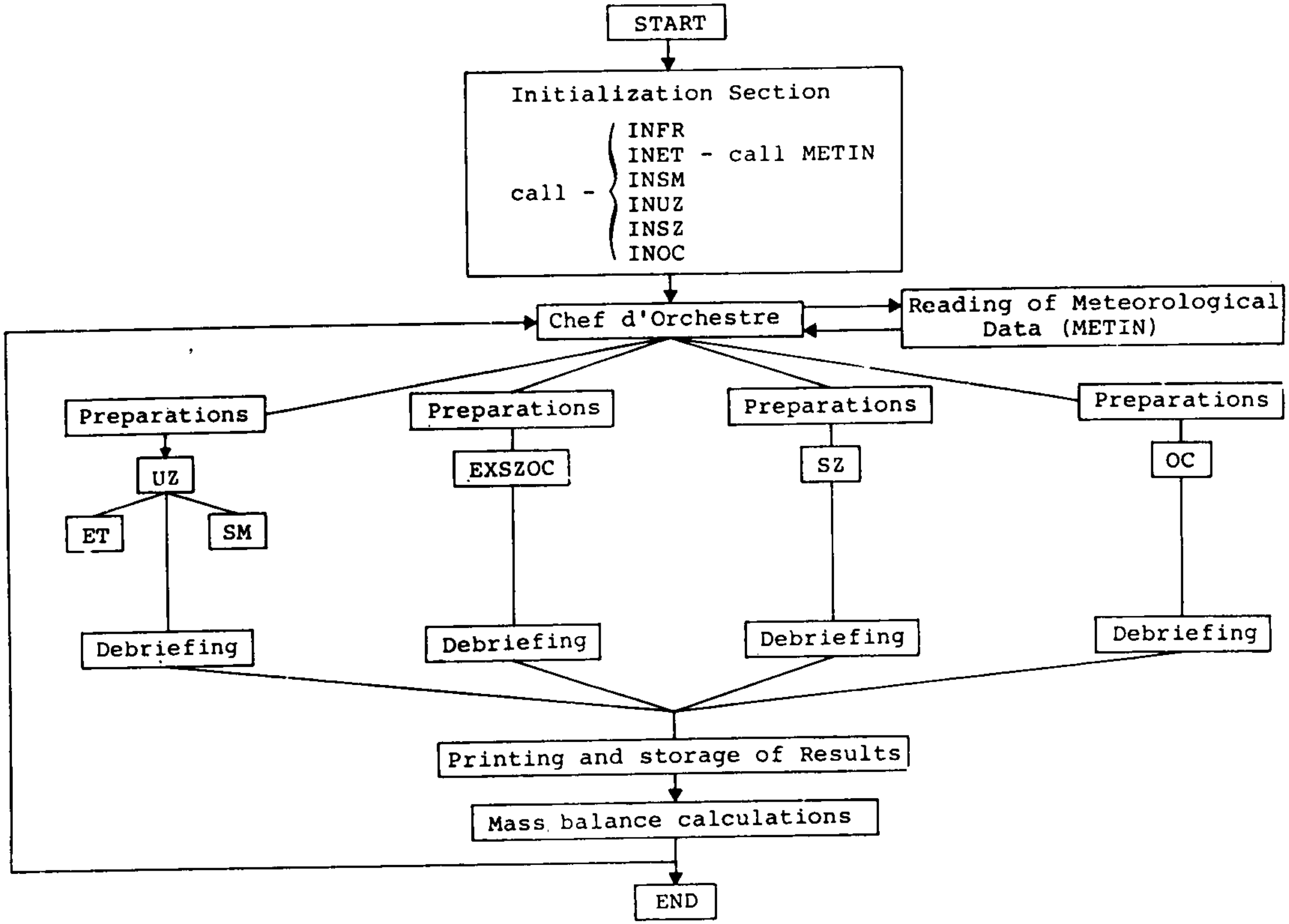

FIGURE 2 - THE PROGRAM STRUCTURE OF SHE

rates are supplied to the unsaturated zone component, which in return provides information on soil moisture conditions in the root zone. Because interception can significantly affect evapotranspiration, the two processes are modelled within the one overall component.

Interception

The interception component calculates net rainfall reaching the ground through the canopy, the amount of water stored on the canopy and evaporation from the canopy. It does not distinguish between throughfall and stemflow, nor does it account for snow or fog interception. Calculations are based on the model developed by Rutter et al.(1971/72) which is essentially an accounting procedure relating rate of change of interception storage to net input (precipitation minus evaporation) and drainage from the canopy.

$$\frac{\partial C}{\partial t} = Q - ke^{b(C-S)} \qquad \ldots(1)$$

where,

C = storage or depth of water on the canopy;

S = canopy storage capacity (the minimum depth of water required to wet all canopy surfaces);

Q = net input;

k and b = drainage parameters; and

t = time.

The equation 1 is solved by analytical integration. In general the canopy storage C and the parameters S, k and b can not be measured directly but must be estimated indirectly from measurements of rainfall, net rainfall below the canopy and evapotranspiration. Although developed initially for trees, the model is used in the SHE for all vegetation since the physical principle is the same, namely that the canopy is considered to have a surface storage which is filled by rainfall and emptied by evaporation and drainage. The model takes into account the proportion of the ground covered by vegetation and the way in which this proportion and other important parameters vary with time, for example over the agricultural cycle.

As an alternative option, the interception process is modelled by introducing an interception ——————→ ——————→ storage, which has to be filled before throughfall to the ground surface takes place. The interception storage is diminished by direct evaporation. The size of the interception storage capacity, I_{max} depends on the vegetation type and its stage of development through the leaf area index, LAI:

$$I_{max} = C_{int} \, LAI \qquad \ldots(2)$$

where,

C_{int} = interception parameter (mm); and

LAI = leaf area index.

The parameter C_{int} is independent of vegetation type but depends on the time resolution. On the basis of interception storage capacities given in the literature for different vegetation types, a typical value of C_{int} is 0.05 mm. The exact value may be assessed from calibration. The leaf area index, LAI varies usually between 0 and 7.

Evapotranspiration

The evapotranspiration component calculates actual evapotranspiration and translates it into a loss term, describing uptake of water by plant roots and its transpiration in a response which is continuous as the canopy varies from a dry, through a partially wetted, to a fully wetted state. The loss term is then used in the calculation of soil moisture changes by the unsaturated zone component.

Several calculation options are available, each one based in some form upon the modification of potential evapotranspiration by vegetation controls and soil moisture. Depending on data availability, the potential rate may be provided from direct measurements (thereby minimizing the amount of calculation) or may be determined from basic principles, taking into account the meteorological conditions e.g. the need for an energy input, a difference in vapour pressure between the evaporating surface and the atmosphere and a means of exchanging surface air for air capable of holding more vapour.

Four calculation options are available. The first two are based on the Penman-Monteith equation, which is a modification of Penman's potential evapotranspiration equation taking into account the average stomatal resistance to vapour flux through a canopy resistance factor (Monteith, 1965).

$$E_a = \frac{R_n \Delta + \frac{\rho c_p \delta_e}{r_a}}{\lambda \left[\Delta + \gamma \left(1 + \frac{r_c}{r_a}\right)\right]} \quad \ldots(3)$$

where,

E_a = actual evapotranspiration rate (m/s);

R_n = net radiation (W/m^2);

Δ = rate of increase with temperature of the saturation vapour pressure of water at air temperature (mb/^oC);

ρ = density of air (kg/m^3);

c_p = specific heat of air at constant pressure ($J/kg/^{\circ}C$);

δ_e = vapour pressure deficit of air (mb);

λ = latent heat of vaporization of water (J/kg);

γ = psychrometric constant ($mb/^{\circ}C$)

$$= \frac{pc_p}{\sigma\lambda};$$

p = atmospheric pressure (mb);

σ = ratio of water vapour density to air density (approximately 0.622);

r_c = canopy resistance to water transport (s/m); and

r_a = aerodynamic resistance to water vapour transport (s/m).

The aerodynamic resistance coefficient r_a represents the resistance to transport of water vapour from the canopy to a plane 2 m above it. The greater the surface roughness, the less is the resistance to water vapour transfer and the lower is r_a, i.e. trees have lower values of r_a than grass. The canopy resistance factor r_c represents the resistance to water transport from some region within or below the transpiring surface to the surface itself. It is equal to zero for a wet canopy (because evaporation of intercepted water is then already satisfying the potential rate) and equal to average stomatal resistance (varying with vegetation type) in dry conditions.

In the first calculation option, r_c is assumed to be constant i.e. vegetation type is then the primary influence, as for wet soils. In the second option, r_c varies also with soil moisture, assuming that this is as important as vegetation type, as for dry soil conditions.

In the third option, actual evapotranspiration is obtained from the potential rate as a function of soil moisture content, thus stressing the control of soil moisture conditions. The method, developed by Feddes et al.(1976), is summarized as follows. If ψ = soil moisture tension, then under conditions drier than some wilting point ψ_w and wetter than some anaerobiosis point ψ_s, plants do not take up water from the soil, so actual evapotranspiration is zero. Between ψ_s and some arbitrary condition ψ_1 at which soil moisture begins to limit plant growth, water uptake and thence evapotranspiration are considered to take place at the potential rate. Between ψ_1 and ψ_w it is assumed that the rate of uptake varies as a linear function of soil moisture content, so that actual evapotranspiration varies linearly as a proportion of the potential evapotranspiration according to soil moisture tension.

The fourth option is similar to the third, being based on measured potential evapotranspiration and alternative functions of soil moisture content and vegetation structure (Kristensen and Jensen, 1975). The transpiration from the vegetation, E_{at} depends on the density of the crop green material described by the leaf area index, LAI and the actual soil moisture content in the nodes in the root zone. It also depends on the root density.

$$E_{at} = f_1 \text{ (LAI) } f_2 \text{ } (\theta) \text{ RDF } E_p \qquad \ldots(4)$$

where,

E_{at} = transpiration;

RDF = root distribution function;

E_p = potential evapotranspiration;

f_1(LAI) = function of leaf area index LAI and the empirical parameters C_1 and C_2 ; and

$$f_2(\theta) = 1 - \left(\frac{\theta_F - \theta}{\theta_F - \theta_W}\right)^{C_3/E_p} \qquad \ldots(5)$$

where,

θ_F = volumetric moisture content at field capacity;

θ_W = volumetric moisture content at wilting point;

θ = volumetric moisture content; and

C_3 = empirical parameter (mm/day).

Equation 4 is applied to all nodes in the root zone. The root distribution function, RDF is calculated in the model assuming a logarithmic variation with the depth in accordance with the usual distribution of the root mass.

The soil evaporation, E_s taken only from the upper layers, consists of a basic evaporation, $E_p f_3(\theta)$ plus evaporation from a possible water reserve in the upper layers, if a vegetation cover does not restrict the energy penetration to the soil surface.

$$E_s = E_p f_3(\theta) + [E_p - E_{at} - E_p f_3(\theta)] f_4(\theta)[1 - f_1(LAI)] \ldots(6)$$

where the functions $f_3(\theta)$ and $f_4(\theta)$ are given by

$$f_3(\theta) = \begin{cases} C_2 \dfrac{\theta}{\theta_W} & \text{for} \quad \theta_M \le \theta \le \theta_W \\ C_2 & \text{for} \quad \theta \ge \theta_W \\ 0 & \text{for} \quad \theta \le \theta_M \end{cases} \qquad \ldots(7)$$

$$f_4(\theta) = \begin{cases} \dfrac{\theta - \frac{1}{2}(\theta_W + \theta_F)}{\theta_F - \frac{1}{2}(\theta_W + \theta_F)} & \text{for } \theta > \frac{1}{2}(\theta_W + \theta_F) \\ 0 & \text{else} \end{cases} \qquad \ldots(8)$$

The reduction E_s/E_p is a function of soil moisture in the upper layers as calculated from equation 6. In the model, the soil evaporation is taken equally from the four upper most nodes. It is seen that the evapotranspiration routine contains three empirical parameters C_1, C_2, and C_3. These are discussed in detail in Kristensen and Jensen (1975).

The various options take into account the proportion of the ground covered by vegetation and the way in which this proportion varies with time, for example over the agricultural cycle. The distribution of plant roots in the soil column is used in the calculation of soil water uptake. The choice of which calculation option to use, depends on data availability and the understanding of the evapotranspiration processes in the particular application.

2.2.3 Overland and channel flow component

This component uses topographic, channel shape and flow resistance parameters to route surface water as overland and channel flow. The depth of surface water available as runoff is determined from the net rainfall and evaporation rates supplied by the interception/evapotranspiration component and from the soil infiltration rate determined by the unsaturated zone component. In addition there is an exchange between channel and aquifer to allow for seepage losses and ground water input.

The SHE uses the theoretical, partial differential equations of mass continuity and force-momentum to simulate the depths, velocities and discharges of overland and channel flow in a methodology known as flood routing. The equations, which are the diffusion wave approximation to the full St.Venant equations, take account of both translation and attenuation effects in flood wave movement. However, the model is aimed at reproducing a hydrological response and should not be considered as a detailed hydraulic model.

Overland flow

For overland flow, a two-dimensional solution is obtained using the equations

$$\frac{\partial h}{\partial t} + \frac{\partial (uh)}{\partial x} + \frac{\partial (v h)}{\partial y} = q \qquad \ldots(9)$$

$$\frac{\partial h}{\partial x} = S_{ox} - S_{fx} \quad \text{(x-direction)} \qquad \ldots(10)$$

$$\frac{\partial h}{\partial y} = S_{oy} - S_{fy} \quad \text{(y-direction)} \qquad \ldots(11)$$

where,

$h(x,y)$ = local water depth;

t = time;

x,y = horizontal cartesian coordinates;

$u(x,y)$, $v(x,y)$ = flow velocities in the x and y directions;

$q(x,y,t)$ = net precipitation minus infiltration;

$S_{ox}(x,y)$, $S_{oy}(x,y)$ = ground slopes in the x and y directions; and

$S_{fx}(x,y)$, $S_{fy}(x,y)$ = friction slopes in the x and y directions.

$$S_{fx} = \frac{u^2}{k_x^2\, h^{4/3}} \qquad \ldots(12)$$

$$S_{fy} = \frac{v^2}{k_y^2\, h^{4/3}} \qquad \ldots(13)$$

where,

$k_x(x,y)$ and $k_y(x,y)$ are the Strickler roughness coefficients for the x and y directions respectively.

These equations are solved in a finite difference scheme using an explicit procedure described by Preissmann and Zaoui (1979).

Channel flow

For channel flow, a one-dimensional solution (i.e. along the channel) is obtained using the equations

$$\frac{\partial A}{\partial t} + \frac{\partial (Au)}{\partial x} = q_L \qquad \ldots(14)$$

$$\frac{\partial h}{\partial x} = S_{ox} - S_{fx} \qquad \ldots(15)$$

$$S_{fx} = \frac{u^2}{k_x^2 h^{4/3}} \qquad \ldots(16)$$

where,

$A(x)$ = flow cross-sectional area;

S_{ox} = channel bed slope;

$q_L(x)$ = source/sink term for evaporation, rainfall, lateral inflow and outflow, stream/aquifer exchange; and

x = distance along the channel.

Allowance is also made for weirs. The eventual solution is carried out by an implicit finite difference scheme (Preissmann and Zaoui, 1979).

2.2.4 Unsaturated zone component

This component determines the soil moisture content and tension, or pressure distributions in the unsaturated zone. The zone extends from the ground surface to the phreatic surface. It is mostly nonuniform in its physical properties and the upper part, the root zone, exhibits considerable fluctuations in moisture content as a result of evapotranspiration and rainfall infiltration. Its lower boundary also varies through time, as the phreatic surface elevation changes. The component plays a crucial role in the SHE since all the other components draw upon the boundary data which it supplies.

Based on the assumption that there is flow in the vertical only, the solution is obtained with the one-dimensional Richards equation:

$$C \frac{\partial \psi}{\partial t} = \frac{\partial}{\partial z} \left(K \frac{\partial \Psi}{\partial z}\right) + \frac{\partial K}{\partial z} - S \qquad \ldots(17)$$

where,

ψ = soil moisture tension or pressure head;

t = time;

z = vertical space coordinate (positive upwards);

$C = \frac{\partial \theta}{\partial \psi}$ = soil water capacity;

θ = volumetric water content;

$K(\theta, z)$ = hydraulic conductivity; and

$S(z)$ = source/sink term for root extraction and soil evaporation.

Two functional relationships are needed to solve the equation. These are the relationship between unsaturated conductivity K and the volumetric moisture content θ and the relationship between soil tension ψ and the volumetric moisture content. The latter, called the retention curve, is known to exhibit hysteresis effects in nature but is approximated by a single-valued relationship in the SHE. A table of θ - ψ values is required and intermediate values are then calculated, using a cubic spline method and tabulated.

For complex situations with non-homogeneous conditions and varying boundary configurations, Richards equation can only be solved by introduction of a numerical approximation. The numerical method is based on subdividing the vertical flow region into finite segments bounded and represented by a series of nodal points at which a solution is obtained. The solution provides a value of the pressure head and moisture content at each nodal point and the flow between the nodal points including the flow exchange between soil and atmosphere and the recharge to the ground water table. The solution is given at discrete times. There are several solution techniques available for solving the one-dimensional unsaturated flow. In the SHE, an iterative implicit finite difference scheme is adopted.

Boundary conditions must be specified for each time step and when transient flow conditions are considered, the initial condition is also required. The upper boundary may either be a specified flux (net precipitation) or a specified head. The latter case is considered when the net rainfall rate reaching the ground exceeds the infiltration capacity of the soil and ponding occurs. A pressure head will then be specified as long as water is located at the ground surface. The lower boundary condition is usually a pressure head boundary determined for the first nodal point below the ground water table. Since the position of the water table is changing during a simulation run, the extent of the unsaturated zone also varies. Special cases may arise during the wet season where the unsaturated zone can completely vanish at a particular grid square in the horizontal grid network.

2.2.5 Saturated zone component

This component computes the phreatic surface level and the flows, assumed to be horizontal only, in the saturated zone. At present only single layer, unconfined aquifers can be modelled. However, the component is designed so that it can easily be expanded to account for confined and multilayer aquifers in the future. Otherwise allowance is made for spatial variations in aquifer permeability and the impermeable bed level. The component receives net percolation rates from the unsaturated zone calculations and supplies in return the phreatic surface level as a lower boundary condition for those calculations. Stream/aquifer interactions, ground water seepage at the ground surface and artificial pumping are also simulated.

The variation through time of the phreatic surface level at each square is modelled by the nonlinear Boussinesq equation. This combines Darcy's law and the mass conservation of two-dimensional laminar flow in an anisotropic, heterogeneous aquifer, to give

$$S \frac{\partial h}{\partial t} = \frac{\partial}{\partial x} \left(K_x H \frac{\partial h}{\partial x}\right) + \frac{\partial}{\partial y} \left(K_y H \frac{\partial h}{\partial y}\right) + R \qquad \ldots(18)$$

where,

$S(x,y)$	=	specific yield;
$h(x,y,t)$	=	phreatic surface level;
$k_x(x,y)$, $K_y(x,y)$	=	saturated hydraulic conductivities in the x and y directions respectively;
$H(x,y,t)$	=	saturated thickness;
t	=	time;
x,y	=	horizontal cartesian coordinates; and

R(x,y,t) = instantaneous vertical recharge into the saturated zone.

This can be expressed by,

$$R = \Sigma q - \frac{\partial}{\partial t} \int_{h}^{gs} \theta \, dz \qquad \ldots(19)$$

where,

Σq = transpiration + soil evaporation + infiltration + stream/aquifer exchange + external boundary flows;

$\theta(z,t)$ = soil moisture content in the unsaturated zone; and

gs = ground surface level.

Equation 18 is solved by a finite difference approximation using an alternating-direction, non-iterative implicit scheme. Allowance is made for both the complete disappearance of the saturated zone and the rise of the phreatic surface to the ground surface. Stream/aquifer interactions are simulated for the following cases:

(a) phreatic surface in direct contact with a flowing stream;

(b) phreatic surface in direct contact with a dry stream;

(c) phreatic surface lying below a flowing stream; and

(d) phreatic surface lying below a dry stream.

In addition, the channel boundary can be assigned a hydraulic conductivity different from that of the surrounding aquifer. This is to account for the higher or lower conductivities which may characterize the sediments in the immediate vicinity of the channel.

2.2.6 Snowmelt component

This component uses snowpack and vegetation parameters, along with meteorological input data, to predict the transfer of moisture resulting from the process of

(i) snowfall addition to the snowpack;

(ii) snowmelt from the snowpack;

(iii) spatial variations in snowpack conditions; and

(iv) interception and evapotranspiration in the presence of a snowpack and at air temperatures below freezing.

Its aim is to model the snowpack thickness as it is affected by precipitation and melting and to model the rate of delivery of meltwater from the snowpack to the soil surface. The component is structured so that first the total heat flux to the snowpack is calculated, then the amount of melting engendered by this flux is determined and finally the meltwater is routed through the snowpack. Thus both energy and mass fluxes within the snowpack are modelled.

Depending on the availability of data or on general requirements, two different calculation modes can be used to determine the total heat flux. The simplest is an adaptation of the degree-day method giving

$$H = K T_a S \rho_w L_i \qquad \ldots(20)$$

where,

H = heat flux;

K = degree-day factor;

T_a = air temperature;

S = specific gravity of snow;

ρ_w = density of water; and

L_i = latent heat of fusion of ice.

Because of its empirical nature, this method is used only when available data are limited to air temperatures.

At a more sophisticated level, the heat flux is determined from a budget of the energy inputs and outputs. Contributions from all the fluxes are calculated for the pack as a whole, giving

$$H = C + P + E + G + R_n \qquad \ldots(21)$$

where,

- C = heat gained by convection from the air;
- P = heat gained from precipitation;
- E = heat gained from condensed vapour;
- G = heat conducted from the underlying rock or soil; and
- R_n = net radiation.

Vertical variations in snowpack parameters are neglected and each parameter is assumed to be uniform through depth. The snowmelt resulting from the total heat flux is derived from an energy balance equation, in which due account is taken of the latent heat gained by movement of water into the snowpack. Any meltwater is then routed through the snowpack, the time which it takes to reach the soil being given by

$$t_m = 0.745\, Z^2 + 1.429\, Z \qquad \ldots(22)$$

where,

- t_m = time of travel from the top to the bottom of the snowpack, in hours; and
- Z = snowpack depth at the beginning of the meltwater flow, in metres of snow.

Equation 22 was derived empirically from the experimental data of Anderson (1968).

2.3 Parameter and Data Requirements

The distributed and physically-based nature of the SHE requires that in each application study, a vast amount of data and parameters describing the physical characteristics of the catchment are available. Different types of applications and different hydrological regimes being considered may call for various degrees of accuracy in the estimation of the individual basin parameters and the evaluation of some parameter values may simply be based on experience. The data availability however, will in any case determine the degree of reliability which can be put into the simulation results.

In the following a brief introduction to the required data is listed. These comprise of

1. Catchment geometry:

- Topography (from toposheets on scale 1:50,000)
- Soil depths (depth to impervious layer)
- River geometry (cross-sections, route of the river and information about structures)

2. Land use and soil parametric data:

- The spatial distribution of soil and vegetation types

For each vegetation type:

- Temporal variation of either (i) root depth and leaf area index or (ii) canopy drainage parameters, soil shading indices and canopy and aerodynamic resistances

For each soil type:

- Soil moisture tension/content relationship
- Unsaturated hydraulic conductivity as a function of moisture content

- Saturated hydraulic conductivities for horizontal flow and vertical flow

3. Surface parametric data:

These data are required for each grid square and include

- Strickler roughness coefficient for overland flow and river flow
- Cracking/bypass coefficients
- Depth to drains and subsurface drainage coefficients

4. Snowmelt parametric data:

- Initial snowpack depth
- Degree-day factor
- Initial snow temperature

5. Input data:

- Rainfall and meteorological station network and records of data obtained at these stations (including potential evapotranspiration data)
- Streamflow data
- Boundary and initial conditions
- Other relevant data which can be utilized in the model calibration and validation e.g. water table, soil moisture data etc.

In order to conduct a successful application study with the SHE, major emphasis should be devoted to the data collection/assembly and data processing phase, Lack of information on some basin parameters may require that a short term programme of field measurements is carried out with the aim of improving the parameter data base and also to gain a first hand knowledge about the hydrological regime in the catchment to be studied.

2.4 Data Provision Methodologies for the SHE

Direct field measurement of the parameters and their spatial distributions is prohibitively expensive. Therefore, a few measurements can be carried out at representative sites in the catchment (concentrating on those parameters having the most influence on simulation results). These measurements are then assumed, on the basis of their physical nature, to apply to other areas of the catchment having the same basic characteristics i.e. data provision is accomplished by transfer from representative site to the whole basin. Some calibration will still be needed.

Calibrate the model for a subcatchment of the main catchment and then apply the calibrated parameters to the main catchment. Calibration for a subcatchment requires less data collection, so it may be feasible to carry out a field measurement programme for the subcatchment whereas this would be prohibitive for the main catchment. Transfer of the calibrated parameters to the main catchment is feasible as long as the subcatchment is representative of the main catchment and as long as scale problems are not important i.e. if different grid square sizes are used in the subcatchment and main catchment, do the parameters calibrated for the subcatchment squares remain representative at the larger scale of the main catchment squares.

Remote sensing offers long term hope of providing spatially and temporally distributed data averaged at different grid scales. At present, remote sensing can map distributions of vegetation, land use and topography. It is so far less useful for mapping soil type and soil moisture conditions, although ground penetrating radar can measure phreatic surface levels in certain circumstances.

2.5 Application Capabilities

Development of the SHE represents a new approach to modelling, based solidly on scientific hydrology and with the aim of attacking the full range of problems which appear in water resources engineering. Table 1 summarizes some possible fields of application for the SHE at different operation scales. In particular, the physical basis of the SHE suits it to predictions of the hydrological consequences of man-made changes in a catchment and for pollutant and sediment transport studies. However, the flexibility of the SHE also makes it possible for the one modelling system to perform predictions for a wide range of hydrological problems and at various levels of complexity.

During the initial development (1977-81), the SHE was tested on several catchments and further its components have been tested independently. In addition, within the last five years, the SHE has been applied in the following projects:

(i) A study of the effects of land use change on floods and sediment loads on catchments in Thailand. The study included field studies as well for modelling of three catchments ranging from 50 sq.km. to 600 sq.km.

(ii) A study of the environmental impacts of applying nitrogen fertilizers. This study included very detailed modelling of water flow, nitrogen transport and degradation in two geologically different catchments of 150 sq.km. to 500 sq.km. size in Denmark.

(iii) A study of contaminant transport and degradation of contaminants from chemical/municipal dumps in landfills in Denmark.

Table 1 : Fields of Application for the SHE at Different Operation Scales

S.No.	Topic*	Primary Hydrological Process**	Possible Scale of Operation
1.	Irrigation schemes:		
	Irrigation water requirement	ET/UZ	field
	Crop production	ET/UZ	project
	Waterlogging	ET/UZ	field
	Salinity/irrigation management	UZ	field
2.	Land use change:		
	Forest clearance	ET/UZ/SZ	catchment
	Agricultural practices	ET/UZ/SZ	field/ catchment
	Urbanization	ET/UZ/SZ	catchment
3.	Water developments:		
	Ground water supply	SZ	catchment
	Surface water supply	ET/UZ/SZ	catchment
	Irrigation	UZ/SZ	project/ catchment
	Streamflow depletion	SZ/OC	catchment
	Surface water/ground water interaction	ET/UZ/SZ	project/ catchment
4.	Ground water contamination:		
	Industrial and municipal waste disposal	UZ/SZ	field/ catchment
	Agricultural chemicals	UZ/SZ	field/ project/ catchment
5.	Erosion/sediment transfer	OC/UZ	project/ catchment
6.	Flood prediction	OC/UZ	catchment

* For some of the topics, a water quality component would need to be added to the existing water quantity model.

** ET = evapotranspiration; UZ = unsaturated zone; SZ = saturated zone; OC = overland and channel flow.

(iv) A water supply planning project for the city of Arhus (Denmark). This study included a 800 sq.km. regional five layered ground water model and also focused on the interaction between ground water and streams.

(v) A comparative study of different models ability to simulate runoff from medium size catchments in Zimbabwe and Denmark.

(vi) A study on transport and dispersion of radionuclides from deep disposal sites through the near-surface and surface hydrological system in the UK.

(vii) A study of the effects of irrigation development with focus on sub-basins of river Narmada in India.

3.0 GENERAL DESCRIPTION OF STUDY AREA AND DATA AVAILABILITY

3.1 The Cauvery Basin

The Cauvery basin extends over an area of 87,900 sq.km. in the states of Kerala, Karnataka and Tamil Nadu and lies between the longitudes $75^{O}29'$ and $79^{O}45'$ and north latitudes $10^{O}05'$ and $13^{O}30'$. The basin is bounded on the west by the western ghats, on the east and south by the eastern ghats and on the north by the ridges separating it from the Tungabhadra and the Penner basins. The basin is somewhat rectangular in shape, the maximum length and breadth being 360 km and 200 km respectively. The three main physiographic divisions of the basin are (i) the western ghats, (ii) the plateau of Karnataka, and (iii) the delta. The western ghat region is mountainous and covered with thick vegetation. The plateau of Karnataka with an average elevation of 750 m slopes gently towards the east/south-east. The delta is the most fertile tract in the basin and covers the major portion of the Tiruchirapalli and Thanjavur districts of Tamil Nadu and is eminently suited for intensive cultivation.

The Cauvery is one of the major inland rivers of the peninsula, flowing east and draining into the Bay of Bengal. It rises at Talakaveri on the Brahmigiri range of hills ($12^{O}25'$ N, $74^{O}34'$ E) in the western ghats in the Coorg district of Karnataka state, at an elevation of 1,341 m above mean sea level. The total length of the river from the head to its outfall into the sea is 800 km, of which about 320 km are in Karnataka, 416 km in Tamil Nadu and the remaining length of 64 km forms the common boundary between the states of Karnataka and Tamil Nadu. The important tributaries which join the Cauvery within the Karnataka state are the Harangi, the Hemavati, the Simsha and the Arkavathi on the north (left bank) and the Lakshmanathirtha, the Kabbani and the

Suvarnavathi on the south (right bank). In Tamil Nadu, all the main tributaries of the Cauvery are from the south (right bank). They are the Bhavani, the Noyil and the Amravathi.

3.2 The Hemavati Basin

The Hemavati, also known as Yennehole, is one of the important tributaries to join the Cauvery on its northern bank. It rises in Ballalarayanadurga in the western ghats in the Mudigere taluk of Chikmagalur district. The Hemavati, after traversing a length of 193 km in Hassan and Mandya districts, joins the river Cauvery in the water spread of Krishnarajasagar reservoir near Akkihebbal. Figure 3 shows Hemavati sub-basin in Cauvery river basin.

Hemavati river, in its early reaches, passes through a very heavy rainfall region in the vicinity of Kotigehara and Mudigere. Important tributaries of the Hemavati are the Yagachi and the Algur. The river Yagachi, flowing in a meandering course along NNW-SSE to SSW-NNE directions drains into the Hemavati river at Gorur. The river Algur joins the Hemavati from the south near Algur. In addition to these major streams, a number of other minor streams join the river all along its course. The river drains an area of 5,200 sq.km. The annual rainfall varies from a maximum of 5080 mm to a minimum of 762 mm. Average rainfall for the period 1942-71 is 2972 mm in the Hemavati basin.

The economy of the basin is primarily dependent on agriculture which is the chief occupation of the people. In the hilly region, there are number of small check dams constructed across the river during the 19th century which till to date are being used for irrigation. In the undulating plain, tank irrigation is common. Efforts are being made to increase the irrigation potential of the area and bring more area under

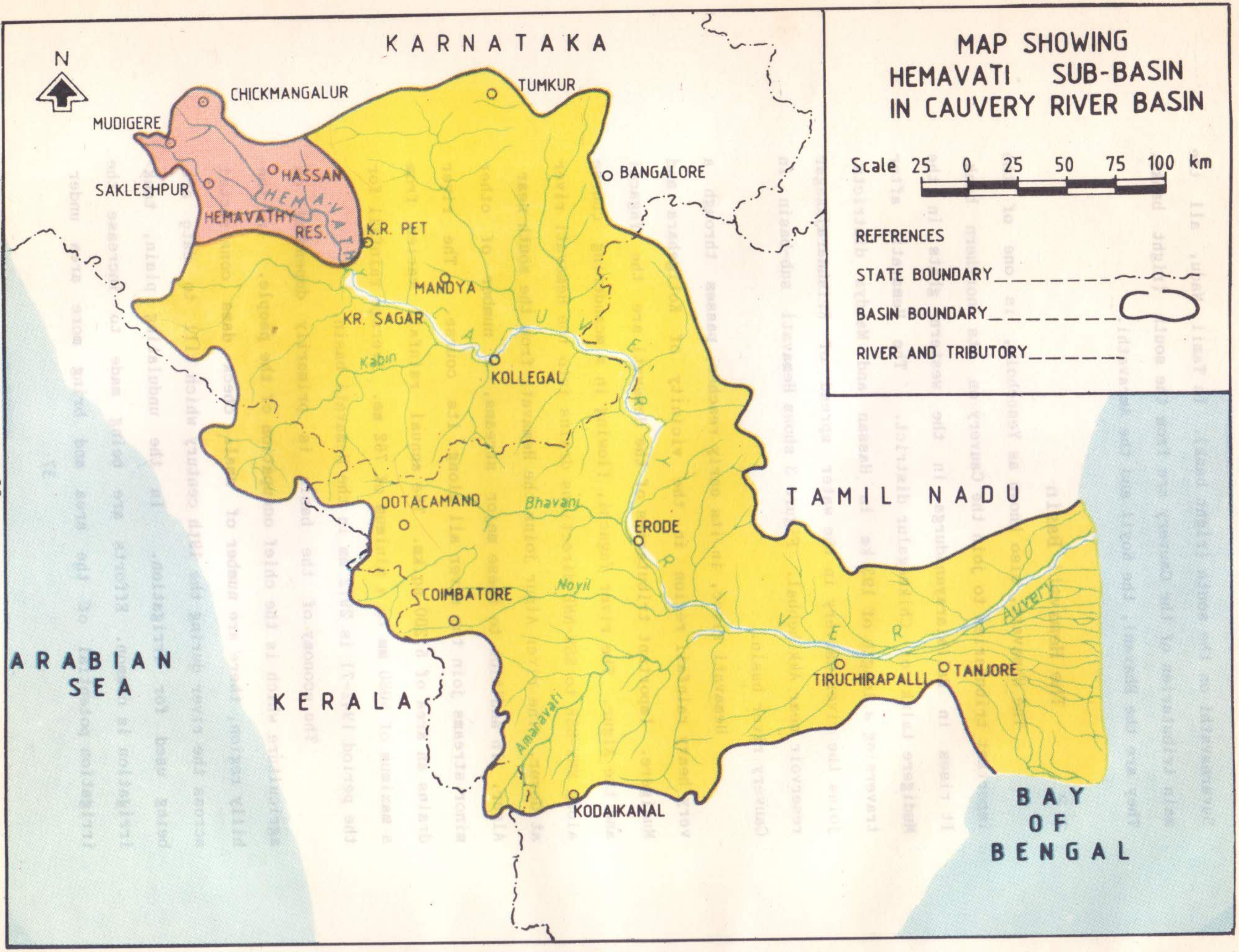

FIGURE 3 - HEMAVATI SUB-BASIN IN CAUVERY RIVER BASIN

cultivation. With this object, Hemavati reservoir project comprising of a composite dam with central masonry and earthern flanks, has been constructed across Hemavati river near Gorur about 1 km upstream of the road bridge on Hassan-Arkalgud road. The catchment covers an area of about 2810 sq.km. and the uppermost reaches of catchment forms hilly and forest zone and the lower reaches are in moderate conditions.

3.3 The Study Area

The Hemavati, a tributary to the Cauvery, takes its [illegible] Javali in Mudigere taluk of Chikmagalur district in Karnataka and follows south easterly course in the study area which comprises the 600 sq.km. head water catchment of the Hemavati defined by the W.R.D.O. gauging site at Sakleshpur, where the river length is about 55.13 km.

The Hemavati (upto Sakleshpur) basin is situated between 12°55' and 13°11' north latitudes and 75°29' and 75°51' east longitudes and lies in the south western part of the state of Karnataka covering parts of the Chikmagalur and Hassan districts. The area is covered under Survey of India toposheet nos. 480/8, 480/12, 480/16, 48P/9 and 48P/13. The total extent of the basin is 600 sq.km. upto Sakleshpur gauging site. The Sakleshpur taluk of the Hassan district rests on the brow of the western ghats and comprises some of the most beautiful scenery in Karnataka state.

Climate and rainfall

The climate during the summer months viz., March to May is generally cool, healthy and agreeable. Rainy season extends from June to October and is characterized by heavy to very heavy rainfall. Winter season extends from November to February. Severe cold climate is experienced during these months. Mean monthly temperatures and potential evapotranspiration at Hassan ($13^{o}00'$ N $76^{o}09'$ E, height 960 m above MSL), near to the basin, are presented in table 2.

Topography

Physiographically the area represents a highly dissected country. General elevation in the basin ranges from 890 m to 1240 m above the mean sea level. Topographically, the basin can be divided into three distinct zones (figure 4):

(i) Low land (valley lands),

(ii) Semi-hilly (gently sloping lands), and

(iii) Hilly (hill ranges with steep to moderate slopes).

Figures 5 and 6 present the topography of the basin in 1 km x 1 km and 2 km x 2 km grid networks respectively.

River network

The basin is heavily dissected by the stream network, as shown in figure 7. The largest tributary in the basin has a length of approximately 20 km. The total length of the Hemavati river from the head to Sakleshpur gauging site is around 55 km. The lengths of the various streams in the basin are given in table 3.

Geology

The main geological formations are schists, granites and gneisses all of precambrian age. Schists are exposed to the western part of the basin and as scattered patches in eastern portions. The belt chiefly consists of epidiorites, hornblende schists, chlorite schists, quartzites and ferruginous quartzites. On account of their superior resistance to weathering, the quartzites and magnetite quartzites form hard cores standing out

Table 2 : **Mean Monthly Temperatures and Potential Evapotranspiration at Hassan**
(Based on observations from 1931-1960)

Month	Mean Monthly Temperature (°C)	Potential Evapotranspiration (PET) (mm)
January	21.4	110.8
February	23.2	119.2
March	25.6	156.8
April	26.7	149.4
May	25.9	146.0
June	23.1	110.7
July	21.9	100.4
August	22.2	103.6
September	22.6	105.7
October	23.1	104.7
November	22.0	98.1
December	20.9	100.0
Annual Average	23.2	1405.4

Source: Temperature - Gazetteer of India, Hassan district, 1971.
PET - Report of National Commission of Agriculture, Part IV, 1976.

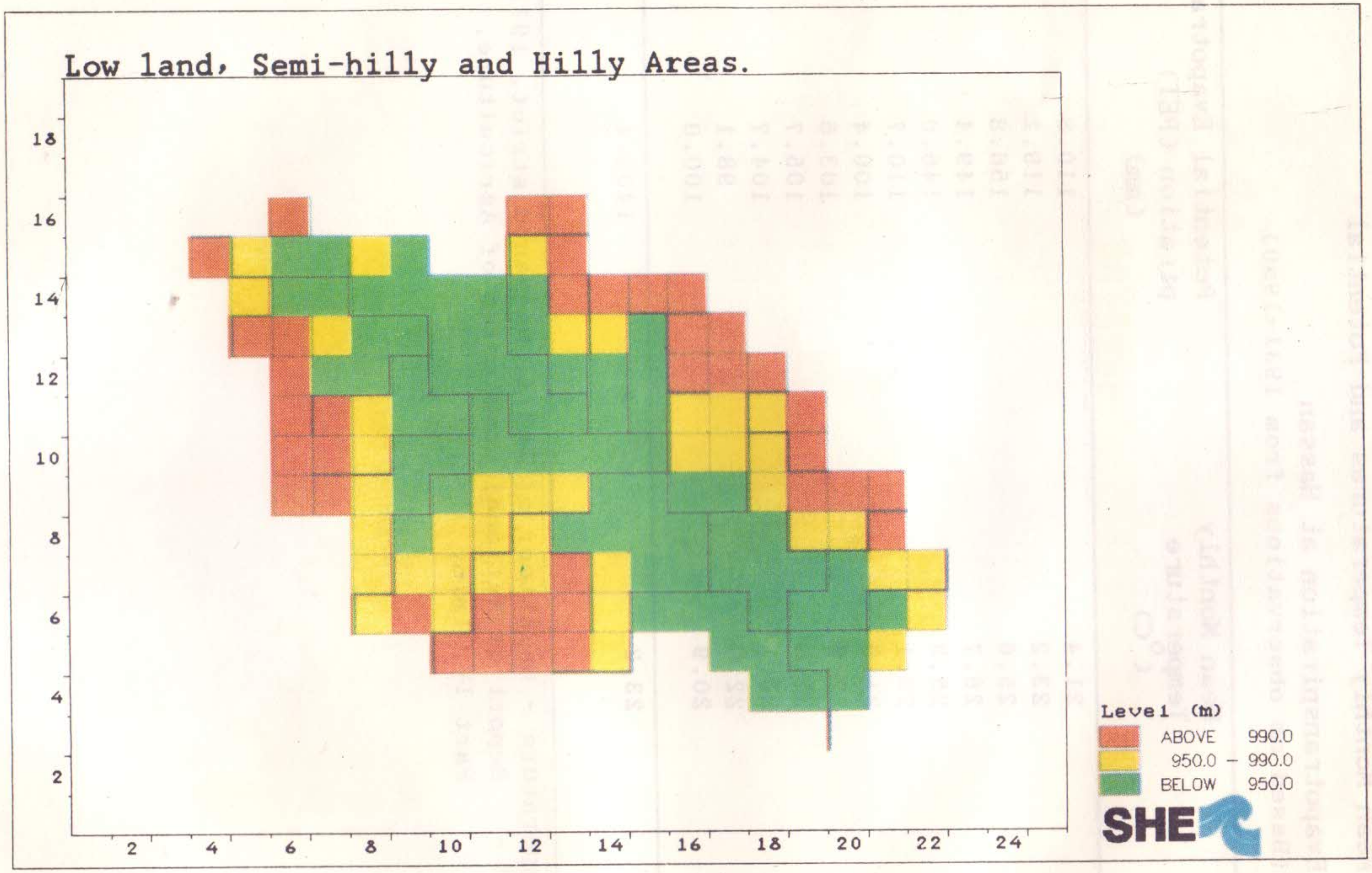

FIGURE 4 - LOW LAND, SEMI-HILLY AND HILLY AREAS

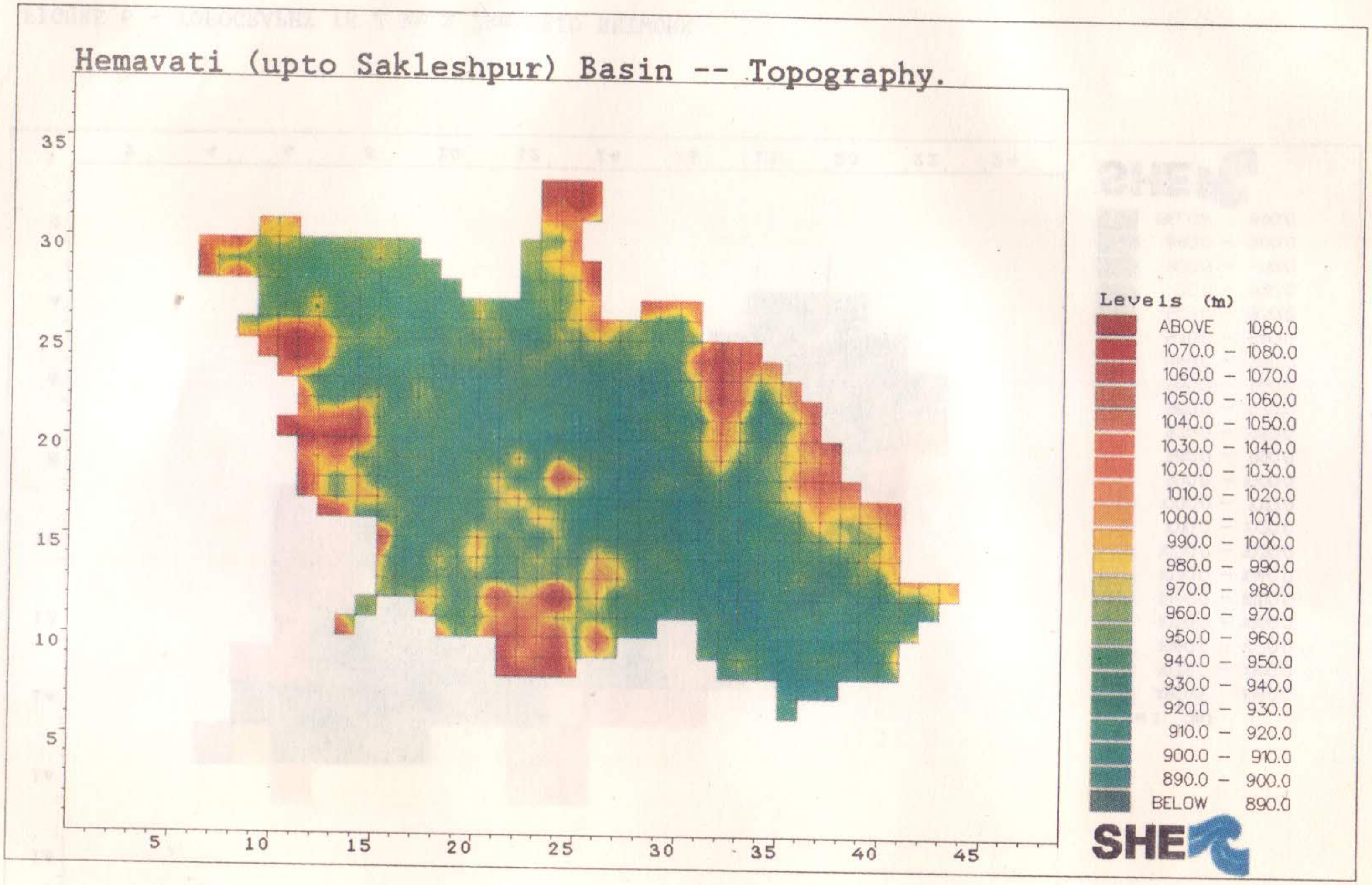

FIGURE 5 - TOPOGRAPHY IN 1 km x 1 km GRID NETWORK

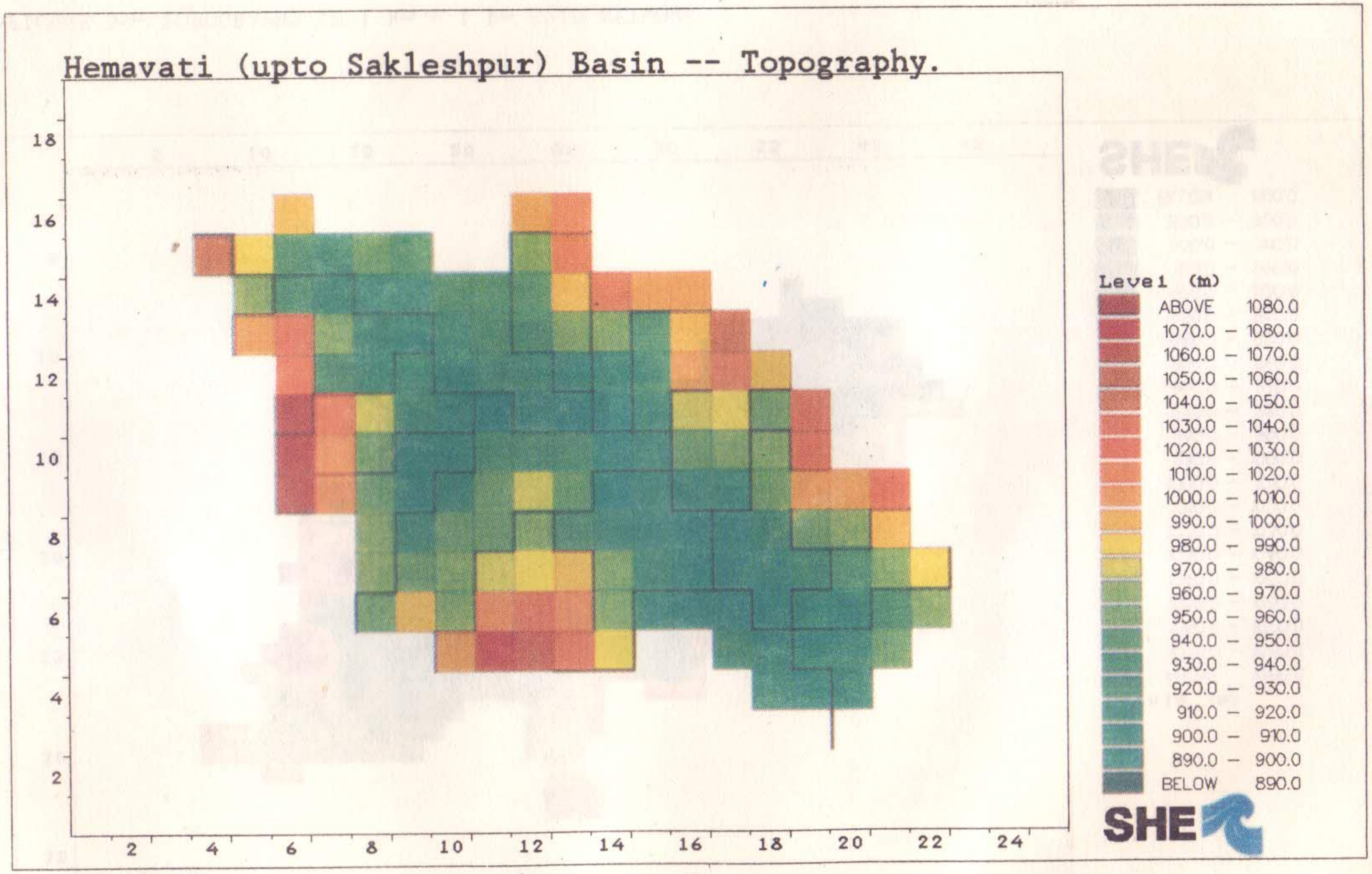

FIGURE 6 - TOPOGRAPHY IN 2 km x 2km GRID NETWORK

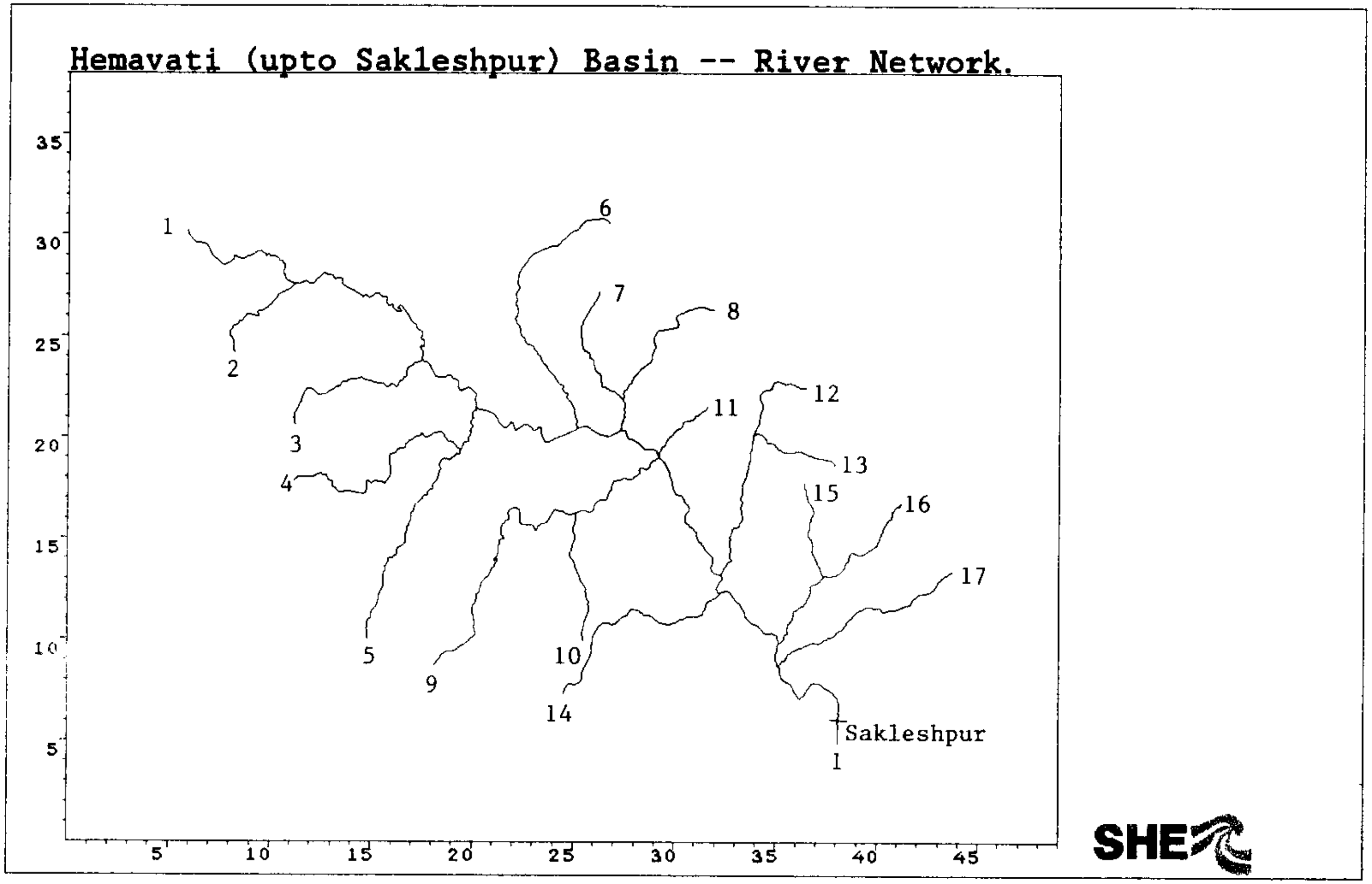

FIGURE 7 - RIVER NETWORK IN THE BASIN

Table 3 : Lengths of Streams in the Basin

Stream No.	Name	Length (km)
1.	Hemavati	55.13
2.	*	5.56
3.	Bakki Halla	9.13
4.	*	11.89
5.	*	15.63
6.	*	14.77
7.	Sunnada Halla	6.60
8.	*	9.20
9.	Japavati Hole	20.51
10.	Benagina Halla	6.78
11.	*	3.66
12.	*	12.33
13.	*	4.62
14.	Chitna Halla	11.47
15.	*	4.96
16.	Byadin Halla	10.44
17.	Kadaban Halla	10.60

* No specific names mentioned in the respective toposheets.

as prominent ridges.

The gneisses and granites are well exposed on the hillocks and valleys in all parts of the basin except in the western portion. They are characterised by medium to coarse grained texture, grey colour. They are weathered and decomposed upto 18 to 21 metres yielding white to buff coloured clay.

Land use

Agriculture and plantation are the main industries in the basin. Principal crops grown are coffee, paddy and cardamom. Coffee plantations occupy hill slopes and valleys are occupied by paddy fields. Cardamom is grown in all parts of the basin. The land use was split into the basic divisions of forests, coffee plantations and unirrigated crop land. The spatial distribution of these land uses in the basin at the 2 km x 2 km grid scale is shown in figure 8. The proportion of basin occupied by each land use is given in table 4.

Soils

The principal soil types found in the basin are red loamy soils and red sandy soils. Soils in the forest area and coffee plantations are greyish due to high humus content. Generally, red soils are less fertile. Unlike the heavy black soils, red soils do not retain moisture well and are therefore unable to sustain a good crop after the main rainy season. The normally loamy structure of the red soils or the intermixture of fine and thick particles makes them suitable for the cultivation of a larger variety of crops than the black soils.

Figure 9 presents the soil distribution in the basin at the 2 km x 2 km grid scale. The proportion of basin occupied by each soil type is given in table 5. The following soil types

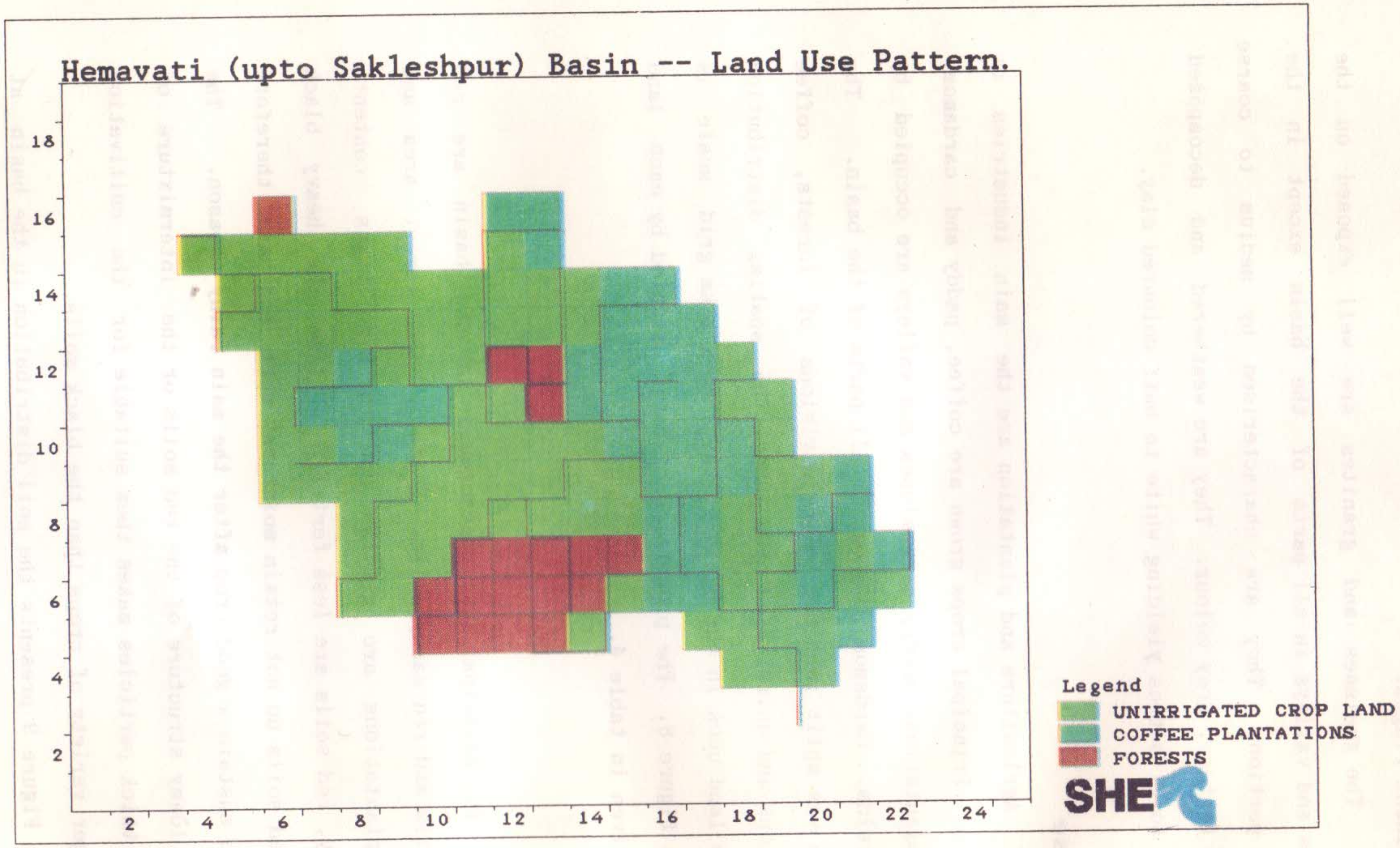

FIGURE 8 - LAND USE PATTERN IN THE BASIN

Table 4 : Land Use Pattern in the Basin

S. No.	Land Use	Area Covered (km^2)	Proportion of Basin Covered
1.	Forests	72	12.00 %
2.	Coffee Plantations	172	28.67 %
3.	Unirrigated Crop Land	356	59.33 %

Table 5 : Soil Distribution in the Basin

S. No.	Soil Type	Area Covered (km^2)	Proportion of Basin Covered
1.	Red Loamy Soils	400	66.67 %
2.	Red Sandy Soils	200	33.33 %

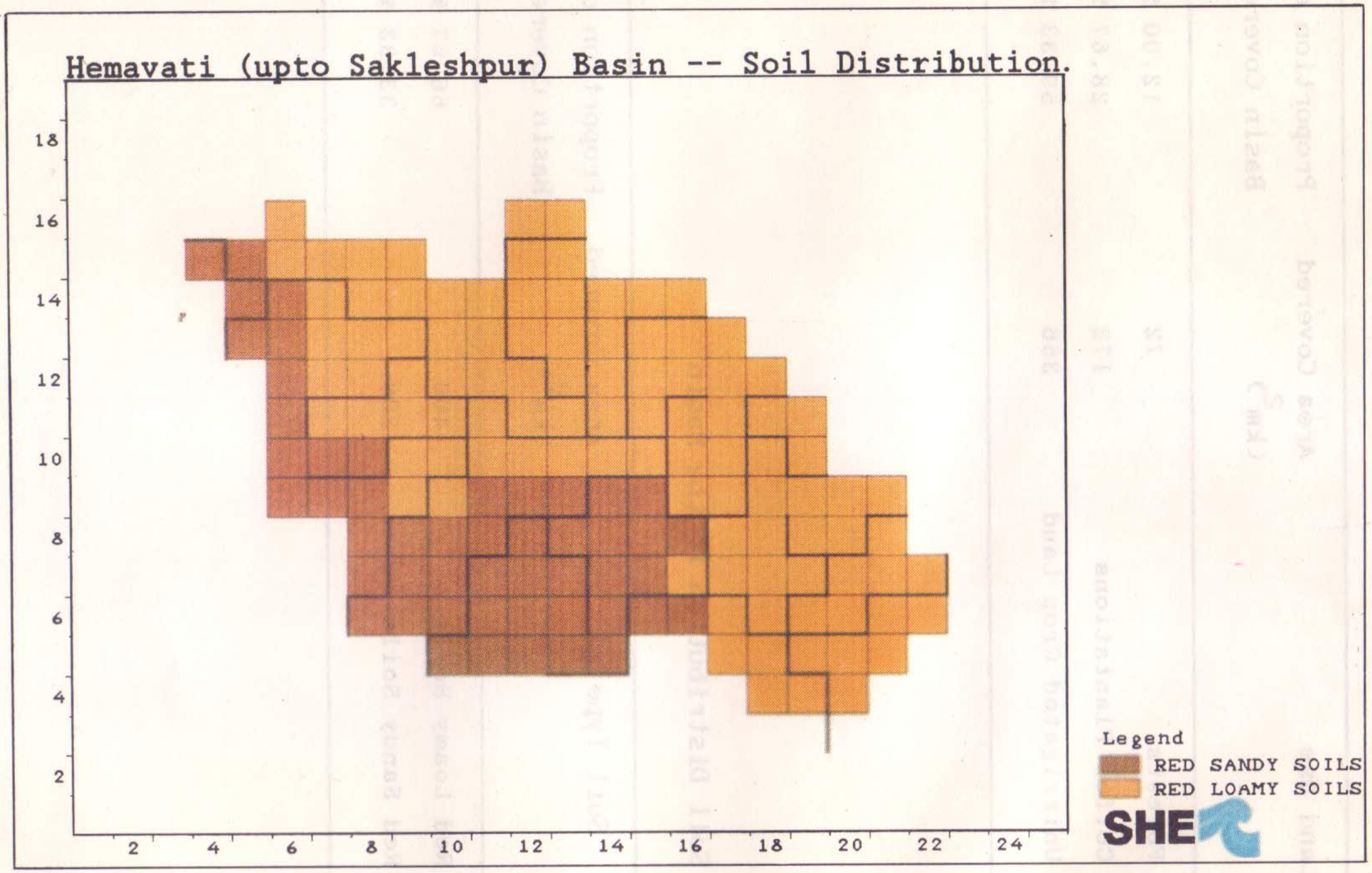

FIGURE 9 - SOIL DISTRIBUTION IN THE BASIN

(Alfisols) are found in the basin:

(a) Red Loamy Soils - Haplustalfs, Paleustalfs, Rhodustalfs

(b) Red Sandy Soils - Haplustalfs, Paleustalfs, Rhodustalfs

Soil Texture - Very fine sandy loam and loamy sand

Soil Reaction - Neutral (pH 6.5 to 7.5)

Ground water occurrence and development

Ground water occurs in the weathered rocks under water table conditions. The main source for ground water is from atmospheric precipitation and to a lesser extent through seepage of water from rivers, streams, storage tanks, canals and water used for irrigation. Depth to water table ranges from 1.5 to 18 metres depending upon the season and topographical location of wells. The diameter of dug wells ranges from 1.25 to 2.45 metres and the depth ranges from 3 to 35 metres. The fluctuation in water table between summer and monsoon ranges from 3 to 15 metres.

Because of the highly undulating character of the ground, the deep weathering resulting in heavy clay over burden, there is large fluctuation in water table. Clay being not quite permeable does not allow water to freely flow into the well. Open wells, except in the valley regions, are not likely to be successful. For any large scale development of ground water resources, deep bore wells have to be preferred. These bore wells have to pass 15 to 18 metres in the jointed hard rock to intersect satisfactory supplies.

The main source for ground water is atmospheric precipitation. No accurate data relating to surface runoff and loss due to evapotranspiration are available. Because of the continuous rains and steep slopes, a good part of the rainfall is lost through surface flow. The thick forest cover also transpires considerable quantities of water. On account of these features, it can be considered safe to assume a recharge of only 5 % of the rainfall into the ground water body. Again, much of this is lost through base flow in the months following the rainy season. This accounts for the large fluctuation in water levels between the rainy season and summer season.

Well irrigation is not practiced in the basin. The reason for this may be the assured rainfall, availability of water from perennial sources, deep-seated character of the water table, the soft clayey material encountered in well sinking requiring costly protective lining and the high fluctuation in water table. At present, agriculture is mainly rainfed. It is possible to grow more than one crop in a year through the utilization of ground water. Bore wells are to be preferred over open wells. The bore wells can be expected to yield a minimum of 65 to 75 cubic metres of water per day. Better yields can be expected by going deeper. Because of high fluctuation in water table between seasons, wells have to be sunk deeper 10 to 15 metres. Even so the recuperation is not likely to be good because of the clayey character of the weathered rock. Open wells preferably of smaller diameter 2 to 3 metres, to a depth of 10 to 13 metres, lined with concrete rings may be sunk in favourable valley regions which are expected to yield between 60 to 70 cubic metres per day.

3.4 Basin Response

A sound understanding of basin behaviour is essential for successful field application of the SHE. Using reports on the general region, the characteristic basin response was documented for use in interpreting the simulation results. For the valley lands with deep soils, the initial monsoon rains are absorbed by the soil moisture reservoir. Once this reservoir is full, further rainfall is lost as surface runoff, interflow in the upper layers of the profile or evaporation. During the dry season, moisture in the root zone is lost through evapotranspiration while the deeper ground water reservoir drains slowly, contributing to deep storage or river base flow. Less is known about the hydrology of the hill ranges with shallow soils. However, runoff is likely to be relatively rapid because of the thin soils, steep slopes and greater prevalence of small channels.

3.5 Data Availability

The SHE simulates all the major aspects of the land phase of the hydrological cycle. Consequently its application requires the evaluation of a large number of parameters and their spatial distributions, along with the necessary time series of data for calibration, validation and operation of the model.

A data assembly programme was carried out to provide the hydrometeorological data and basin parameters (e.g. soil, vegetation and topographic characteristics) needed to support SHE simulations of the basin. Collection of the data involved visiting a number of different offices in Karnataka, photocopying the data sheets and finally transferring the data onto the computer files. Data were assembled for the period 1975-81. It was not expected that the full range of requirements would be satisfied by the available data. The data base for the basin is presented in table 6. Comments on the individual items are as follows:

Rainfall

There are five raingauge stations in the basin situated at Mudigere, Kotigehara, Sakleshpur, Hanbal and Arehalli. The available periods of record for each raingauge are shown in table 6. The area represented by each raingauge station are shown in figure 10. These raingauge stations provide representative

Table 6 : Data Availability for the Hemavati (upto Sakleshpur) Basin

Data Type	Data Availability
Rainfall	**Daily**
	Mudigere : June 1975 - May 1981
	Kotigehara: June 1975 - May 1981
	Sakleshpur: June 1975 - May 1981
	Hanbal : June 1975 - May 1981
	Arehalli : June 1975 - May 1981
	Hourly
	Mudigere : 1975 (June - December)
	1976 (January, February, April-July, December)
	1977 (January, February, June-October, December)
	1978 (January - December)
	1979 (January - December)
	1980 (January - December)
	1981 (January - May)
	Kotigehara: 1975 (September-November)
	1976 (January, February, April, June, August, September, November, December)
	1977 (January, June-December)
	1978 (January-December)
	1979 (January-December)
	1980 (April-December)
	1981 (January-May)
Discharge	Gauge and discharge data
	Sakleshpur (outlet): June 1975 - May 1981 (2 to 5 times a day)
Evaporation	Daily pan evaporation data
	Banbalore*: March 1975 - August 1977
	Gorur* : September 1977 - May 1981
Channel Cross-section	Plan and longitudinal section of dam at Gorur*
Rating Curves	Depth-discharge curve table for river Hemavati at Sakleshpur, based upon the data of 1971-73
Ground Water Level Observations	Monthly ground water level observations
	Mudigere : March 1975 - May 1981
	Kotigehara: March 1975 - May 1981
	Sakleshpur: March 1975 - May 1981
	Arehalli : March 1975 - May 1981

*lies outside the basin.

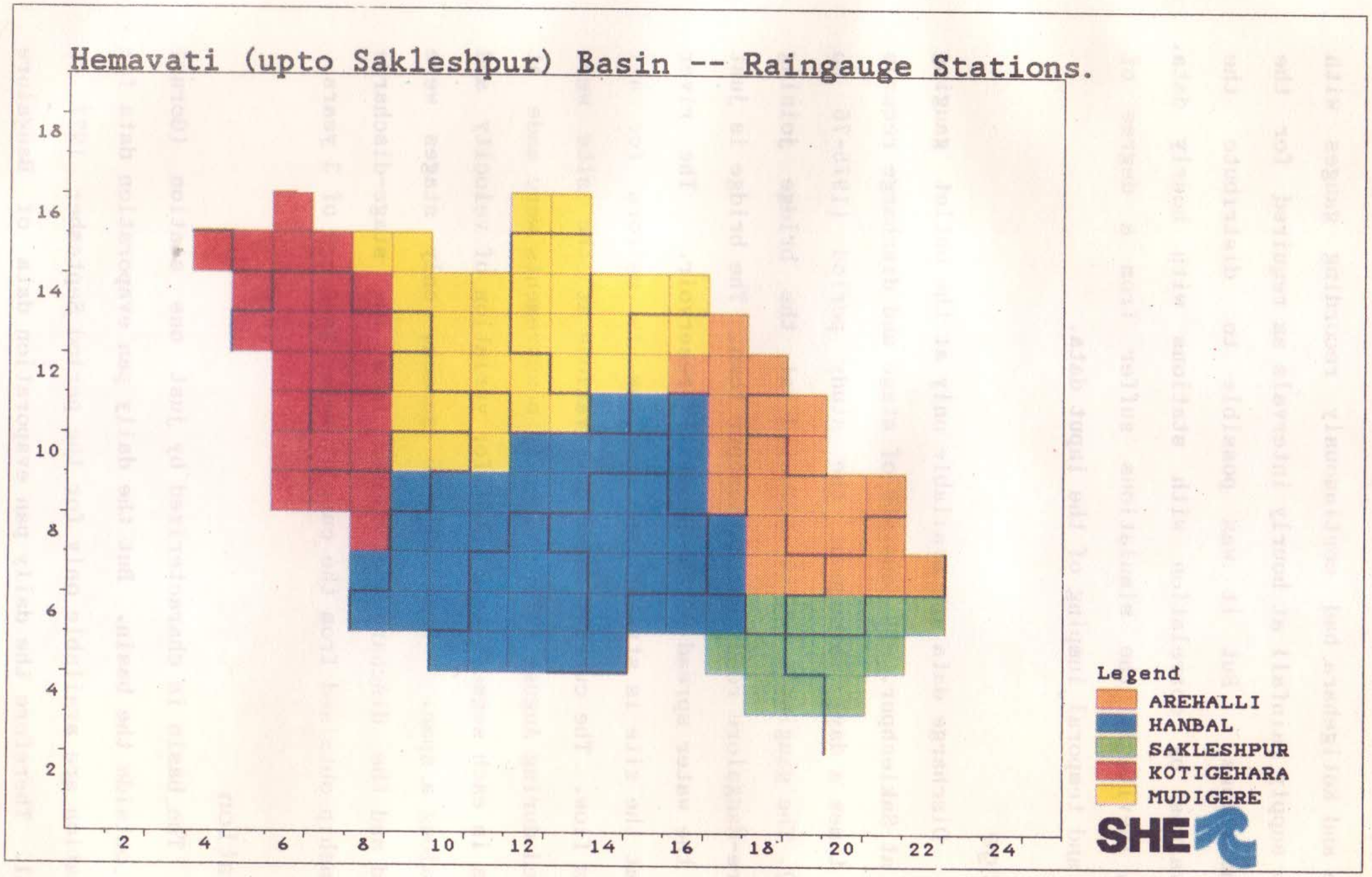

FIGURE 10 - THIESSEN POLYGONS OF RAINGAUGE STATIONS

coverage of spatial variability throughout the basin. However Sakleshpur, Hanbal and Arehalli recorded daily rainfall only. Mudigere and Kotigehara had continuously recording gauges with which to supply rainfall at hourly intervals as required for the SHE simulations. But it was possible to distribute the daily values by correlation with stations with hourly data. However, inevitably the simulations suffer from a degree of spatial and temporal lumping of the input data.

Discharge

Discharge data are available only at the outlet gauging station at Sakleshpur. It consists of stage and discharge records (2 to 5 times a day) throughout the study period (1975-76 to 1980-81). The gauging site is situated at the bridge joining Bangalore-Mangalore road near Sakleshpur town. The bridge is just outside the water spread of the Hemavati reservoir. The river course at the site is straight and the flow is uniform for all depths of flow. The current meter observations at the site were commenced during August 1971. Velocity measurements were made at 3 places in each segment to account for variation of velocity and depths along a span. From 1974-75 season, only stages were observed and the discharges computed from the stage-discharge relationship obtained from the current meter gaugings of 3 years.

Evaporation

The basin is characterized by just one station (Gorur) located outside the basin. But the daily pan evaporation data for this station are available only for the period September 1977 to May 1981. Therefore the daily pan evaporation data of Bangalore was used for the remaining study period i.e. March 1975 to August 1977. Evaporation tends to be more spatially uniform than does rainfall (at least over periods of a week or more) but even so it is likely that the spatial lumping involves some error.

Topography

In all cases land and channel elevations in the basin were taken from the following toposheets issued bythe Survey of India:

Scale	Toposheet No.
1:250,000	48O, 48P
1: 50,000	48O/8, 12, 16
	48 P/9, 13

Land use

The land use in the basin was obtained from 1:1,000,000 scale map in the 'Agricultural Atlas of India'. The general distribution of major land uses (forests, coffee plantations and unirrigated crop land) is presented in figure 8.

Soil distribution

The soil distribution in the basin was obtained from 1:2,000,000 scale map in the 'Agricultural Atlas of India'. Figure 9 presents the distribution of soil types (red loamy soils and red sandy soils) in the basin.

Soil and vegetation properties

There is a general lack of direct informationon soil hydraulic dsproperties (saturated condutivity, retention curve and related information), depth to bed rock, vegetation properties, root depths, vegetation growth and cropping pattern for the basin. Consequently the necessaryinformationwas provided indirectly from reports and papers on neighbouring areas.

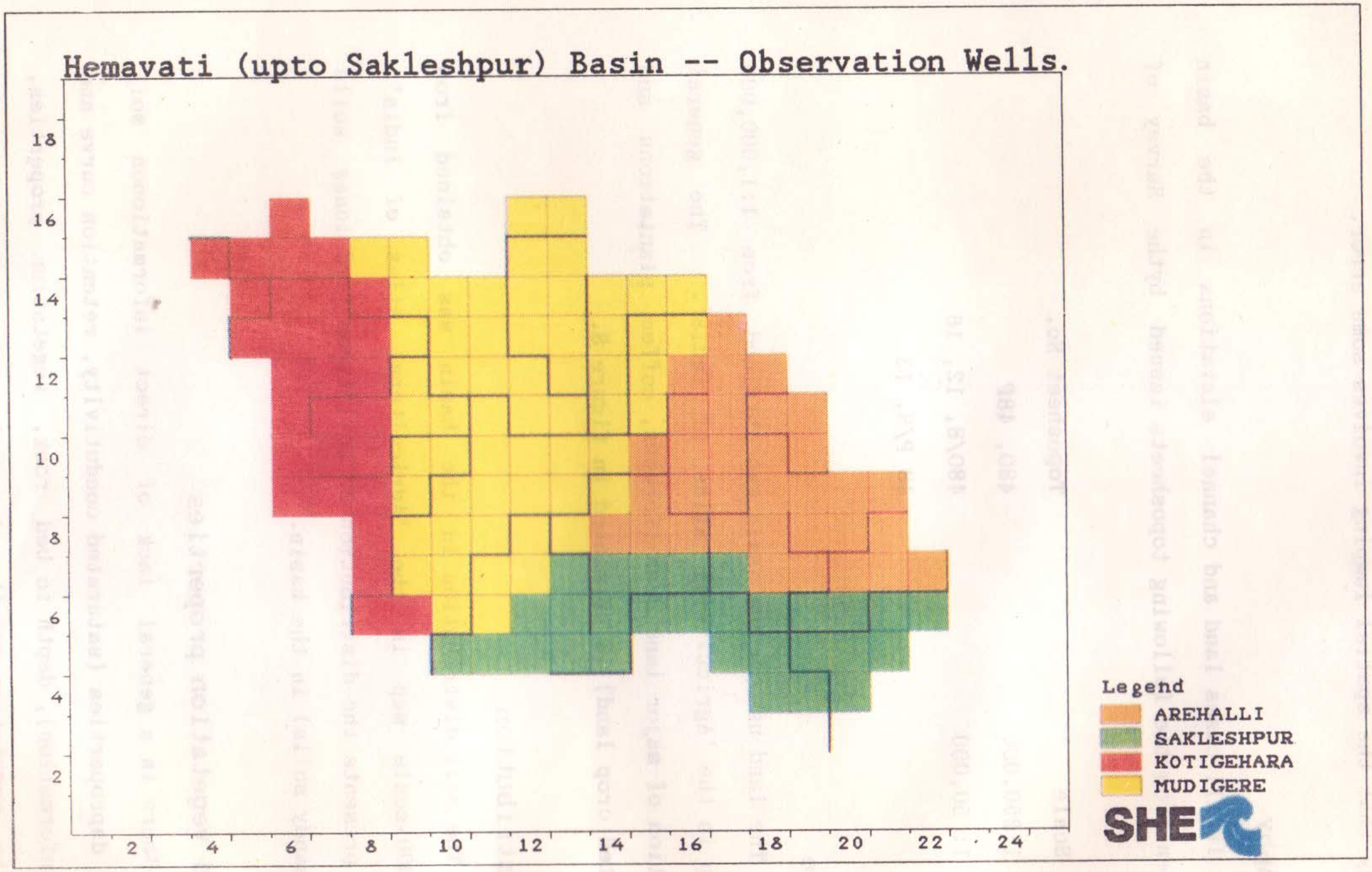

FIGURE 11 - THIESSEN POLYGONS OF GROUND WATER OBSERVATION WELLS

Channel cross-section

Cross-sectional dimensions are available only at the composite dam site (outside the basin) at a distance of 24 km from Hassan. The dimensions for the system were therefore estimated byscaling according to the upstreamchannellengths and using the empirical relationships for bed width, top width and bankfull depth.

Ground water observations

There are four observation wells in the basin situated at Mudigere, Kotigehara,Sakleshpur and Arehalli and maintained by the Department of Mines and Geology (Ground Water and Minerals) of Karnataka state. The available periods of record for each observation well are shown in table 6. The network of observation wells in the basin is presented in figure 11.

4.0 DATA PROCESSING AND PREPARATIONS

4.1 General

In every application of the SHE, a large amount of data (temporally and spatially distributed) are both required and produced. A suite of auxiliary routines is available for filling in data files and displaying these and the SHE results in a convenient way. The organization of the data files and the data flow between the various auxiliary routines in the SHE software package is illustrated in figure 12. The data input necessary to run SHE successfully can be divided into four categories:

i. Program organizational data

ii. Catchment organizational data

iii. Physical characteristic data

iv. Meteorological data.

The first three types of data are read in during the initialization phase while the meteorological data are read currently during the simulation phase. The major part of the program organizational data are read from the FRAME component. This includes information about organization and operation of the simulation e.g. length of simulation, grid square setup and times at which data should be stored or printed. Codes describing the soil and vegetation type distribution, and rainfall and meteorological station network are also read from FRAME. The distributions are presented as an array of codes, allocated to each grid square. A code number signifies a particular characteristic. The physical data associated to these characteristics are read from the different process components where the data are used. The data inputs needed are stored on several of the following data files:

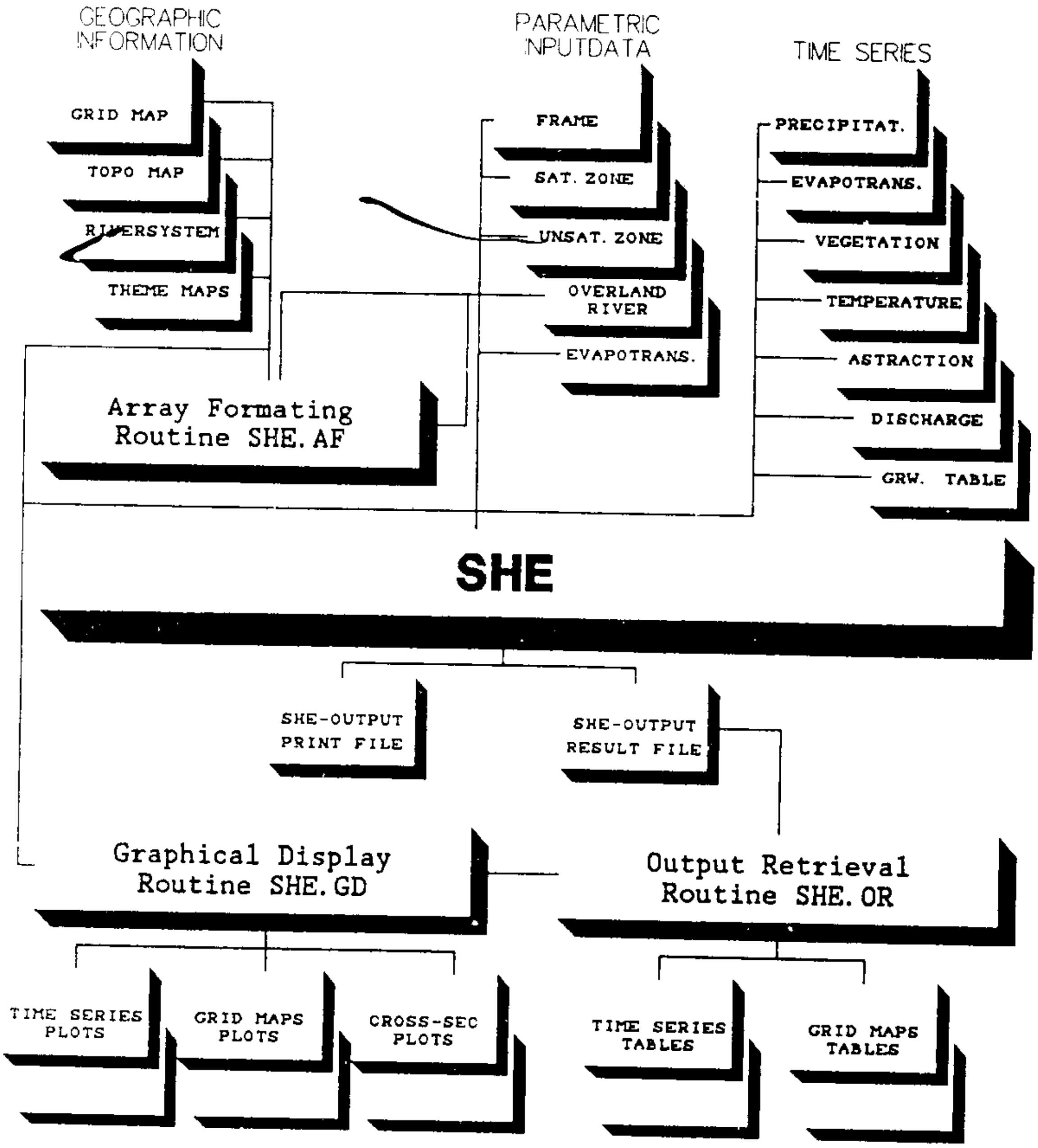

FIGURE 12 - FLOW CHART OF THE SHE PROGRAM PACKAGE

1.	HEMA.FRD	Frame
2.	HEMA.ETD	Interception/Evapotranspiration
3.	HEMA.OCD	Overland and Channel Flow
4.	HEMA.UZD	Unsaturated Zone
5.	HEMA.SZD	Saturated Zone
6.	HEMA.SMD	Snowmelt
7.	HEMA.MED	Meteorological data
8.	HEMA.PRD	Rainfall data
9.	HEMA.EPD	Potential Evaporation data
10.	HEMA.VED	Root Depth and Leaf Area Index data
11.	HEMA.TED	Temperature data
12.	HEMA.EXD	Ground Water Abstraction Rates
13.	HEMA.QOD	Observed Discharge data
14.	HEMA.POD	Observed Ground Water Heads.

Here 'HEMA' is the mnemonic name defining the specific simulation project (Hemavati). Each of the first six mentioned files contains parametric data. The eight last data files contain time series data. A major part of the data (maps, codes etc.) in the input files, are generated by employing the SHE Array Formating Routine SHE.AF. It is recommended to be careful when preparing the data card files and checks that the data read by the program are correct. This will save time. Wrong data may not only cause 'blow up', but perhaps unintentional simulation results, which may be difficult to trace back to the input data files.

4.2 Data Handling Procedures

The current trend in the SHE applications, where progressively larger amounts of data are being processed, has called for a powerful data handling package. The package attached to the SHE comprises of SHE Array Formating Routine (SHE.AF), SHE Output Retrieval Routine (SHE.OR), and SHE Graphical Display Routine (SHE.GD).

4.2.1 SHE Array Formating Routine

SHE requires a huge amount of spatial distributed data, concerning e.g. catchment geometry, hydrogeology, land use pattern and meteorological station networks. It is therefore, a very time consuming and tedious process to prepare the input files for SHE in the particular format required. Especially, the river system setup requires a vast number of data information concerning levels and cross-sections at each link in the computational grid square network to which the river system is approximated The data are often available on maps of different scales. It is therefore, convenient to provide the data on the scales available and then automatically setup the spatially distributed data on the scale, which has been selected for the numerical computation.

The SHE Array Formating Routine (SHE.AF) has been developed in order to facilitate the data preparation. By applying SHE.AF the entire data preparation can be finalized within short time for grid systems comprising of several thousands squares. SHE.AF is a very powerful tool in connection with digitization of the spatial data. The routine constructs the SHE input files and sets up automatically a river network in the scale chosen.

The SHE.AF reads a series of data files containing various arrays of spatial distributed data, transforms these data to an appropriate format and includes them in the existing SHE input files. The array data files may have various forms, as shown in figure 12. The Data Identification Code (DIC) is used by SHE.AF to identify the form of the data in the file and which type of processing is required.

The grid identification code determines the degree of discretization (sizes of grid squares) to be used in the SHE application. All other data can be given with both a coarser and a finer discretization than the grid identification code. In case of uniform distributed data, one single default value can be applied for a series of the data. A brief description of various data files is given below.

i. Grid code data files

- assigns the grid codes inside and outside the model area.

ii. Point data data files

- point data such as topographical data etc. given as point values for the catchment.

iii. Grid averaged data data files

These data files can be prepared either directly from the SHE input files or prepared through the SHE Output Retrieval Routine SHE.OR. The latter is particularly useful, if e.g. the elevation of the ground water table calculated in a SHE simulation is used as initial conditions in a new SHE simulation.

iv. River setup data files

The computational river node system can be established by use of the SHE.AF. The following data are required:

- A series of data points given as coordinates.
- Bank levels at a series of points along the river system. A value at each end of a river section is obligatory.
- A table defining the cross-section at each end of a river section.

The river system is divided into a series of sections. For each section an array of points can be defined. The numbering should be given in increasing order in the upstream direction, starting with the main river, and each river section is finalized at one time. A point should always be given at the outlet of a tributary. This point is then starting point for that particular tributary. The SHE.AF calculates the cross-section for each link by linear interpolation between the two cross-sections in each river section. The river setup comprises a setup of the following files:

RIVER.DIG	digitized river system,
RIVER.NUMB	connections of river system,
RIVER.CROSS	cross-sections for actual river section,
RIVER.BOU	boundaries for river, and
RIVER.QST	defines the position of discharge stations, used to specify corresponding link.

After preparation of the required data files, the SHE input files are established by running the SHE.AF Routine in an interactive mode. SHE.AF requires a set of existing SHE input files (HEMA.FRD, HEMA.OCD, HEMA.SZD, HEMA.UZD), which are read and stored again with the appropriate new data arrays. Table 7 shows a sample of data requirements for SHE.AF. Zero is used for no setup for actual SHE component and a default value indicates that uniform grid is prepared (a negative default value indicates a distance below ground surface).

It is recommended to run the SHE only a few time steps after having prepared the SHE data files. This serves to check the river system setup. In some cases, the interpolated river bank elevations become higher than the ground surface elevations of the adjacent grid squares. In these cases, a warning message is given

Table 7 : Data Requirements for SHE.AF (SETUP.2000)

TOPIC	DATA FILE
1. Frame ********	
FRD , Filename	HEMA.FRD
GRID , Filename	[.MAPS]GRID.2000
TOPO , Filename	[.MAPS]TOPO104.2000
IMP. , Filename	[.MAPS]IMP.2000
MET. , Filename	1
PREC., Filename	[.MAPS]PRECIP.2000
VEG. , Filename	[.MAPS]LAND.2000
SOIL1, Filename	1
SOIL2, Filename	1
2. OC *************	
OCD , Filename	HEMA.OCD
CATR , Filename	1.0
HRI , Filename	[.MAPS]TOPO104.2000
DET , Filename	0.01
RIVER.DIG	[.MAPS]RIVER.DIG
RIVER.NUMB	[.MAPS]RIVER.NUMB
RIVER.CROSS	[.MAPS]RIVER.CROSS
RIVER.BOU	0
RIVER.QST	0
3. SZ *************	
SZD , Filename	HEMA.SZD
SZD , Nlay	0
SZD , CON	10.0
SZD , HSZO	[.MAPS]HSZO.2000
SZD , HBOU	0
SZD , QBOU	0
SZD , ZDR	-1.00
SZD , CDR	0.01
4. UZ *************	
UZD , Filename	HEMA.UZD
UZD , Filename	0

by the OC component and corrections in the river setup data files are required. The SHE.AF can then be executed again. The SHE output print file contains various results and warning and error messages. Stored results may be retrieved and presented by applying the routines SHE.OR and SHE.GD.

4.2.2 SHE Output Retrieval Routine

The purpose of the SHE Output Retrieval Routine, SHE.OR is to retrieve data stored on the SHE result file HEMA.RES for presentation. The HEMA.RES file is binary and the output data from SHE are stored as single values or arrays with one record for each data type. It is only possible to retrieve data from SHE result file, if specified in the SHE frame file, that the data type should be stored in the result file. The user types SHE.OR on the home data directory and a suite of questions appears on the screen. Data can be retrieved as a time series for a specified period or as a map at a fixed time.

4.2.3 SHE Graphical Display Routine

The SHE Graphical Display Routine, SHE.GD can be applied either for display of SHE results which are retrieved by applying the SHE.OR or directly be applied for display of in data to the SHE. In case SHE results are plotted, the concerned data should be stored temporarily after retrieval on a data file, which then is read by SHE.GD. Three different types of data can be presented - time series data, grid data and cross-section data. The graphical routines are written in FORTRAN and uses the UNIRAS-software plotting routines. Some of the plots can be produced in colours. The SHE.GD can run interactively by typing SHE.GD and uses the SHE-standard data format.

4.3 Data Processing

All the data processing, including transfer of the rainfall, discharge and evaporation records to computer files, detailed evaluation of the hydrometeorological records and other data records assembled and corrections for errors and incompatibilities, digitization of the river system etc., were carried out prior to model setup and simulation work. A large number of reports were referred for obtaining the relevant information on basin properties. Details of individual items are given below.

Rainfall

The rainfall data of different stations reveal that rainfall goes on decreasing from Kotigehara in the west to Arehalli in the east. Thus the rainfall over the basin is not uniformly distributed. The bulk of the rainfall is received during the months of June to August. Significant rainfall also occurs during the months of May, September and October.

Missing hourly records were filled up by using the corresponding daily rainfall records, based upon the following criteria:

i. If rainfall in a day is less than 1.2 mm, assume it as a single total value in the 18th hour (i.e. 1.30 AM to 2.30 AM).

ii. If rainfall in a day is greater than 1.2 mm, distribute it uniformly over 24 hours.

The daily rainfall records were distributed on an hourly basis according to the patterns measured at the Mudigere recording gauge. Distribution of domains for each rainfall station was based on Thiessen polygon approach. Correlation between the rainfall patterns throughout the basin is by no means assured, so this method of distributing rainfall temporally forms a considerable source of uncertainty in the inputs. This uncertainty is further exacerbated by the infilling necessary to close gaps in the measured time series.

Thiessen weights and area represented by each raingauge station are shown in table 8. The variations of mean rainfall over the basin are presented in figures 13 and 14 for the period 1975 to 1980 (monsoon seasons).

Table 8 : Thiessen Weights of Raingauge Stations

S.No.	Raingauge Station	Thiessen Weight	Area Represented (km^2)
1.	Mudigere	0.247	148.20
2.	Kotigehara	0.173	103.80
3.	Sakleshpur	0.087	52.20
4.	Hanbal	0.333	199.80
5.	Arehalli	0.160	96.00
	Total	1.000	600.00

Discharge

The discharge values for the outlet (Sakleshpur) were obtained from the measured stage values (2 to 5 times a day) for the study period (1975-76 to 1980-81). The rating curve was that derived by the Major Irrigation Investigation Division, Hassan based upon the measured stage and discharge data for the period 1971-72 to 1973-74. Errors in using the curve arise from its derivation, as a power law, from arithmetically averaged data and from its presentation as a single valued function which does not allow for event and seasonal hysteresis effects. Typical monsoon peak discharges for the simulation period are upto 1390 cumecs at

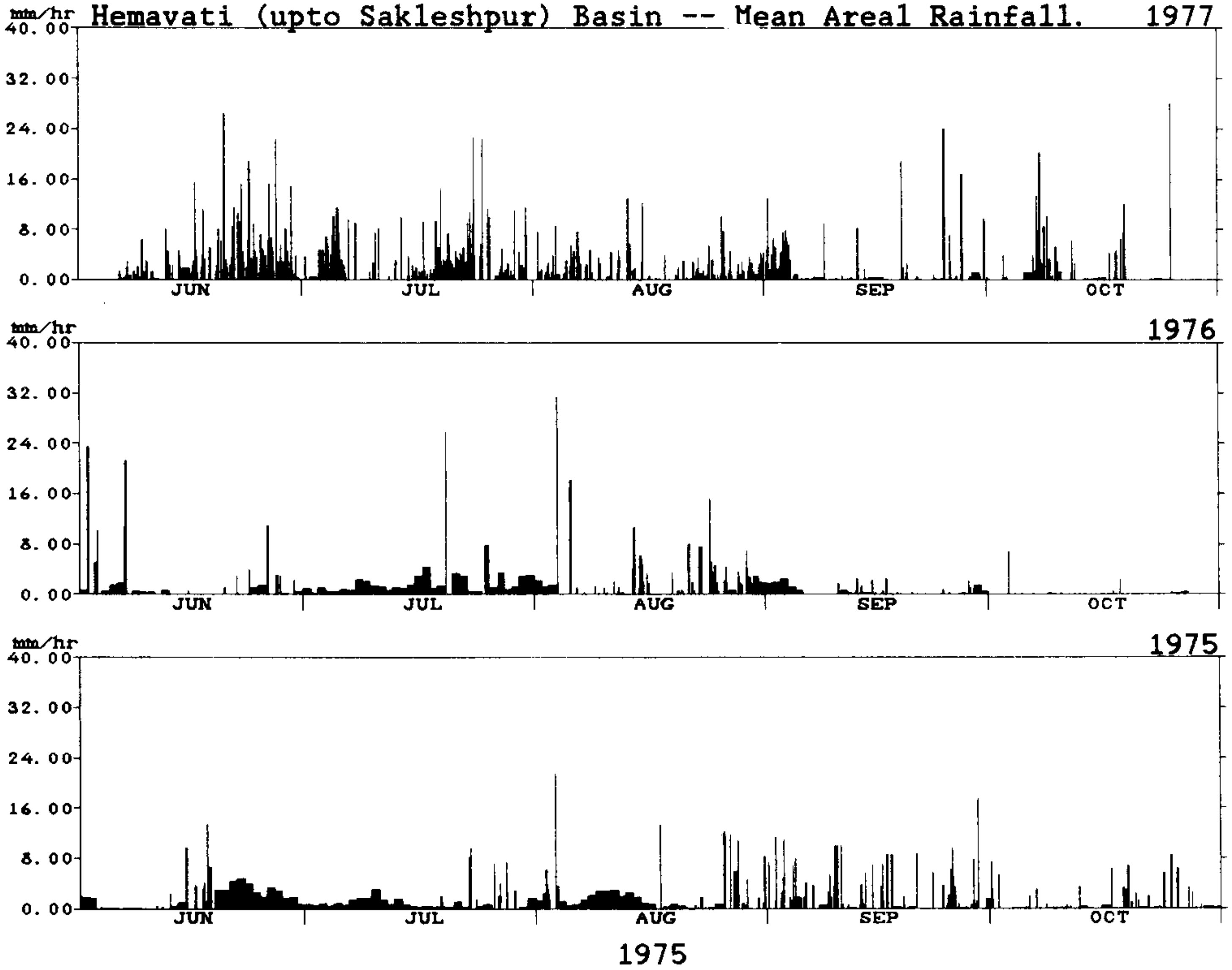

FIGURE 13- VARIATION OF MEAN RAINFALL OVER THE BASIN FOR THE PERIOD 1975-77(MONSOON SEASONS)

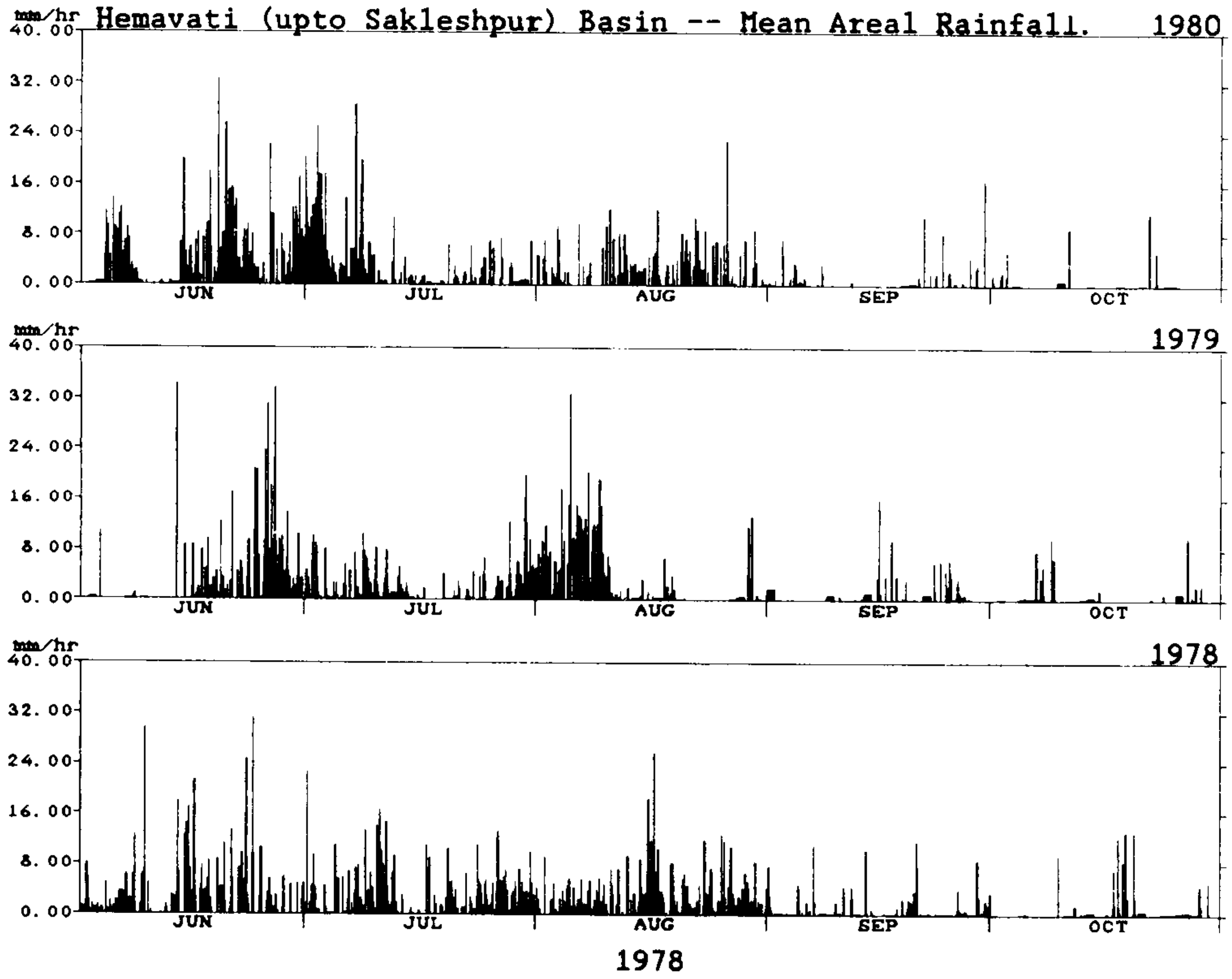

FIGURE 14 - VARIATION OF MEAN RAINFALL OVER THE BASIN FOR THE PERIOD 1978-80(MONSOON SEASONS)

the Sakleshpur gauging site. Figures 15 and 16 present the observed hydrographs at Sakleshpur for the period 1975-76 to 1980-81.

Evaporation

Potential evaporation was assumed to be given by the pan evaporation data of Bangalore (March 1975 to August 1977) and Gorur (September 1977 to May 1981), multiplied by a factor (0.7) and to apply uniformly in the basin. The provision of hourly evaporation rates from the daily records involves considerable temporal lumping. Figures 17 and 18 present the variations of potential evaporation for the period 1975-76 to 1980-81.

A summary of the observed monthly areal mean rainfall, discharge and potential evaporation values is presented in table 9.

River system

The basin boundary and river system were digitized from the topographical maps (scale 1:50,000) and by making use of 'DIGTOSHE' (a SHE-related service program), data were written in SHE format on the following files:

GRID.DIG	basin boundary,
RIVER.DIG	river system.

Figures 19 and 20 show the digitized boundary and digitized river system respectively.

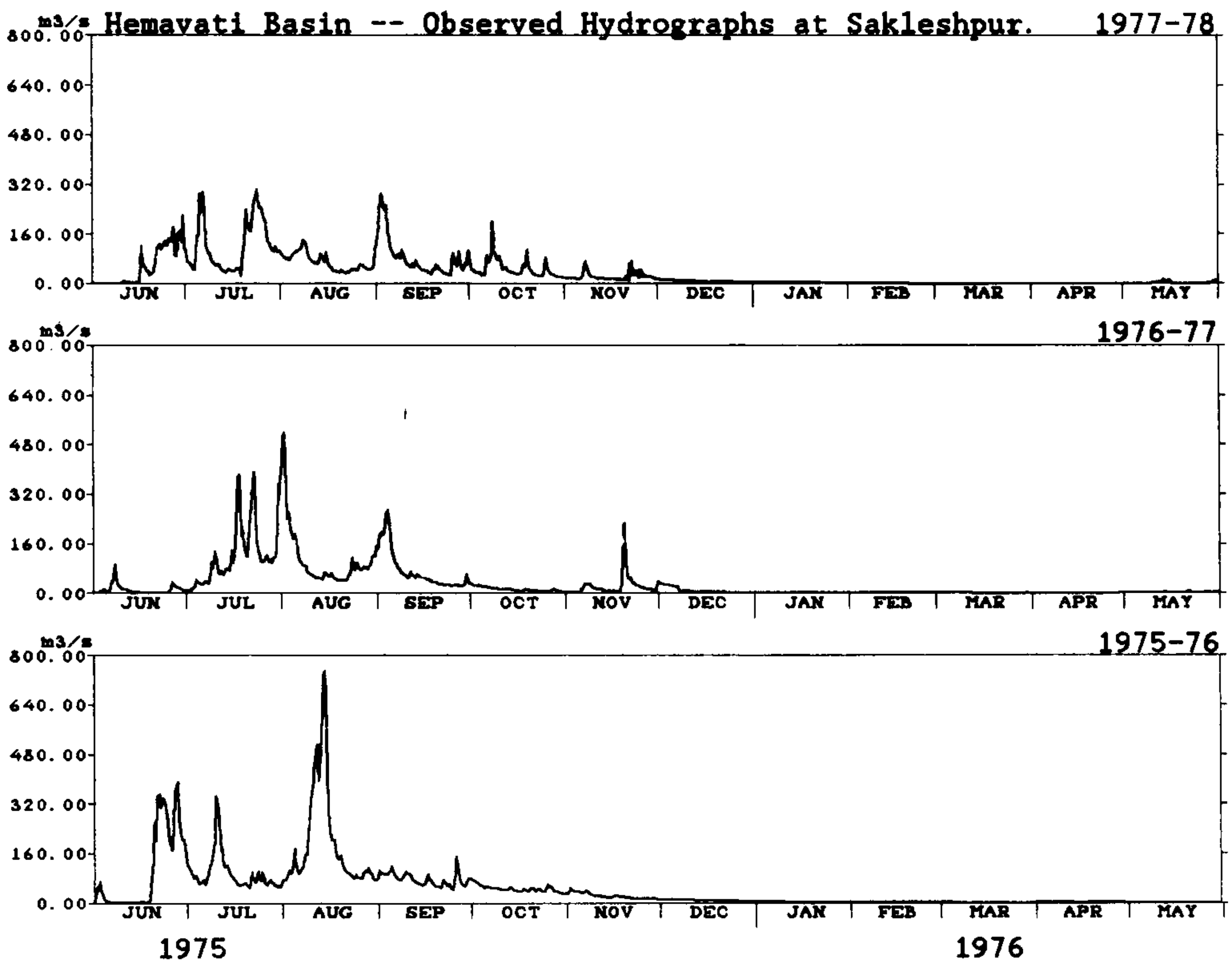

FIGURE 15 - OBSERVED HYDROGRAPHS AT THE SAKLESHPUR GAUGING SITE FOR THE PERIOD 1975-76 TO 1977-78

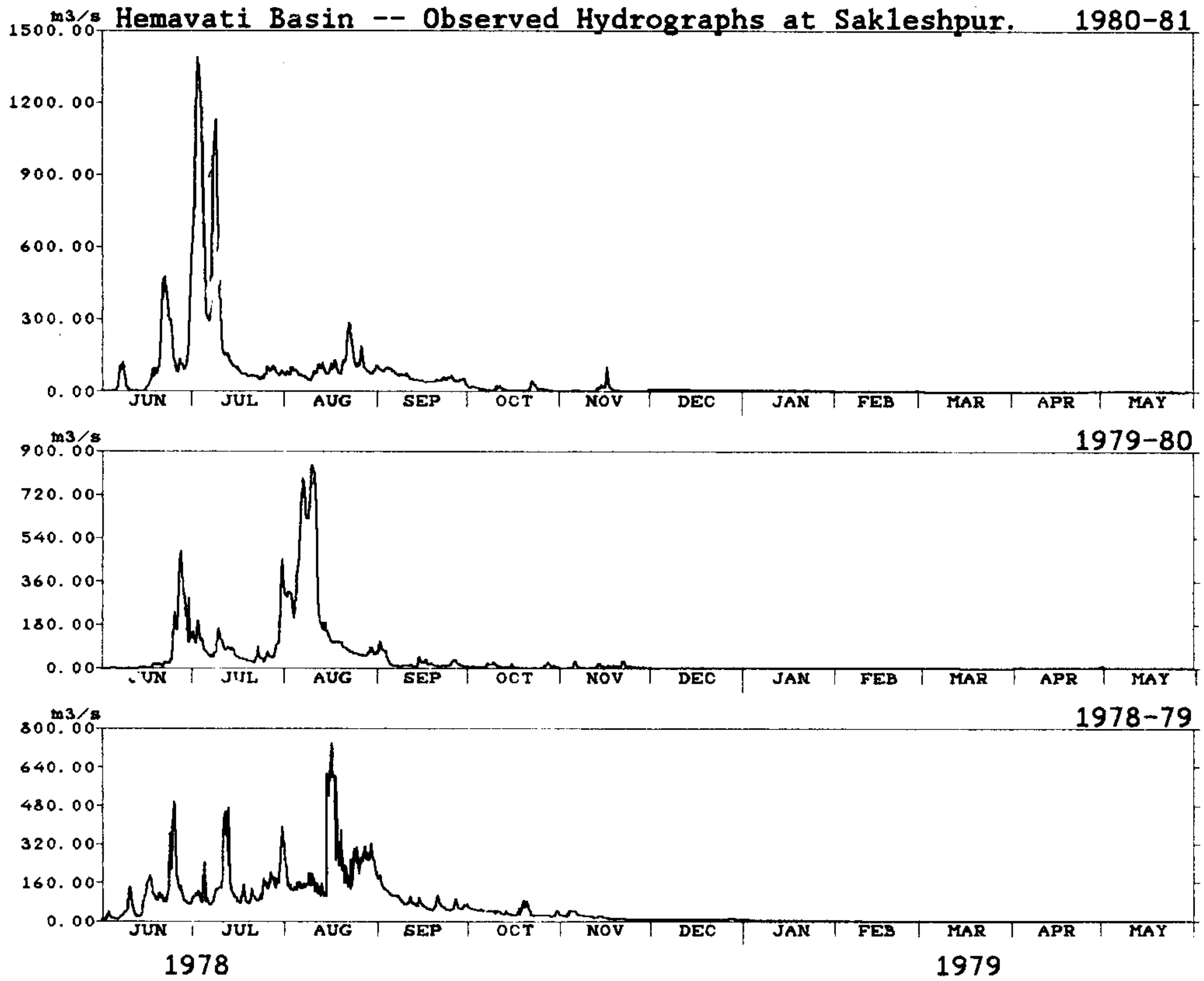

FIGURE 16 - OBSERVED HYDROGRAPHS AT THE SAKLESHPUR GAUGING SITE FOR THE PERIOD 1978-79 TO 1980-81

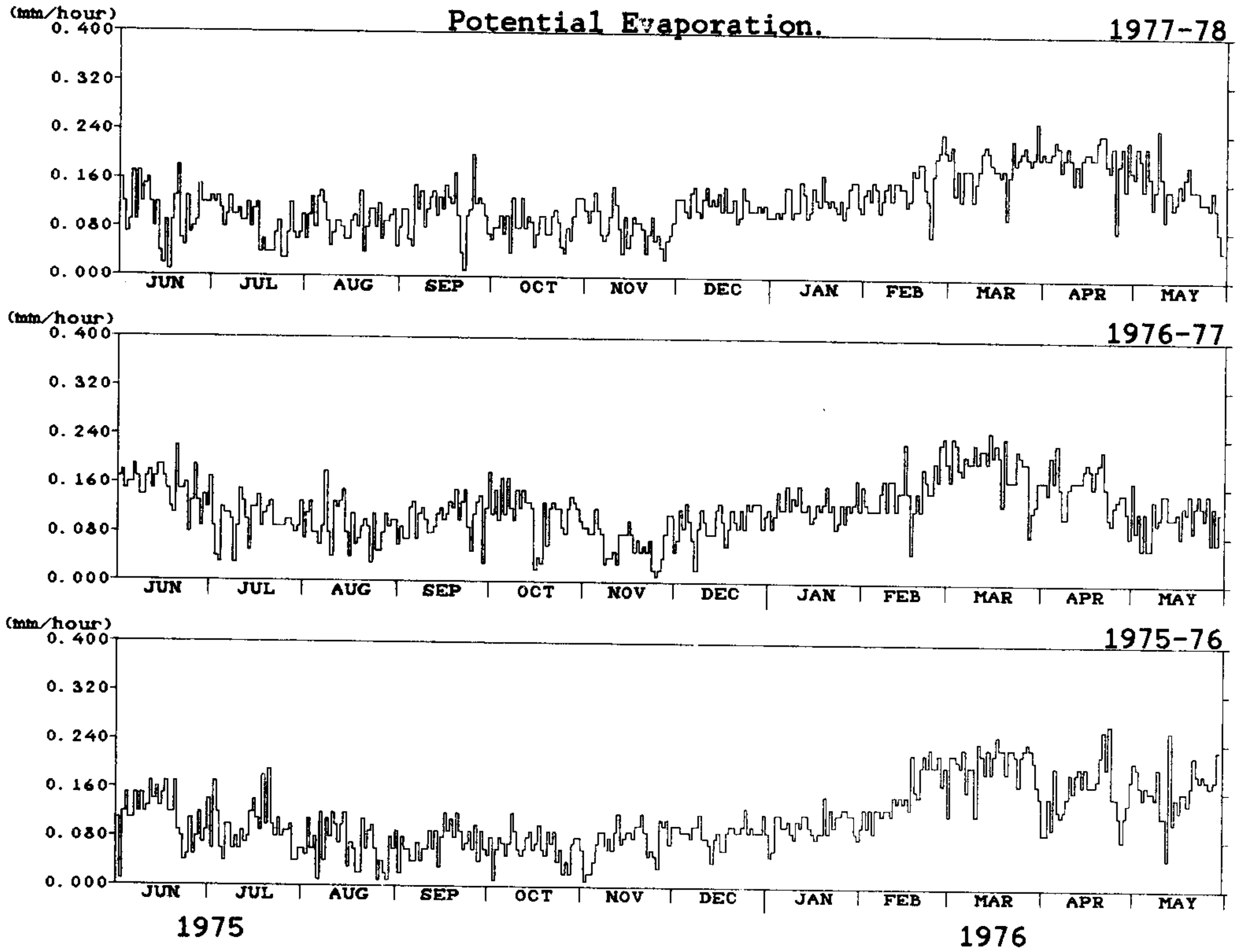

FIGURE 17 - VARIATION OF POTENTIAL EVAPORATION FOR THE PERIOD 1975-76 TO 1977-78

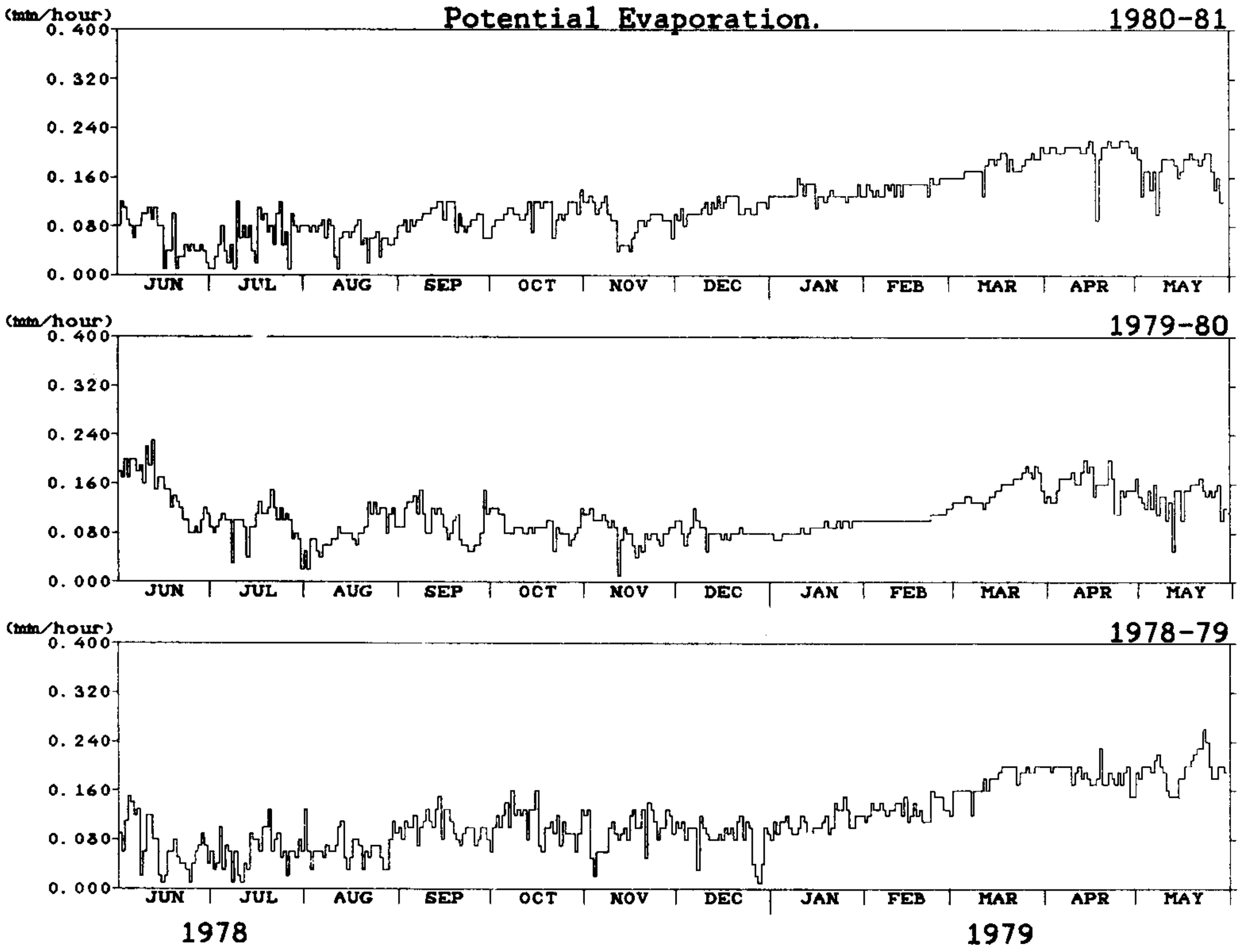

FIGURE 18 - VARIATION OF POTENTIAL EVAPORATION FOR THE PERIOD 1978-79 TO 1980-81

Table 9 : Observed Monthly Rainfall, Discharge and Potential Evaporation

Year	Month	Areal Mean Rainfall (mm)	Discharge at Sakleshpur (outlet)(mm)	Potential Evaporation (mm)
1975-76	June	978.77	467.04	81.36
	July	561.17	430.08	70.80
	August	752.34	870.22	49.68
	September	314.53	336.06	51.60
	October	116.74	208.94	48.48
	November	80.95	102.07	53.04
	December	0.00	49.30	67.44
	January	0.00	25.49	76.80
	February	0.00	15.06	108.96
	March	30.26	13.41	152.88
	April	69.93	15.06	116.40
	May	29.92	11.94	125.52
1976-77	June	373.15	58.14	110.88
	July	1041.61	584.53	74.40
	August	459.21	480.97	67.44
	September	281.46	318.50	73.92
	October	31.20	66.17	85.44
	November	208.35	106.64	47.52
	December	2.61	46.65	73.44
	January	0.00	15.92	93.12
	February	3.20	11.30	102.96
	March	8.73	9.84	144.00
	April	78.28	8.97	115.44
	May	153.87	17.28	85.44
1977-78	June	681.84	241.21	76.08
	July	706.80	560.48	63.60
	August	312.95	318.49	67.20
	September	353.76	367.64	78.72
	October	253.79	228.63	64.80
	November	130.76	106.91	59.28
	December	0.00	43.22	90.00
	January	0.00	20.62	93.12
	February	1.06	6.36	105.36
	March	6.63	3.30	138.96
	April	76.69	2.36	142.80
	May	173.52	12.07	110.40

1978-79	June	762.02	427.33	49.68
	July	748.52	681.38	44.88
	August	847.16	1090.19	48.48
	September	202.39	365.93	72.48
	October	154.24	177.75	78.72
	November	55.22	82.54	68.16
	December	26.13	40.81	63.36
	January	0.00	25.26	80.88
	February	16.03	13.67	87.60
	March	10.16	11.41	131.52
	April	45.53	7.37	133.92
	May	60.83	6.28	146.40
1979-80	June	790.83	270.21	106.80
	July	600.22	405.10	70.32
	August	877.52	1125.09	60.72
	September	216.62	109.41	69.36
	October	150.03	42.64	66.72
	November	167.43	39.30	58.80
	December	0.00	15.14	61.20
	January	0.00	10.96	65.28
	February	0.00	15.56	71.76
	March	30.92	7.77	112.08
	April	153.51	13.44	114.24
	May	103.08	11.58	98.88
1980-81	June	1189.18	468.76	47.04
	July	1028.39	1377.23	46.56
	August	552.66	457.26	46.80
	September	126.79	263.42	66.72
	October	107.66	53.62	75.60
	November	132.93	41.89	64.08
	December	0.00	40.12	81.84
	January	0.00	27.64	99.12
	February	0.00	11.26	97.68
	March	9.88	6.75	132.00
	April	77.12	6.36	146.88
	May	112.64	11.14	126.48

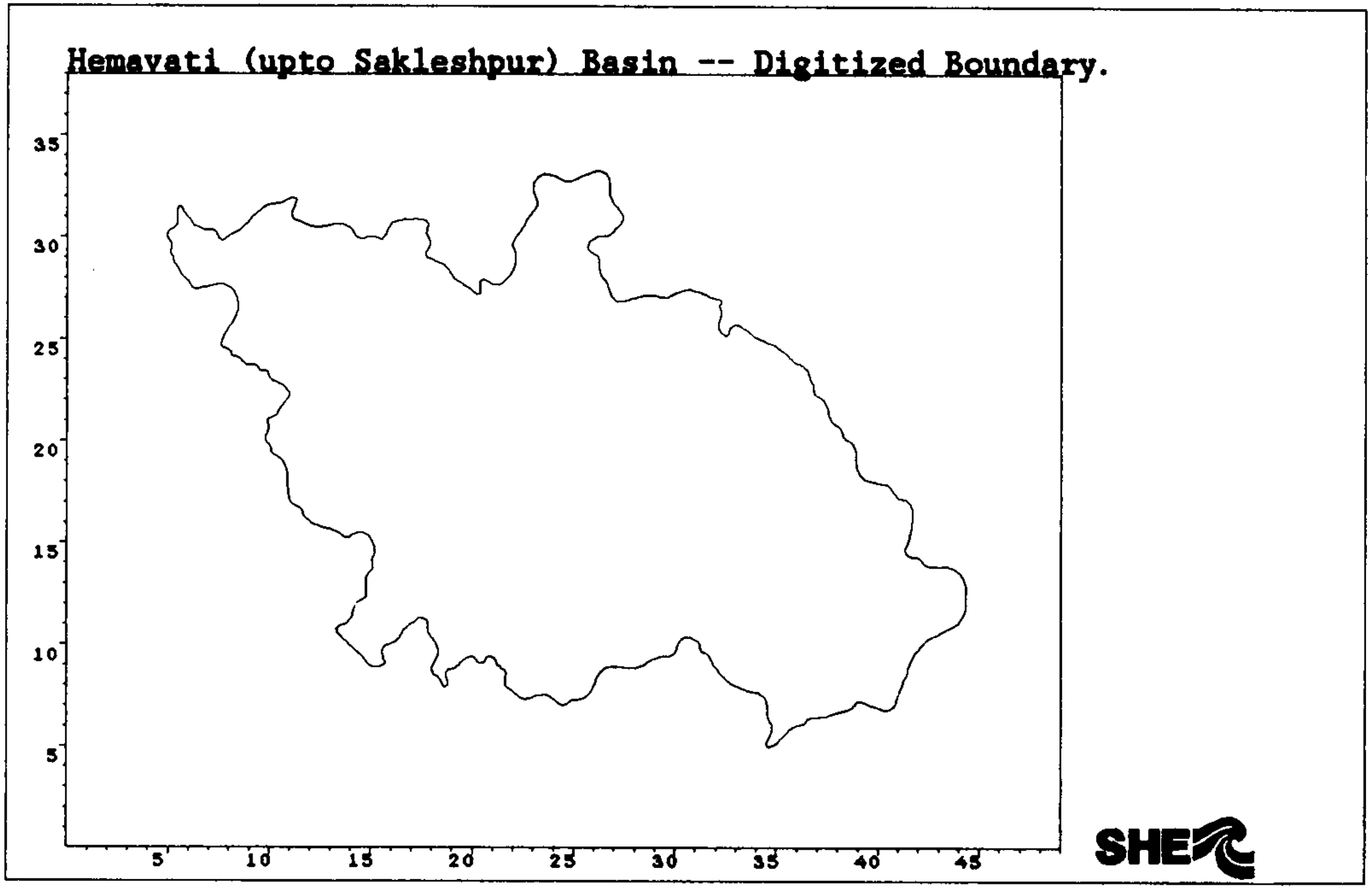

FIGURE 19 - DIGITIZED BOUNDARY OF THE BASIN

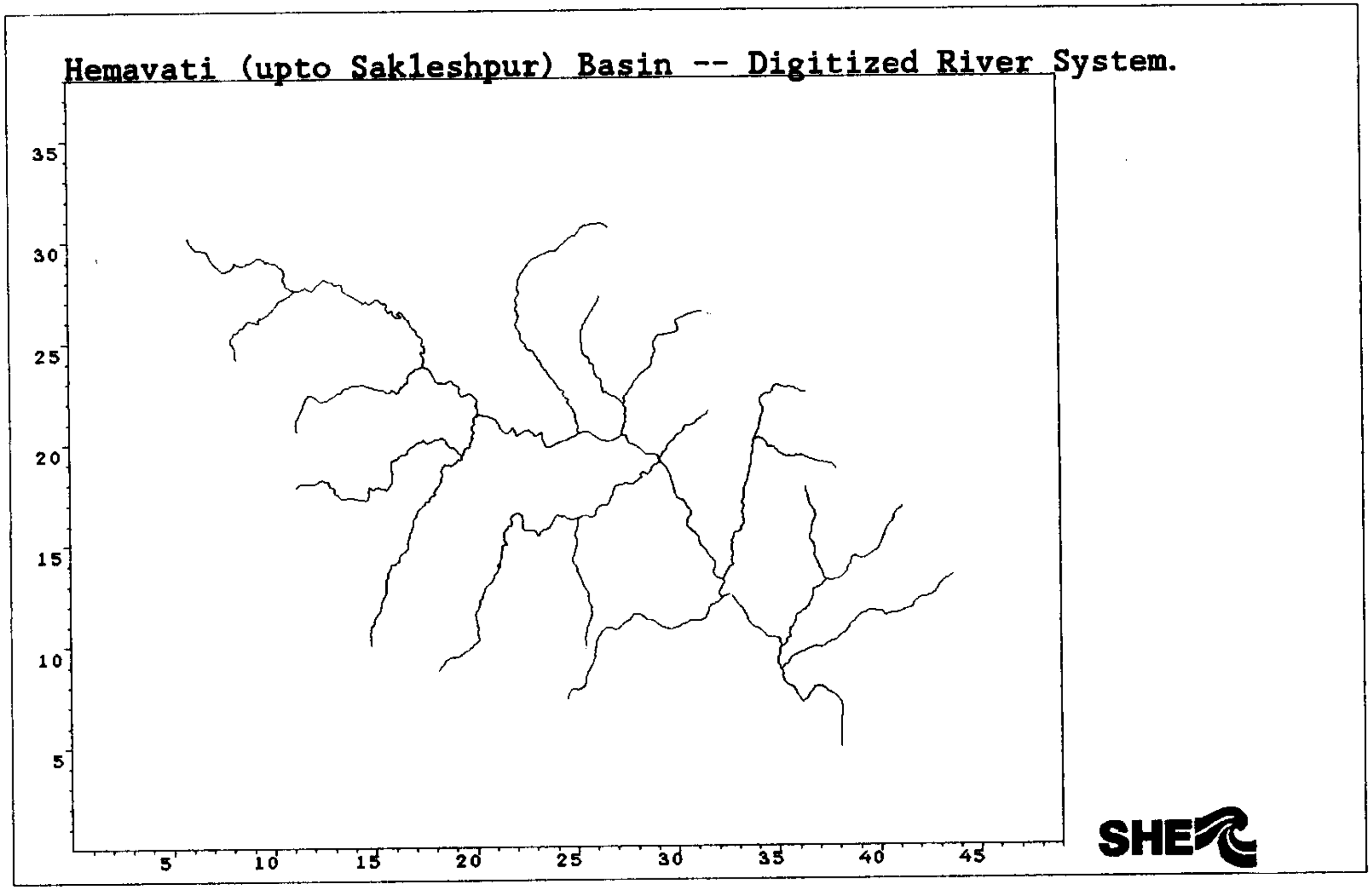

FIGURE 20 - DIGITIZED RIVER SYSTEM OF THE BASIN

Topography

Topographic elevations were read from 1:50,000 scale contour maps superimposed on a grid system of 1 km x 1 km (2 cm x 2 cm). The elevations were read at the corners of the grid squares. The grids were connected to the longitudinal and latitudinal coordinates to have identical origin in the coordinate system. Figure 21 presents the average grid elevations in the basin for 2 km x 2 km grid network.

Land use and soil distribution

To describe land use type areas and soil type areas in the SHE system, grid code maps are used. The polygons enclosing the areas were digitized, using the polygon type and written in SHE format by making use of 'DIGTOSHE'. Figures 22 and 23 present the digitized land use pattern and digitized soil distribution respectively. Grid code maps were then made by 'SHEOL' (SHE overlay maker) from digitized polygons with associated code values.

The land use can further be split into components for low land (< 950 m), semi-hilly (950-990 m) and hilly (> 990 m) areas, giving a total of nine categories. The distributions for the basin are shown in table 10 and figure 24.

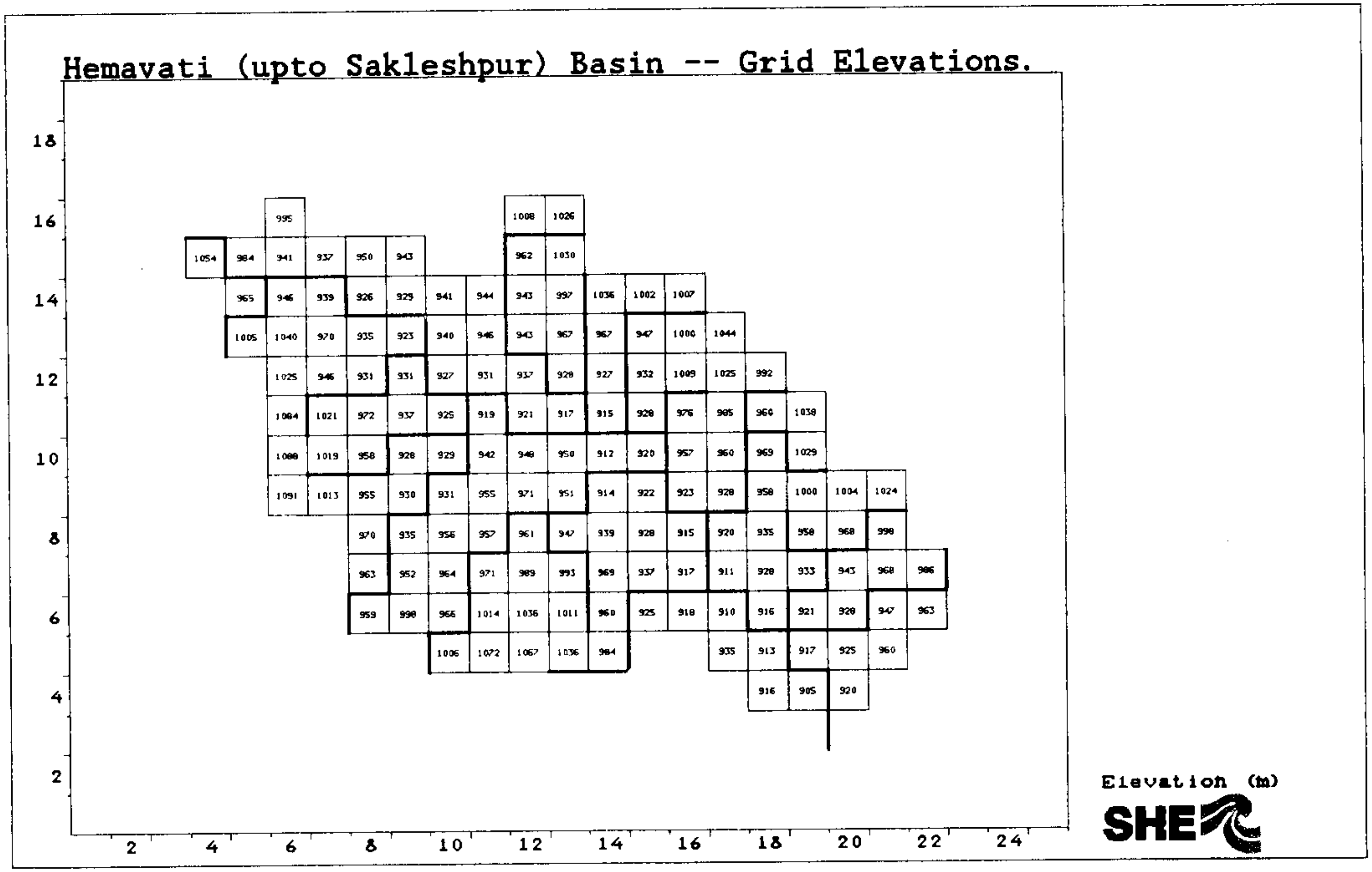

FIGURE 21 - AVERAGE GRID ELEVATIONS IN 2km x 2 km GRID NETWORK

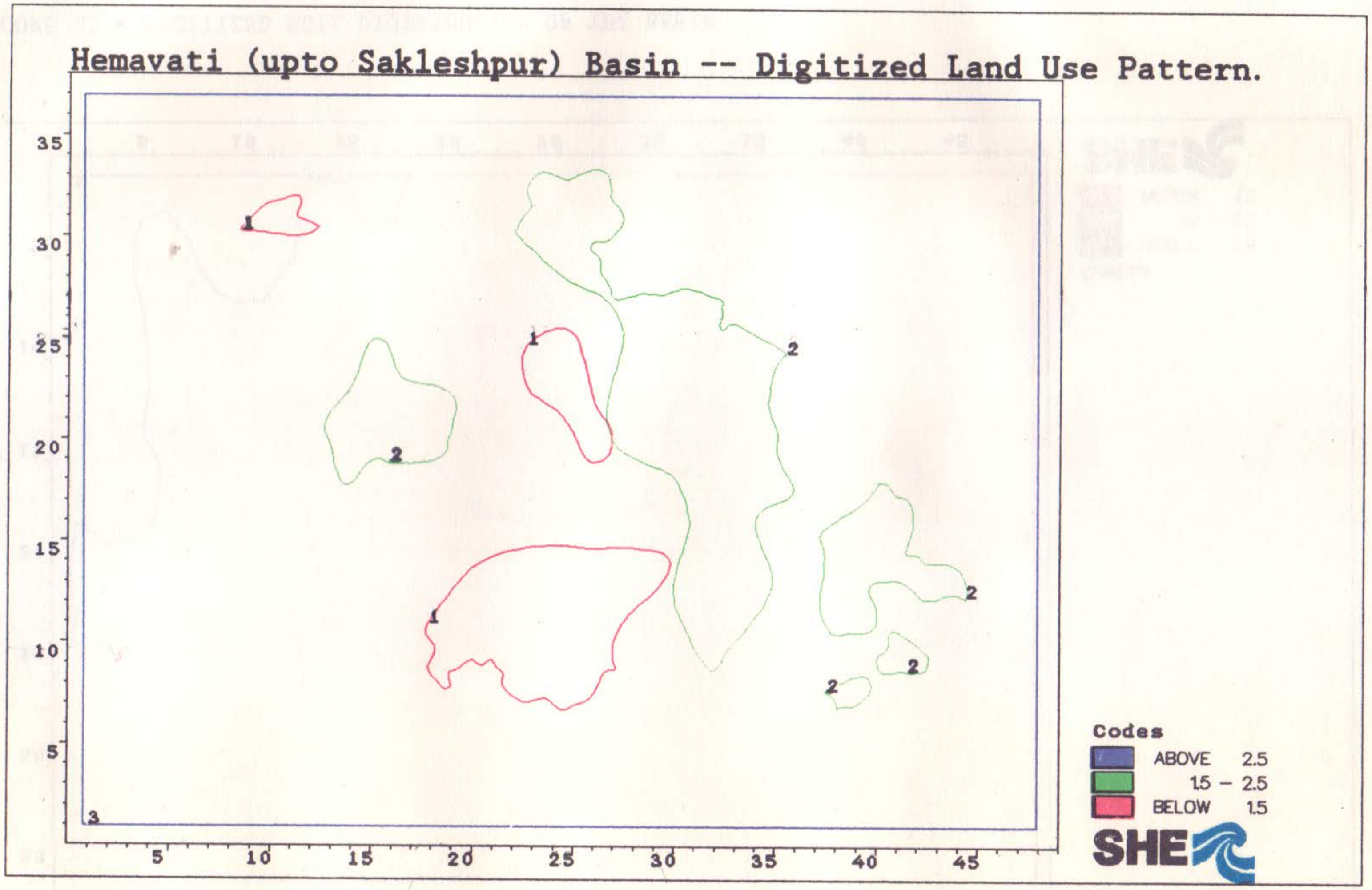

FIGURE 22 - DIGITIZED LAND USE PATTERN OF THE BASIN

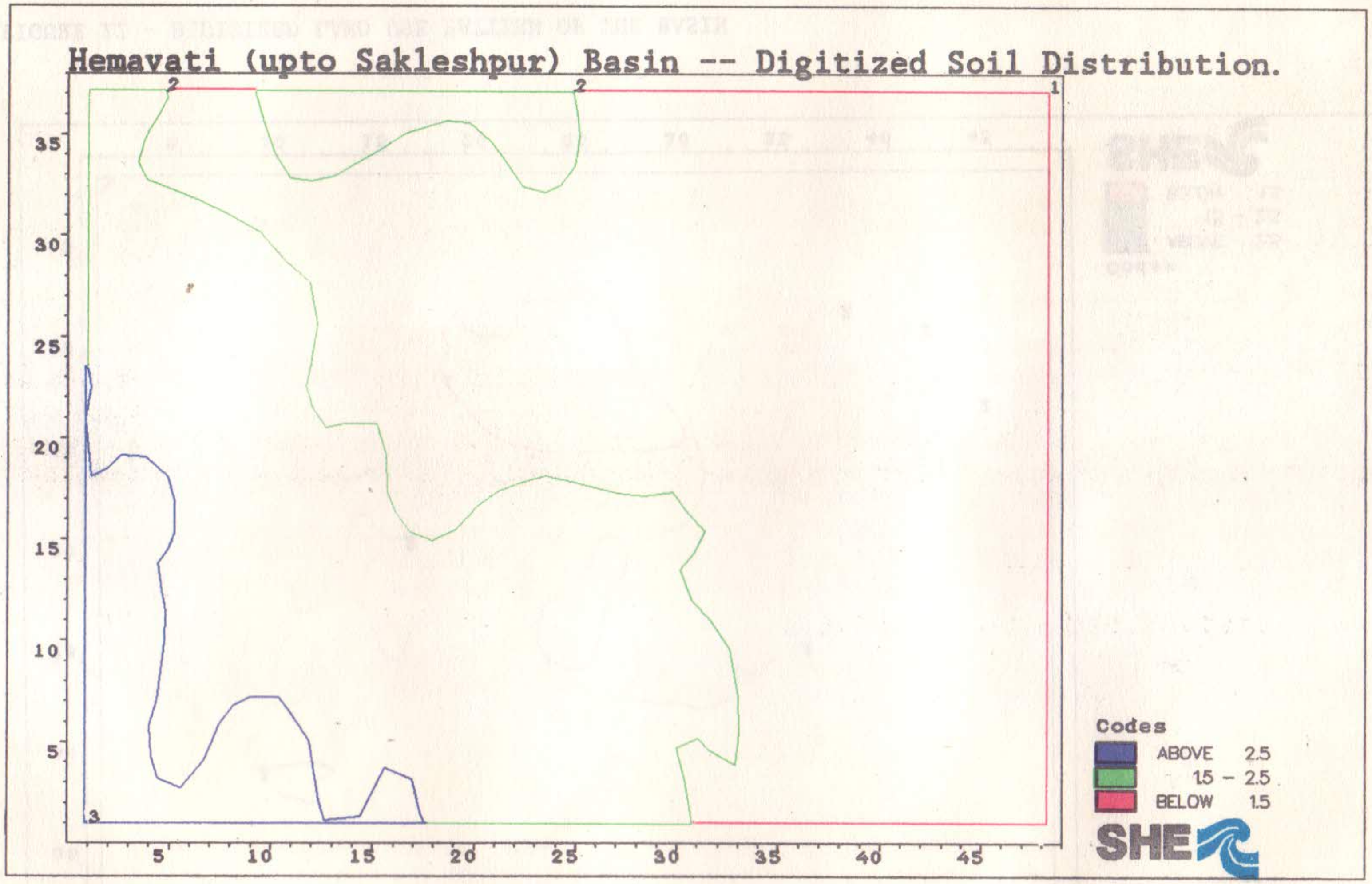

FIGURE 23 - DIGITIZED SOIL DISTRIBUTION OF THE BASIN

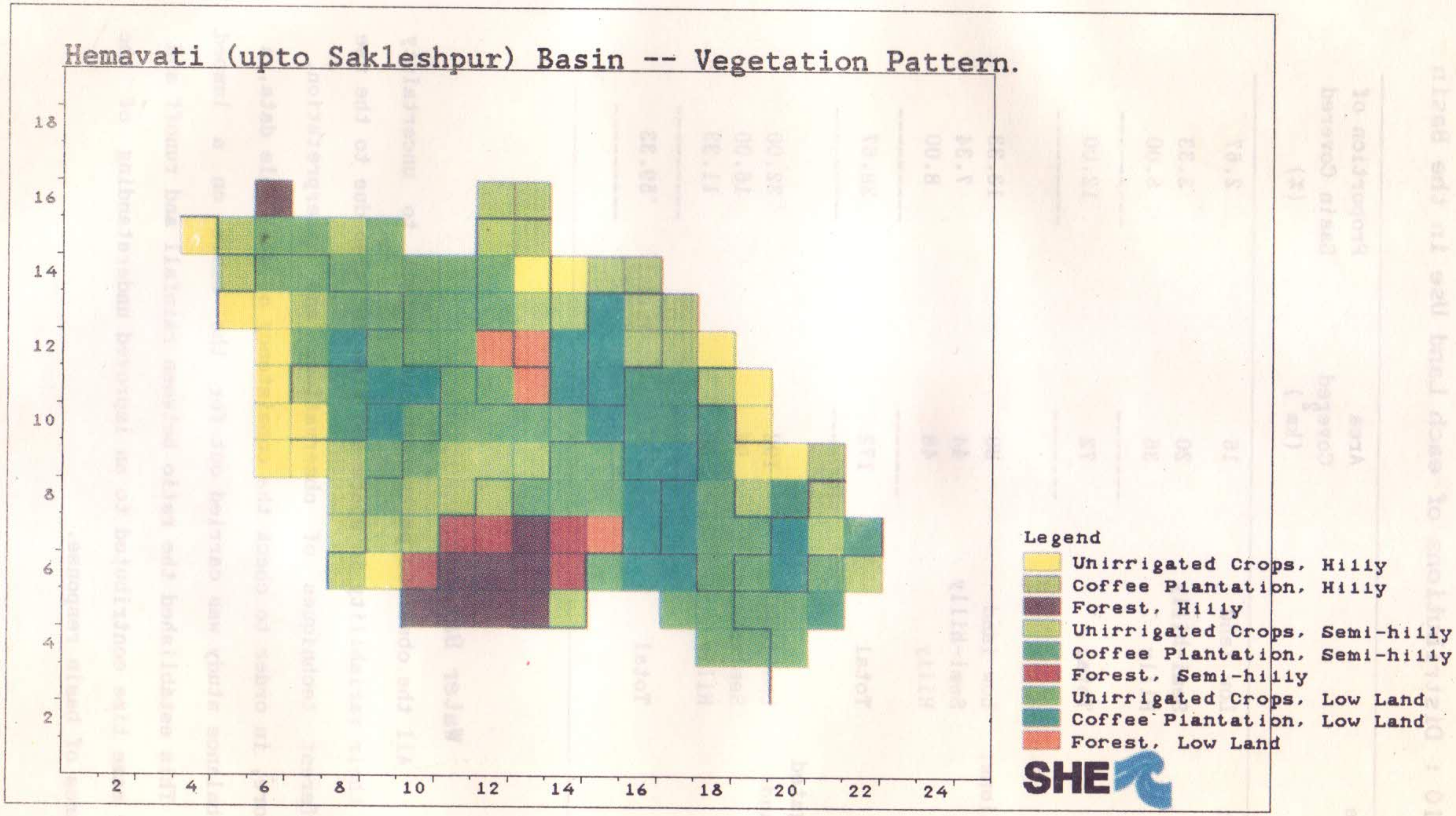

FIGURE 24 - VEGETATION PATTERN IN THE BASIN

Table 10 : Distributions of each Land Use in the Basin

Land Use		Area Covered (km^2)	Proportion of Basin Covered (%)
Forests:	Low land	16	2.67
	Semi-hilly	20	3.33
	Hilly	36	6.00
	Total	72	12.00
Coffee Plantations:	Low land	80	13.33
	Semi-hilly	44	7.34
	Hilly	48	8.00
	Total	172	28.67
Unirrigated Crop Land:	Low land	192	32.00
	Semi-hilly	96	16.00
	Hilly	68	11.33
	Total	356	59.33

4.4 Water Balance

All the observed parameters are subject to uncertainty due to their variability in space and time and also due to the use of different techniques of observations and interpretation. Therefore, in order to check the consistency of available data, a water balance study was carried out for the basin on a lumped basis. This established the ratio between rainfall and runoff and at the same time contributed to an improved understanding of the processes of basin response.

The water balance study was carried out for the basin for monsoon seasons(June to October) from 1975-76 to 1980-81 (table 11). Actual evaporation was assumed to be 95% of the potential evaporation and recharge (from rainfall) to ground water was taken as 8% of the rainfall. The unaccounted water (the discrepancy of water balance) was computed as (rainfall-runoff-actual evaporation-recharge to ground water), the discrepancy being less than 125 mm in all years except in 1978-79. Keeping in view the approximations involved in the computation of actual evaporation and recharge to ground water, this amount of unaccounted water seems to be quite reasonable and within limits. The runoff coefficients were found to vary between 0.69 and 0.87, except for 1978-79. Therefore, the data for all years, except 1978-79, were assumed to be consistent as a result of the above water balance study. However, the data of 1978-79 was also used in the simulations in order to observe its impact on the simulated response.

Table 11 : Water Balance of the Basin

Note : All quantities are in mm.

S. No.	Year	Season	Rainfall (P)	Runoff (Q)	Potential Evaporation (PE)	Runoff Coeff. (Q/P)	Actual Evaporation (0.95PE)	Recharge to G.W. (0.08P)	Unaccounted Water (P-Q-0.95 PE-0.08P)
1.	1975-76	Monsoon	2723.55	2312.34	301.92	0.85	286.82	217.88	- 93.49
2.	1976-77	Monsoon	2186.63	1508.31	412.08	0.69	391.48	174.93	111.91
3.	1977-78	Monsoon	2309.14	1716.45	350.40	0.74	332.88	184.73	75.08
4.	1978-79	Monsoon	2714.33	2742.58	294.24	1.01	279.53	217.15	-524.93
5.	1979-80	Monsoon	2635.22	1952.45	373.92	0.74	355.22	210.82	116.73
6.	1980-81	Monsoon	3004.68	2620.29	282.72	0.87	268.58	240.37	-124.56

4.5 Model Setup

The first stage in the model setup was the construction of the computational grid network and channel system used to represent spatial distribution. For the basin, a basic array for parameter evaluation and distribution was prepared with grid squares of 1 km x 1 km. A topographic elevation, land use type code, soil type code and a meteorological station code were then assigned to each square on the basis of available map information. However, the use of grid squares of 1 km x 1 km resulted in the basin being represented by several hundred squares. In view of the implications for computing time, the basic arrays were not therefore used in the simulation studies. Instead, using the SHE Array Formating Routine, the arrays established with 1 km x 1 km squares were converted into arrays with grid squares of both 2 km x 2 km and 4 km x 4 km. The former scale formed the basis for calibration and validation while the latter was used in the sensitivity analysis. Figures 25 to 28 present the networks with grid squares of 0.5 km x 0.5 km, 1 km x 1 km, 2 km x 2 km and 4 km x 4 km respectively.

Within the SHE, the network is mapped by a series of channel links superimposed on the grid square boundaries. Coarser grid scales produce different drainage densities in terms of the ratio of the number of channel links to the number of grid squares. Table 12 compares the number of grid squares and river links used to represent the basin at different scales.

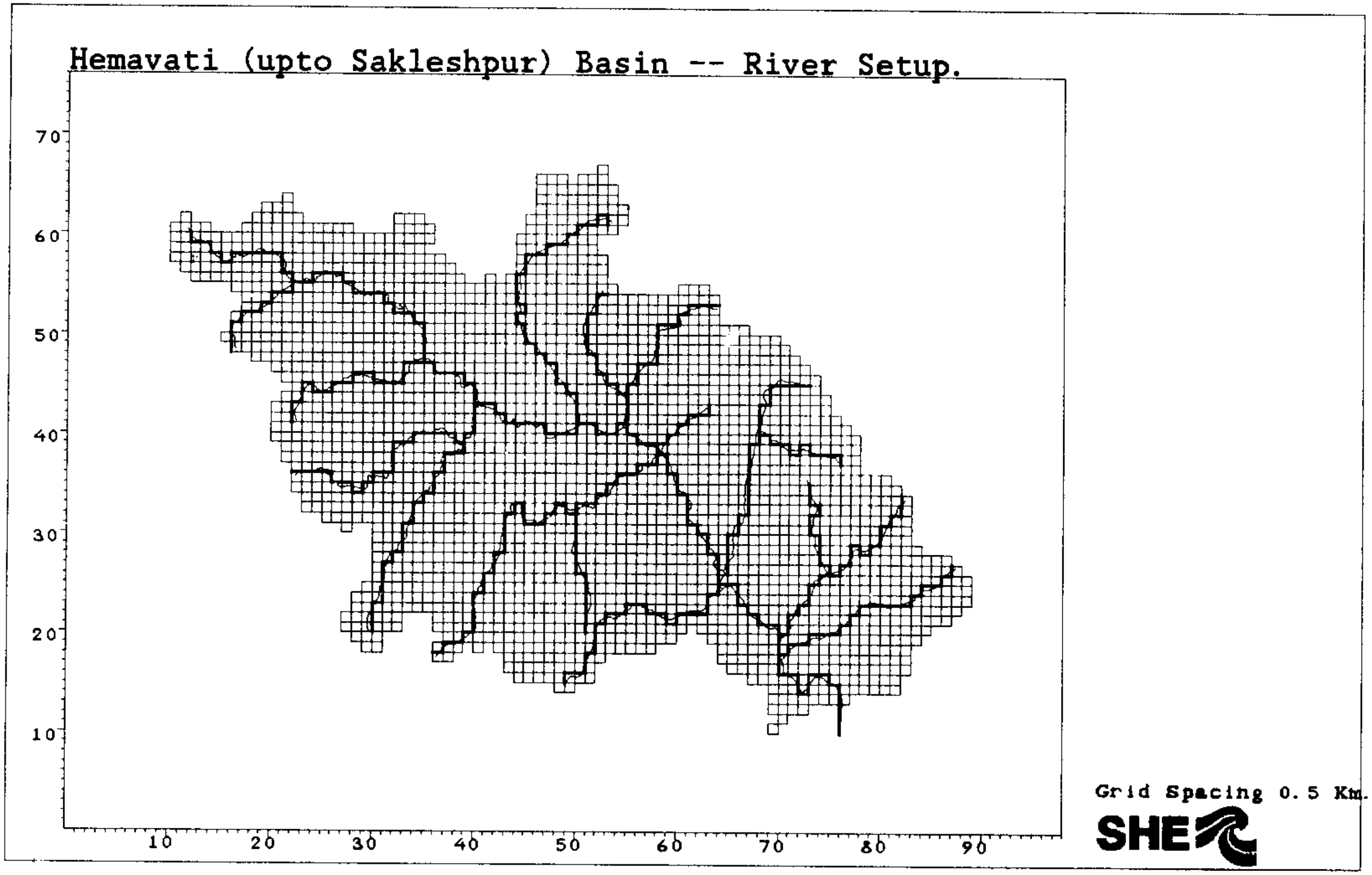

FIGURE 25 - RIVER SETUP IN 0.5 km x 0.5 km GRID NETWORK

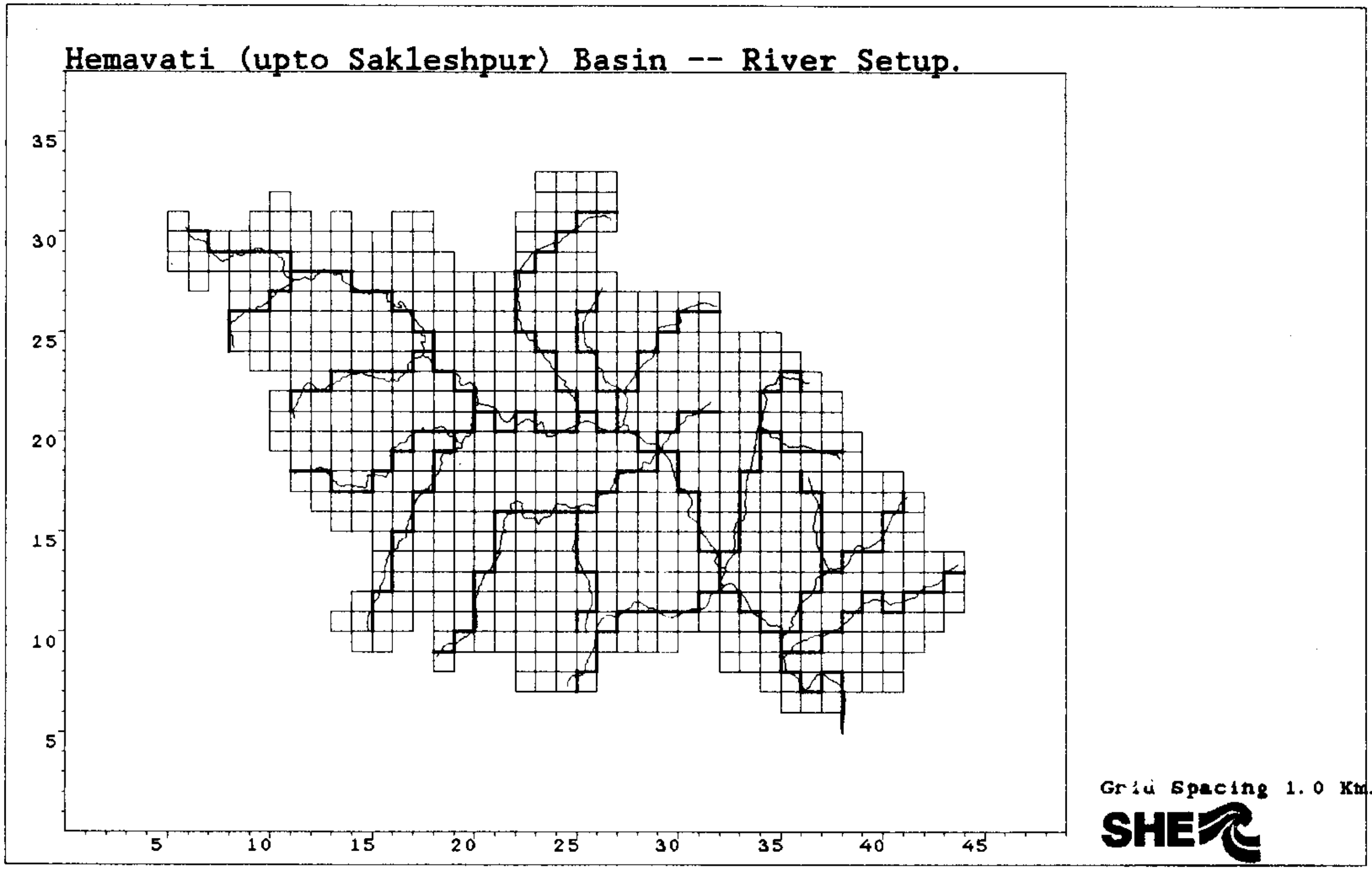

FIGURE 26 - RIVER SETUP IN 1km x 1km GRID NETWORK

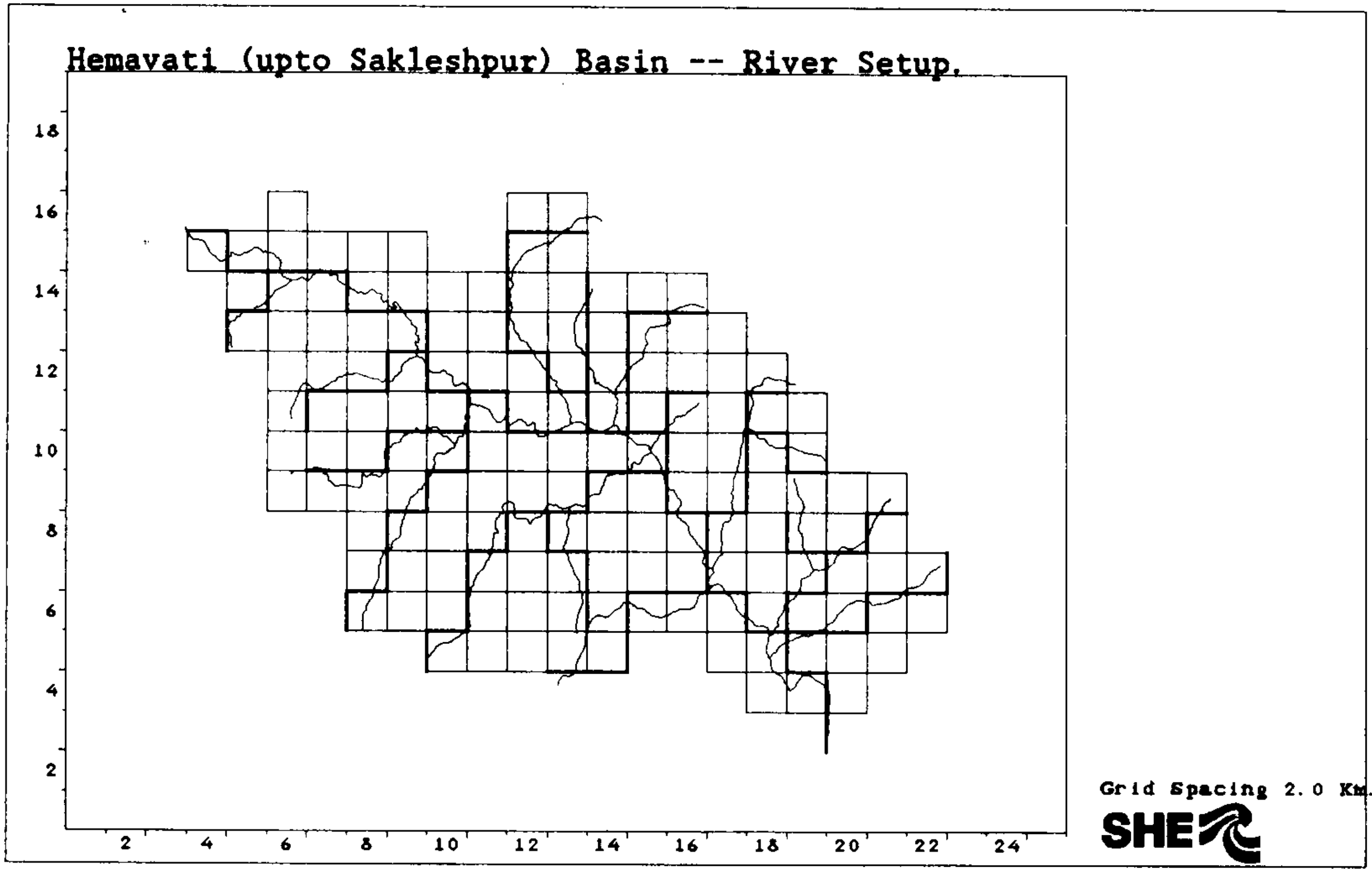

FIGURE 27 - RIVER SETUP IN 2 km x 2 km GRID NETWORK

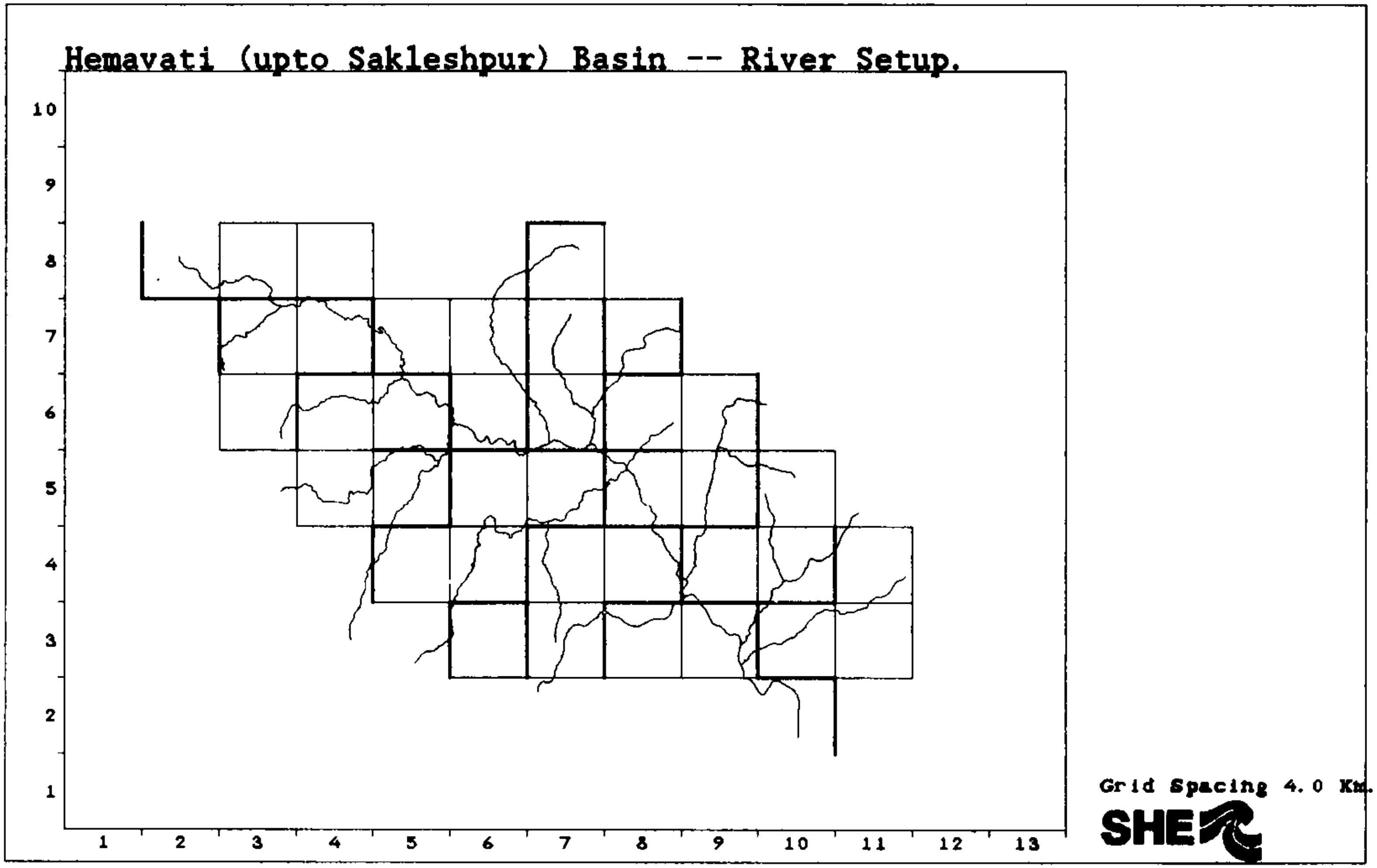

FIGURE 28 - RIVER SETUP IN 4 km x 4 km GRID NETWORK

Table 12 : Grid and Channel Network Dimensions for Different Grid Scales

Grid Square Size (km x km)	Represented Basin Area (km^2)	Number of Grid Squares representing	Number of River Links representing the Basin System	Ratio of Number of Links to Number of the River Squares
0.5 x 0.5	597.00	2388	463	0.194
1 x 1	602.00	602	244	0.405
2 x 2	600.00	150	113	0.753
4 x 4	576.00	36	44	1.222

With the arrays established, initial test runs were carried out to check for errors in the grid arrangements, river links and topographic representations and to ensure that surface flows (overland and channel flows) within the basin could be modelled realistically. At this stage, hypothetical rainfall, evapotranspiration and soil infiltration data were used. These simple tests provided a good 'shake-out' for the basin models and enabled a number of 'teething problems' such as river elevations set higher than bank elevations, to be eliminated. Then the way was clear for simulations with full representations of the basin, based on measured input data, evaluation of soil and vegetation parameters and the available understanding of basin hydrology.

4.6 Parameter Evaluation

Direct measurements of soil and vegetation parameters for the basin were not available and evaluations therefore depended on parameter transfer from the literature on neighbouring areas.

Soil parameters

Soils in the hilly areas are less deep than those in the low land areas but, in general, relevant information is scanty. The relevant parameter values, actually used in the simulations for all soil types, are given in table 13. Only one retention curve was used based on the data given in table 14 and assumed to be the same for low land and upland soils. Three categories of soil depths were defined, for low land areas (deep soils), for semi-hilly areas (intermediate depths) and for hilly areas (shallow soils), the distributions obtained from the topographic maps. The soil depths were determined from analysis of well levels. The values adopted as best estimates for the calibration are shown in table 15 and also presented in figure 29.

Table 13 : Physical Characteristics of Soil

S.No.	Soil Parameter	Value
1.	Water content at saturation (equal to porosity of the soil)	0.478
2.	Effective water content at saturation, adjusted for trapped air volumes	0.450
3.	Water content at field capacity	0.384
4.	Corresponding tension at field capacity	-1.000 m
5.	Water content at wilting point	0.210
6.	Residual water content (inaccessible water content in soil due to adsorption)	0.180
7.	Saturated conductivity	0.100 m/day
8.	Exponent for conductivity/moisture content relation	12.000

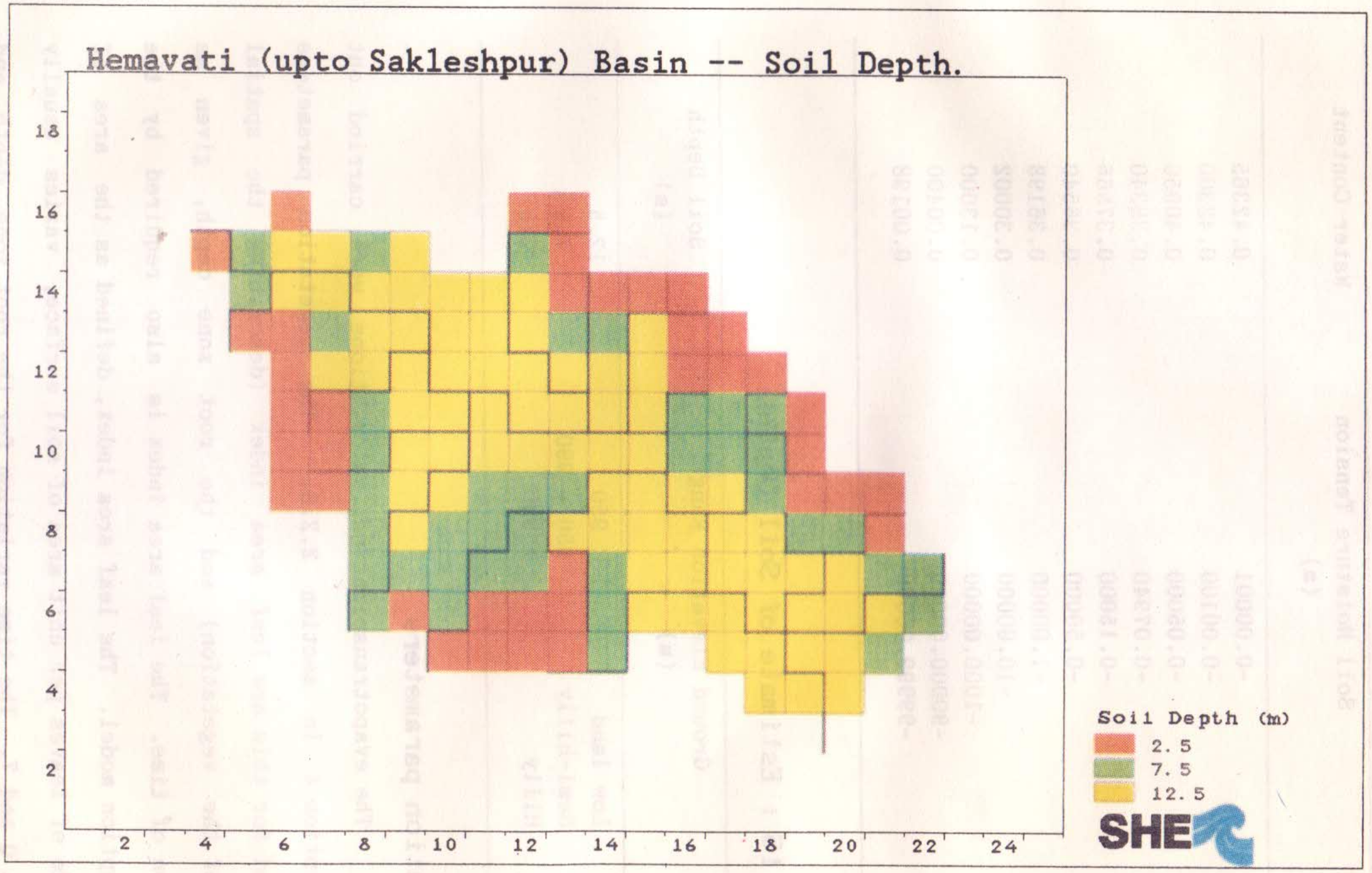

FIGURE 29 - SOIL DEPTHS IN THE BASIN

Table 14 : Retention Curve Table

S.No.	Soil Moisture Tension (m)	Water Content
1.	-0.00001	0.42365
2.	-0.00100	0.42300
3.	-0.05000	0.40950
4.	-0.07940	0.38340
5.	-0.15000	0.37566
6.	-0.50000	0.36540
7.	-1.00000	0.36198
8.	-10.00000	0.30002
9.	-1000.00000	0.13000
10.	-90000.00000	0.00400
11.	-99999.00000	0.00198

Table 15 : Estimate of Soil Depths

S.No.	Ground Elevation Range (m)		Soil Depth (m)
1.	Low land	< 950	12.5
2.	Semi-hilly	950 - 990	7.5
3.	Hilly	> 990	2.5

Vegetation parameters

The evapotranspiration calculations were carried out using option 4 in section 2.2.2. The vegetation parameters required for this are leaf area index (describing the spatial cover of the vegetation) and the root zone depth, given as function of time. The leaf area index is also required by the interception model. The leaf area index, defined as the area of one side of leaves per unit area of soil surface, varies usually between 0 and 7. The time variation for the root zone depth and leaf area index for the three land use types used in the simulations are presented in table 16 and figure 30. Root zone

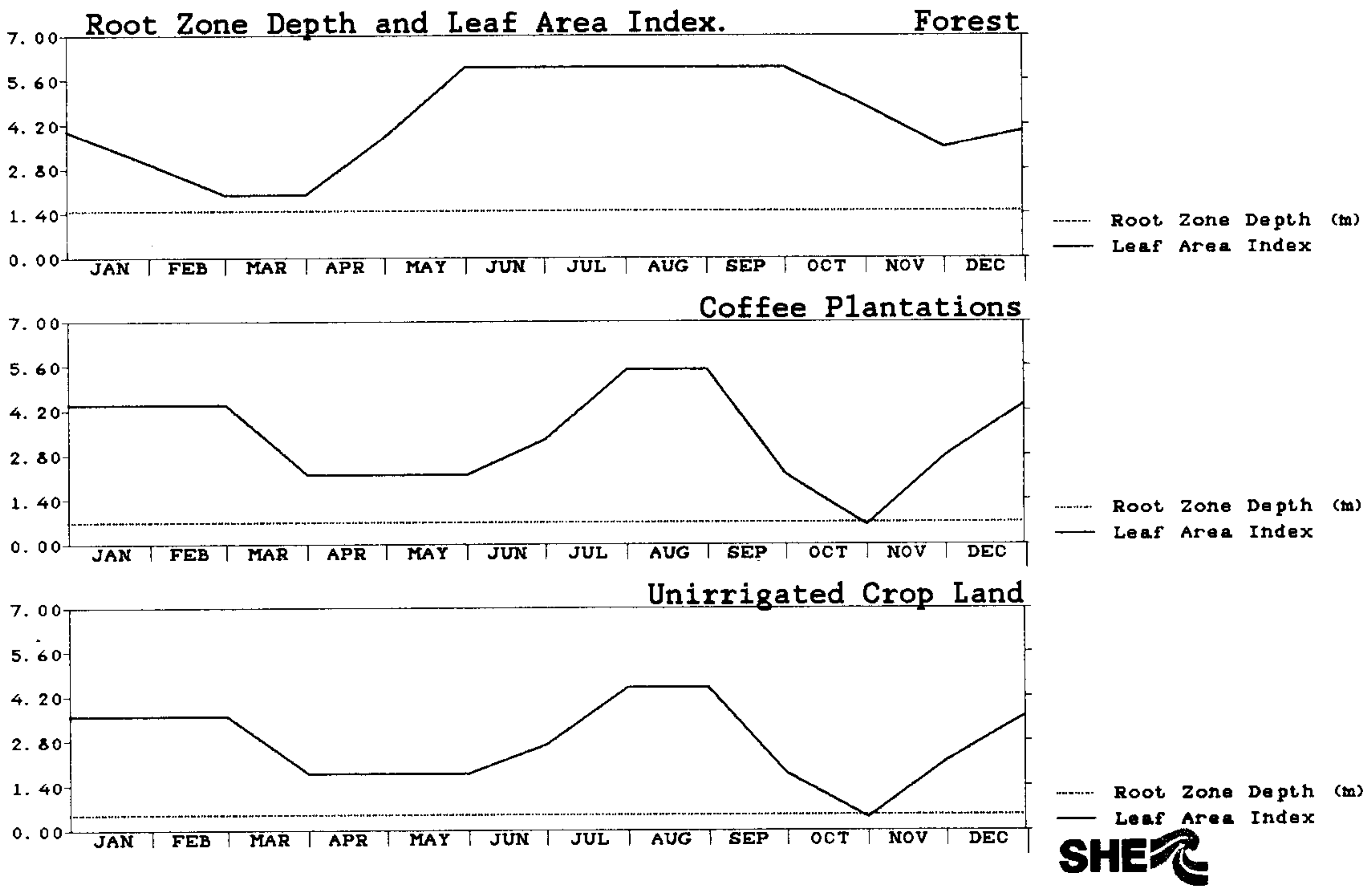

FIGURE 30 - ROOT ZONE DEPTH AND LEAF AREA INDEX

depths varied from 0.5 m in the unirrigated crop land to 1.5 m in forested regions.

Table 16 : Root Zone Depth and Leaf Area Index

Month	Forests		Coffee Plantations		Unirrigated Crop Land	
	Root Zone Depth (m)	Leaf Area Index	Root Zone Depth (m)	Leaf Area Index	Root Zone Depth (m)	Leaf Area Index
January	1.5	4.0	0.7	4.4	0.5	3.6
February	1.5	3.0	0.7	4.4	0.5	3.6
March	1.5	2.0	0.7	4.4	0.5	3.6
April	1.5	2.0	0.7	2.2	0.5	1.8
May	1.5	3.8	0.7	2.2	0.5	1.8
June	1.5	6.0	0.7	2.2	0.5	1.8
July	1.5	6.0	0.7	3.3	0.5	2.7
August	1.5	6.0	0.7	5.5	0.5	4.5
September	1.5	6.0	0.7	5.5	0.5	4.5
October	1.5	6.0	0.7	2.2	0.5	1.8
November	1.5	4.8	0.7	0.6	0.5	0.4
December	1.5	3.5	0.7	2.8	0.5	2.2

Overland and channel flow parameters

The Strickler roughness coefficient for overland flow was assumed to be spatially uniform in the basin. In reality, variations might be expected according to land use and whether the overland flow occurs as sheet flow or in rivulets. However, no information was available on such variations. For overland flow, the Strickler roughness coefficient is likely to lie between about 0.04 (typical of sheet flow in grass) and 2-20 (typical of flow in grass-lined channels). For the simulations, it was varied between 1.0 and 2.5 and used as a calibration factor.

For channel flow, the Strickler roughness coefficient was set within the range 20 - 30. These values, although not evaluated specifically from Hemavati basin data, are characteristic of river channels.

Channel cross-sections

Channel dimensions vary with the upstream drainage area and empirical dependencies can therefore be established to enable the dimensions to be calculated at all parts of the river system. However, drainage area is considered to be inconvenient to measure for more than a few points. A more convenient parameter to measure is upstream channel length, since this also varies closely with upstream drainage area, it can be used as the basis for calculating channel dimensions. The following empirical relationships were therefore used, giving bankfull depth d(m), bankfull (or top) width w_t(m), and bed width w_b(m) as functions of upstream channel length L(km).

$$d = 1.7 L^{0.5} \quad ...(23)$$

$$w_t = 15 L^{0.5} \quad ...(24)$$

$$w_b = 8.5 L^{0.5} \quad ...(25)$$

These relationships were used to define the channel dimensions at all parts of the Hemavati (upto Sakleshpur) river system as defined for the SHE (table 17). However, cross-sectional dimensions at Sakleshpur were based upon the longitudinal section of dam at Gorur.

Initial conditions

Initial conditions for a simulation are specified in terms of the depth of the phreatic surface. In the present case,

Table 17 : Channels Cross-sections (RIVER.CROSS)

N	L	Dd	Wd	Dd	Wd	Dd	Wd	Du	Wu	Du	Wu	Du	Wu	S
1	3	0.0	107.8	7.90	146.1	15.80	184.4	0.0	6.0	0.60	8.3	1.20	10.6	20
2	3	0.0	20.0	2.00	27.7	4.01	35.4	0.0	6.0	0.60	8.3	1.20	10.6	20
3	3	0.0	25.7	2.57	35.5	5.14	45.3	0.0	6.0	0.60	8.3	1.20	10.6	20
4	3	0.0	29.3	2.93	40.5	5.86	51.7	0.0	6.0	0.60	8.3	1.20	10.6	20
5	3	0.0	33.6	3.36	46.4	6.72	59.3	0.0	6.0	0.60	8.3	1.20	10.6	20
6	3	0.0	32.7	3.27	45.2	6.53	57.6	0.0	6.0	0.60	8.3	1.20	10.6	20
7	3	0.0	21.8	2.18	30.2	4.37	38.5	0.0	6.0	0.60	8.3	1.20	10.6	20
8	3	0.0	25.8	2.58	35.6	5.16	45.5	0.0	6.0	0.60	8.3	1.20	10.6	20
9	3	0.0	38.5	3.85	53.2	7.70	67.9	0.0	6.0	0.60	8.3	1.20	10.6	20
10	3	0.0	22.1	2.21	30.6	4.43	39.0	0.0	6.0	0.60	8.3	1.20	10.6	20
11	3	0.0	16.2	1.62	22.5	3.25	28.7	0.0	6.0	0.60	8.3	1.20	10.6	20
12	3	0.0	29.8	2.98	41.2	5.97	52.7	0.0	6.0	0.60	8.3	1.20	10.6	20
13	3	0.0	18.3	1.83	25.2	3.65	32.2	0.0	6.0	0.60	8.3	1.20	10.6	20
14	3	0.0	28.8	2.88	39.8	5.76	50.8	0.0	6.0	0.60	8.3	1.20	10.6	20
15	3	0.0	18.9	1.89	26.2	3.78	33.4	0.0	6.0	0.60	8.3	1.20	10.6	20
16	3	0.0	27.5	2.75	38.0	5.49	48.5	0.0	6.0	0.60	8.3	1.20	10.6	20
17	3	0.0	27.7	2.77	38.3	5.54	48.8	0.0	6.0	0.60	8.3	1.20	10.6	20

N : Number of actual river section.

L : Number of levels.

Dd : Distance (m) between bed level and the level under consideration (downstream section).

Wd : Width (m) at the level under consideration (downstream section).

Du : Distance (m) between bed level and the level under consideration (upstream section).

Wu : Width (m) at the level under consideration (upstream section).

S : Strickler coefficient in river section.

the depths are defined for 1st March for the simulations. The values adopted in simulations are estimates rather than measurements but take into account available information on well levels. Nevertheless, uncertainties associated with definition of the initial conditions are likely to remain. It is therefore recommended that a simulation should include a 'settling down' period before the main event so that the impact of the initial conditions is diffused. Figure 31 presents the initial depth to phreatic surface (as on 1st March, 1975) in the basin.

Unsaturated zone calculations

The unsaturated zone (UZ) plays an important role in the SHE as all other components depend on boundary data from UZ component. The unsaturated zone calculations need to be performed in every grid square in the grid system. For large grid system setups, the UZ component is by far the most time consuming of the components in SHE. It is therefore quite expensive and time demanding to simulate long time series without some sort of approximations. One approximation introduced in the UZ component is that the UZ-calculations are made only in selected grid squares and the boundary conditions from these are transferred to identical grid squares. Homogeneous areas can be defined based on the topography, meteorological input, vegetation type and soil type. An initial selection of homogeneous groups is made by the SHE Array Formating Routine on the basis of the depth to the ground water table and the information of soil, vegetation and climate. The boundary conditions i.e. infiltration rate, evapotranspiration loss and ground water recharge are transferred to the other grid squares within the homogeneous group. This approximation does not introduce any water balance error, but might influence the dynamic of the simulation. However, an

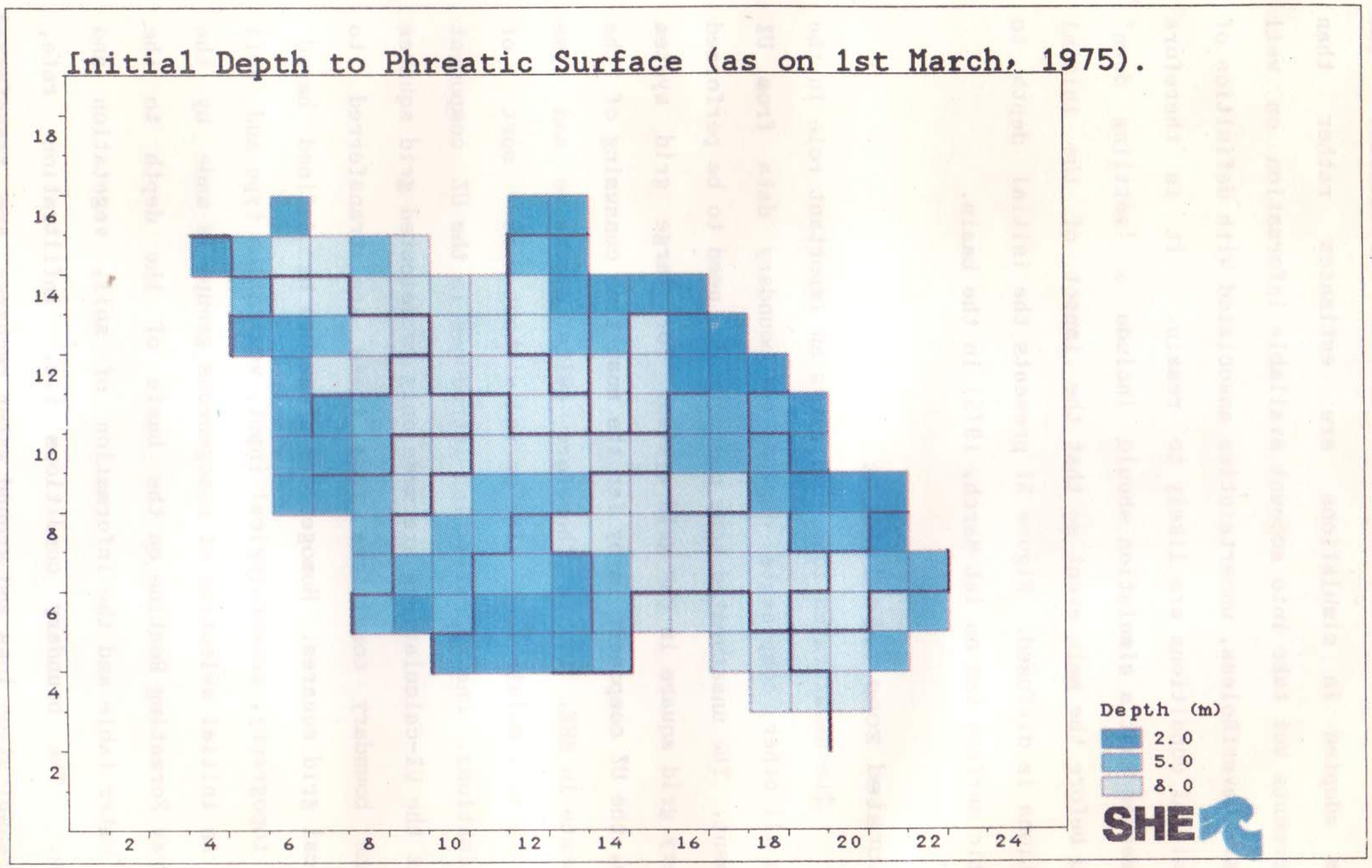

FIGURE 31 - INITIAL DEPTHS TO PHREATIC SURFACE (AS ON Ist MARCH,1975)

intelligent selection of groups of grid squares will reduce the later effect considerably.

With the large number of grid squares and long simulation periods being used for the basin, this facility was therefore used throughout the simulations. Unsaturated zone calculations were carried out directly for 13 specified grid squares out of the total 150 grid squares representing the basin. However, the results are more approximate than if the calculations are carried out for all squares and it is necessary to balance saving in computation time against representation of the basin. Table 18 presents the details of representative grid squares for unsaturated zone calculations.

Table 18 : Representative Grid Squares for Unsaturated Zone Calculations

S. No.	UZ-Code for Representative Grid Square	Location x	Location y	Topography	Raingauge Station	Land Use Type	Soil Type	Number of Grid Squares in the Homogeneous Group
1.	- 2	20	5	low land	3	3	1	11
2.	- 3	10	5	hilly	4	1	1	14
3.	- 4	12	10	low land	4	3	1	24
4.	- 5	21	5	semi-hilly	3	2	1	2
5.	- 6	15	11	low land	4	2	1	12
6.	- 7	21	7	semi-hilly	5	3	1	11
7.	- 8	17	11	semi-hilly	5	2	1	13
8.	- 9	5	15	semi-hilly	2	3	1	21
9.	-10	8	11	semi-hilly	2	2	1	4
10.	-11	15	13	low land	1	2	1	12
11.	-12	11	13	low land	1	3	1	22
12.	-13	13	12	low land	1	1	1	3
13.	-14	6	16	hilly	2	1	1	1

5.0 CALIBRATION AND VALIDATION

5.1 General

Model calibration in general involves manipulation of a specific model to reproduce the response of the catchment under study within some range of accuracy. In a calibration procedure, an estimation is made of the parameters which can not be assessed directly from field data. All empirical (black box) models and all lumped, conceptual models contain parameters whose values have to be estimated through calibration. The fully distributed, physically-based models contain only parameters which can be assessed from field data so that in theory, a calibration should not be necessary if sufficient data are available. However, for all practical purposes the distributed, physically-based models also require some kind of calibration although the allowed parameter variations are restricted to relatively narrow intervals compared with those for the empirical parameters in empirical or lumped, conceptual models.

In principle three different calibration methods can be applied:

a. 'Trial and Error', manual parameter assessment,

b. Automatic, numerical parameter optimization, and

c. A combination of (a) and (b).

The trial and error method implies a manual parameter assessment through a number of simulation runs. This method is by far the most widely used and is the most recommended method, especially for the more complicated models. A good graphical representation of the simulation results is a prerequisite for the trial and error method. An experienced hydrologist can usually achieve a calibration using visual hydrograph inspection within 5-15 simulation runs.

Automatic parameter optimization involves a numerical algorithm which optimizes or minimizes a given numerical criterion. The objective of automatic parameter optimization is to search through the many combinations and permutations of parameter levels to achieve the set which is the optimum or 'best' in terms of satisfying the criterion of accuracy. Several optimization techniques have been used for calibration of hydrological models. However, this method is not used very much today.

Combination of the trial and error and automatic parameter optimization methods could involve, for example, initial adjustment of parameter values by trial and error to delineate rough orders of magnitude, followed by fine adjustment using automatic optimization within the delineated range of physically realistic values. The reverse procedure is also possible, first carrying out sensitivity tests by automatic optimization to identify the important parameters and then calibrating them by trial and error. The combination method can be very useful but does not yet appear to have been widely used in practice.

Finally, given the large number of parameters in a physically-based, distributed model like the SHE, it is not realistic to obtain an accurate calibration by gradually varying all the parameters singly or in combination. A more sensible approach is to attempt a coarser simulation using only the few parameters to which the simulation is most sensitive. These can be determined from sensitivity analysis. However, experience suggests that the soil parameters will usually require the most attention because of their role in determining the amount of precipitation which infiltrates and thence the amount which forms overland flow.

5.2 Calibration Approach

Calibration was carried out for a 2 km x 2 km representation of the basin, mainly by adjusting a few key parameters and examining their effects on the simulated hydrographs. Several trial-and-error runs were carried out by manual parameter assessment. Calibration was carried out primarily by varying the Strickler roughness coefficients for overland and channel flow to calibrate hydrograph peaks, the saturated conductivity for the unsaturated zone to determine the amount of infiltration and thence the runoff hydrograph volume, the saturated zone conductivity to affect base flow discharges, and surface detention submodel to moderate the amount of infiltration and runoff in the early stages of the monsoon. The choice of simulation period was determined by the availability of hourly rainfall and discharge data. The aim of the calibration was to reproduce the following for the catchment:

i. A good agreement between the average simulated and recorded flows, i.e. a good water balance.

ii. A good agreement for the peak flows with respect to volume, rate and timing.

iii. A good agreement for low peaks.

iv. A good overall agreement for hydrograph shape with emphasis on a physical correct model simulation.

The SHE package program does not have a quantitative optimization method to minimize errors in the simulation beyond an arbitrary level and as such simulated and observed hydrographs were compared by eye.

Finally, a model is not validated until, using the calibrated parameter set, it has successfully simulated independent events which have not been used for the calibration. Consequently the technique employed here was 'split-sample test'.

The available data record was divided into two parts. The parameter set was calibrated for the storm events during the period March 1975 to February 1978 and those values were applied in the simulation of the other events during the period March 1978 to February 1981, changing only the initial level of the phreatic surface.

5.3 Calibration

Calibration was carried out for three successive monsoon seasons (1975-77) for the basin. Tests showed that the choice of initial depth of the phreatic surface could have a significant effect on the simulated response to the monsoon rainfall. Therefore, continuous runs linking the consecutive monsoon seasons were carried out so that the simulated antecedent conditions for the later monsoons would be determined by the model. In other words, they would represent a response to the previous monsoon and the intervening dry season and would be less affected by the imposed initial conditions at the start of the simulation.

Parameters were maintained at the 'best estimate' values available at the start of the updating whenever possible. However, some adjustments were needed to improve the calibration. In that case, two runs were made using extreme values bracketing the realistic range and on the basis of the results, the parameter in question was then adjusted within this range to give the best fit. The details of calibration trials for individual parameters are given below

Surface detention

A simple surface detention submodel was used to simulate surface ponding effect. Surface storage of overland flow delays the release of runoff to a river system and thus affects the generation of the hydrograph.

Overland flow

An implicit technique was used in the numerical solution procedure for the overland flow calculations which overcomes the problem of maintaining mass continuity and permits the use of larger calculation time step, thereby reducing CPU time requirements.

The 2 km x 2 km grid representation of the basin was used for the simulations. Initial runs were carried out with the Strickler roughness coefficient for the overland flow set at the value of 2.5. However, simulated hydrograph peaks overestimated the measured peaks while the recessions were steep by comparison with the observed patterns. Coefficients of 2.0, 1.5 and 1.0 were tested and eventually a value of 1.0 was found to produce reasonable agreement between observation and simulation for all the three simulation years. The use of the lower values (implying higher resistance) relative to the values measured elsewhere (around 10.0) with rainfall simulators (Engman, 1986) is justified in terms of scale. Rainfall simulator plots, not more than about 30 sq.m. in area, are relatively uniform and exhibit sheet flow. At the 2 km x 2 km scale of the SHE simulation grids, topography, vegetation and soils are considerably less uniform and both sheet and rivulet overland flows are likely. It is not, therefore, to be expected that the same surface roughness coefficient will apply in both cases. Figures 32, 33 and 34 present the post- monsoon overland flow depths in the basin for the years 1975 , 1976 and 1977 respectively.

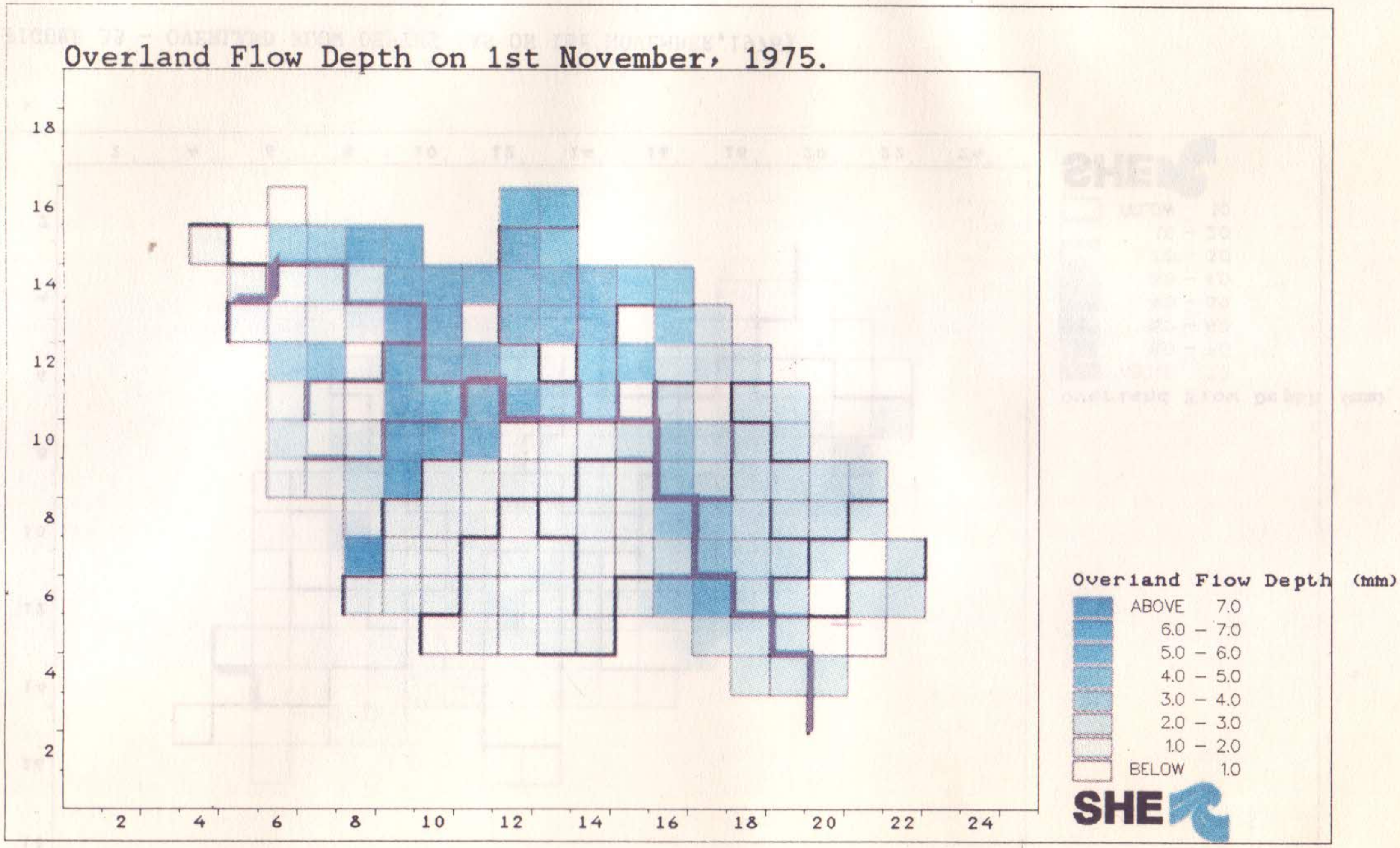

FIGURE 32 - OVERLAND FLOW DEPTHS (AS ON Ist NOVEMBER ,1975)

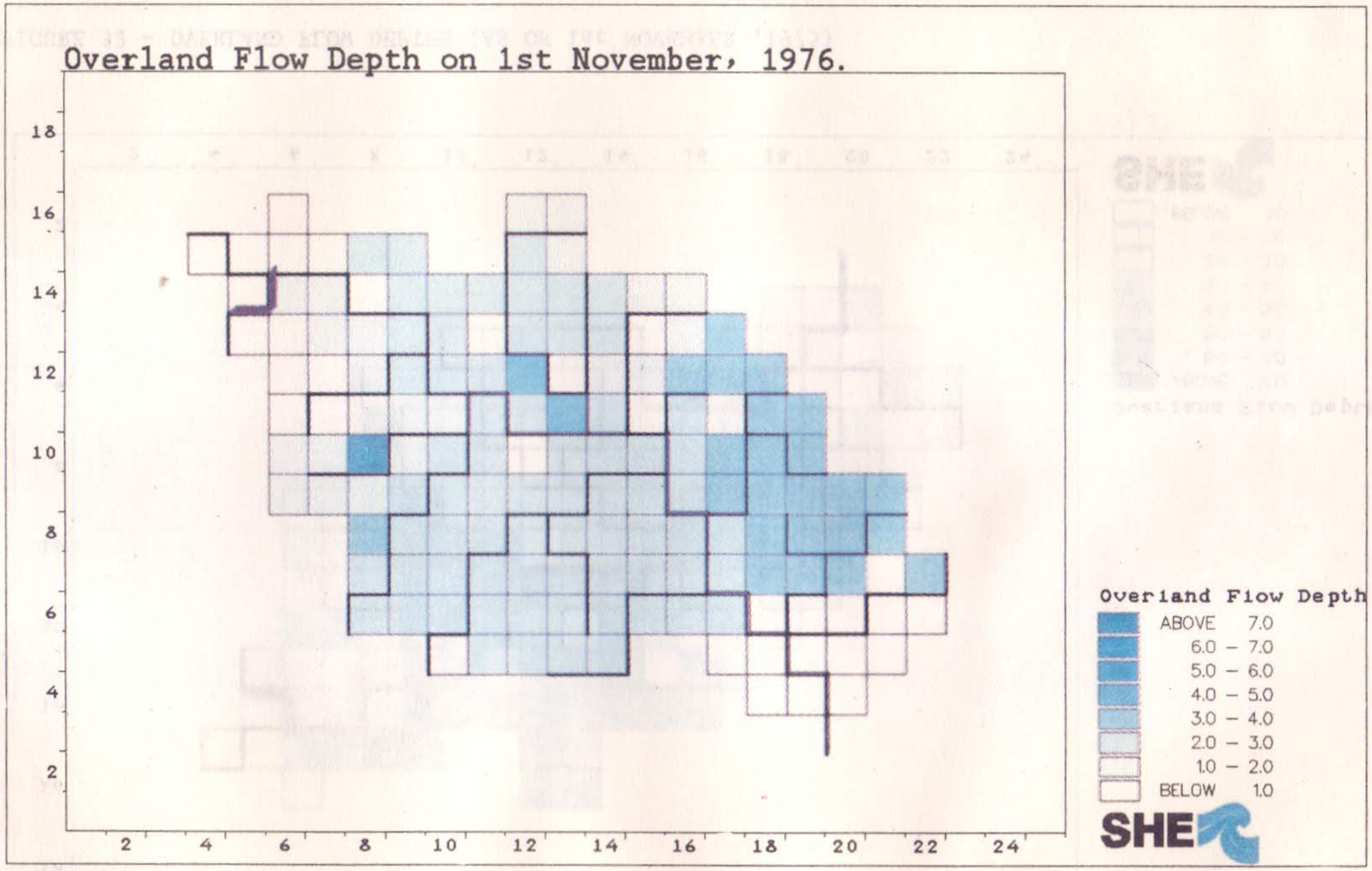

FIGURE 33 - OVERLAND FLOW DEPTHS (AS ON 1st NOVEMBER,1976)

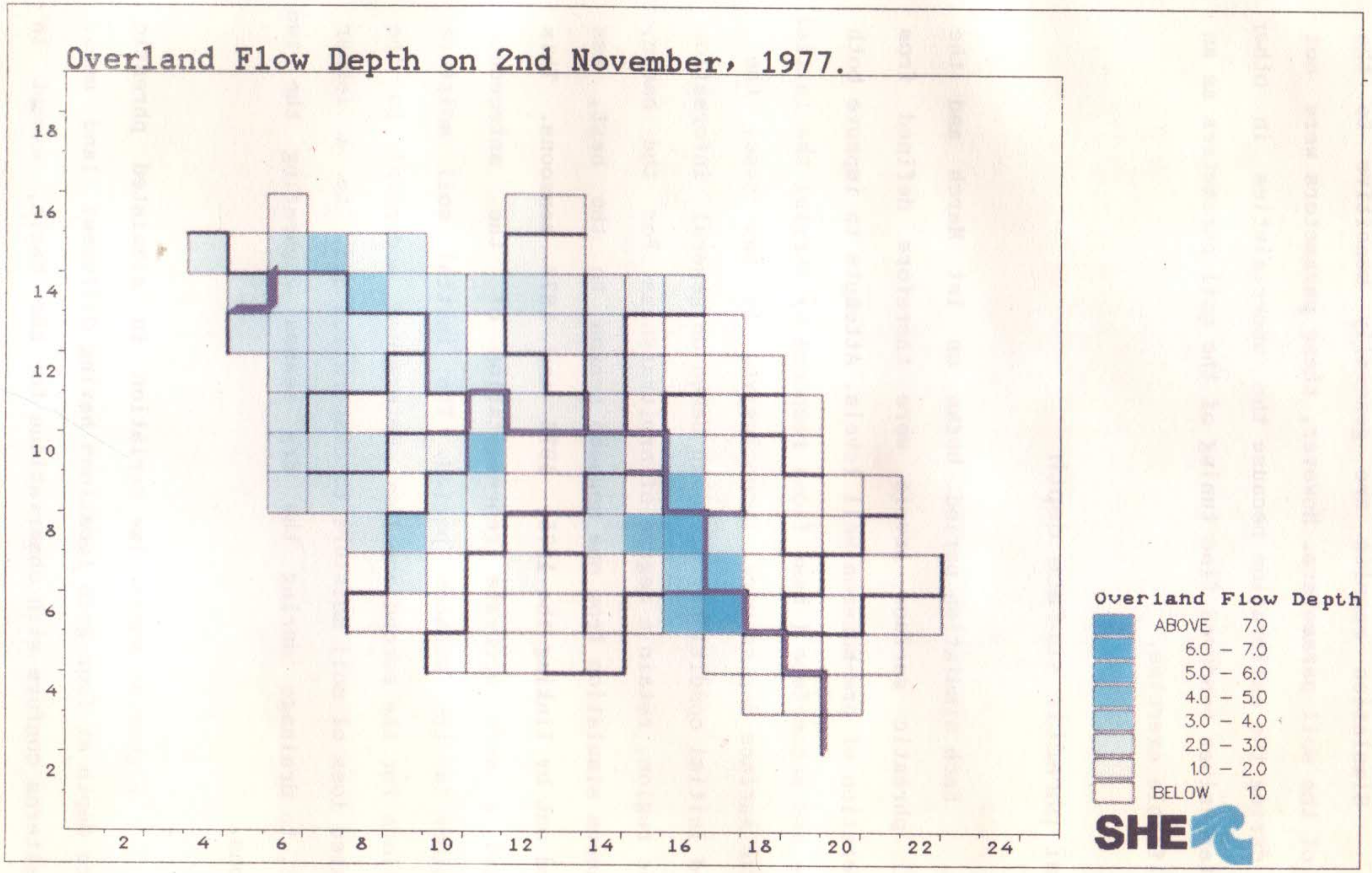

FIGURE 34 - OVERLAND FLOW DEPTHS (AS ON 2nd NOVEMBER,1977)

Soil parameters

Simulation results are generally sensitive to the values of the soil parameters. However, these parameters were not varied during the calibration because the uncertainties in other parameter values rendered fine tuning of the soil parameters as an unjustifiable exercise.

Initial phreatic surface depth

Each simulation period began on 1st March and the initial phreatic surface levels were therefore defined from consideration of pre-monsoon well levels. Attempts to improve both surface and subsurface (base flow) response by varying the initial phreatic surface depths were inconclusive. In any case, the imposed initial conditions, although based on general information for the region, retain a degree of arbitraryness. For the basin, continuous simulation from one monsoon season to the next, was carried out by linking the 1975, 1976 and 1977 monsoons. This provided a more accurate representation of the antecedent conditions for the monsoon period. The initial soil moisture conditions for the second are then determined according to the simulated loss of soil moisture to evaporation and, to a lesser extent, to drainage during the dry season separating the two monsoons.

Figure 35 shows time variation in simulated phreatic surface depth at four grid locations having different land uses. The patterns conform with observations for the basin, except in simulating a relatively long period in which the phreatic surface lies at the ground surface. It seems unlikely that such a period of complete waterlogging in the forest areas occurs in practice

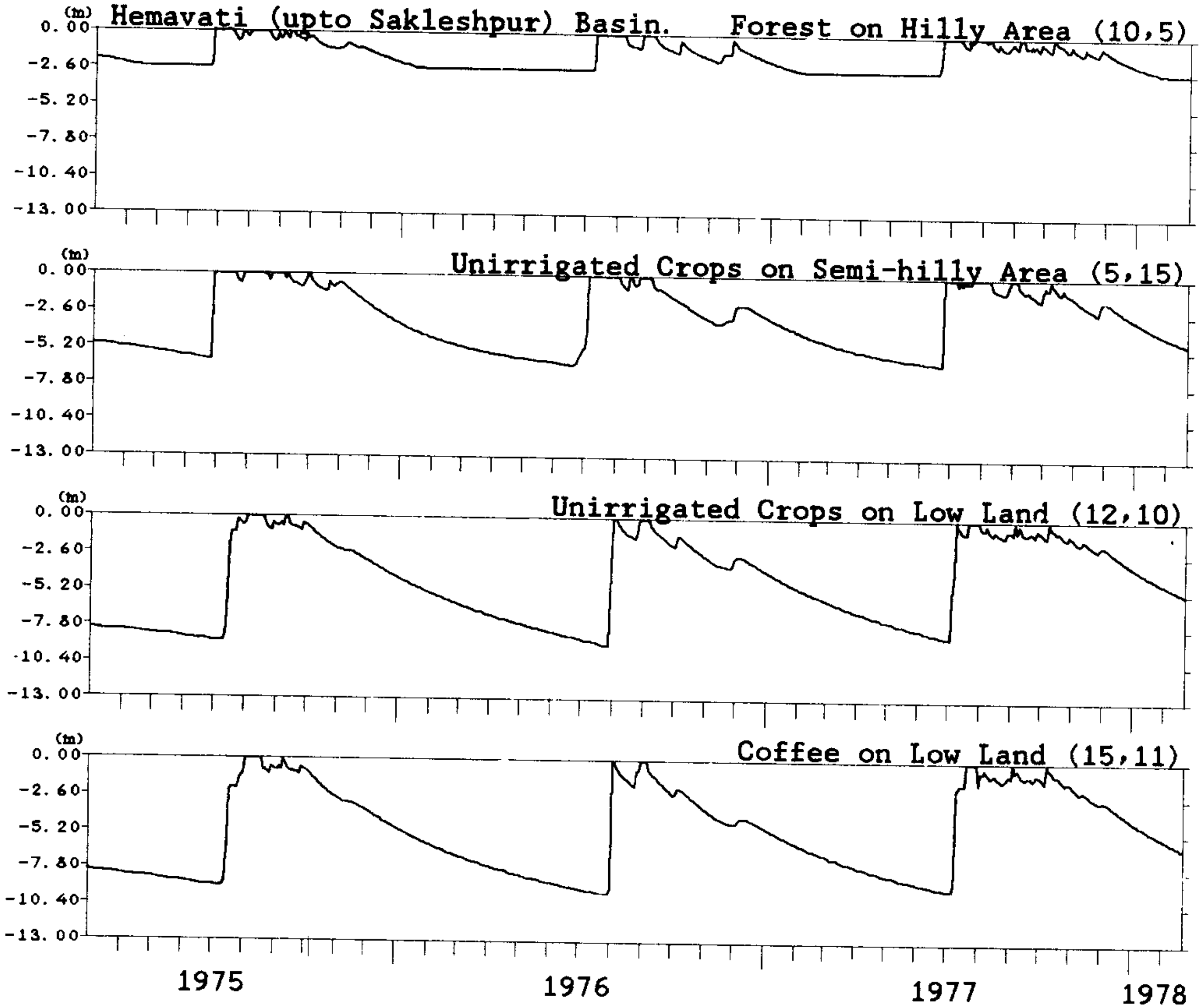

FIGURE 35 - VARIATIONS IN SIMULATED PHREATIC SURFACE DEPTH FOR DIFFERENT LAND USES(CALIBRATION)

since it implies widespread loss of trees. However, the simulated antecedent conditions for successive monsoons return to roughly the same level as the imposed initial conditions. Figures 36, 37 and 38 present the pre-monsoon and post-monsoon phreatic surface depths in the basin for the year 1975 and phreatic surface depths as on 1st March, 1978. Calibration against well data has not been possible but the patterns conform with general observations for the basin.

Unsaturated zone

Under the conditions of heavy rain falling on dry soil, typical of the early monsoon conditions, numerical instabilities and mass balance errors may occur in the simulations if the calculation time step and vertical distance step in the soil column are not kept below critical values. A mass balance check was made for each node point in the vertical for the unsaturated zone calculations. In the mass balance check, the error is tested against a specified tolerance and if it exceeds this value, the dependent variables are corrected and the exercise repeated. The solution of the highly nonlinear equation of unsaturated flow is sensitive to the size of the time step and a careful manual check of the mass balance error, for example, inspection of water table fluctuations is recommended in any simulation run.

Figure 39 shows the unsaturated zone conditions at a grid location (unirrigated crops on low land). It also shows the simulated evapotranspiration variations responsible for producing the variation in unsaturated zone conditions. In line with observations (section 3.4), potential evaporation is satisfied and soil moisture is recharged during the monsoon. During the dry season, soil moisture in the root zone is depleted by

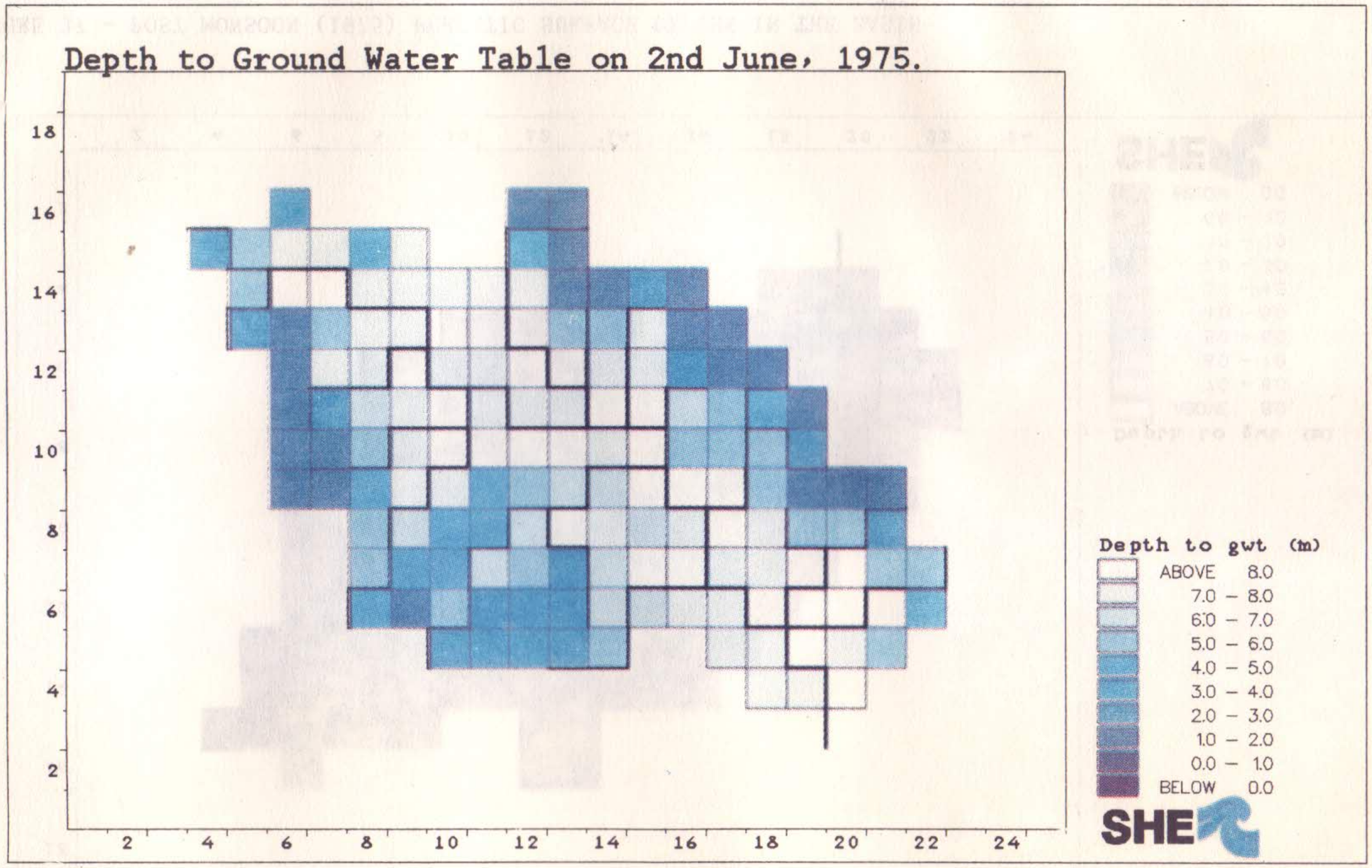

FIGURE 36 - PRE MONSOON (1975) PHREATIC SURFACE DEPTHS IN THE BASIN

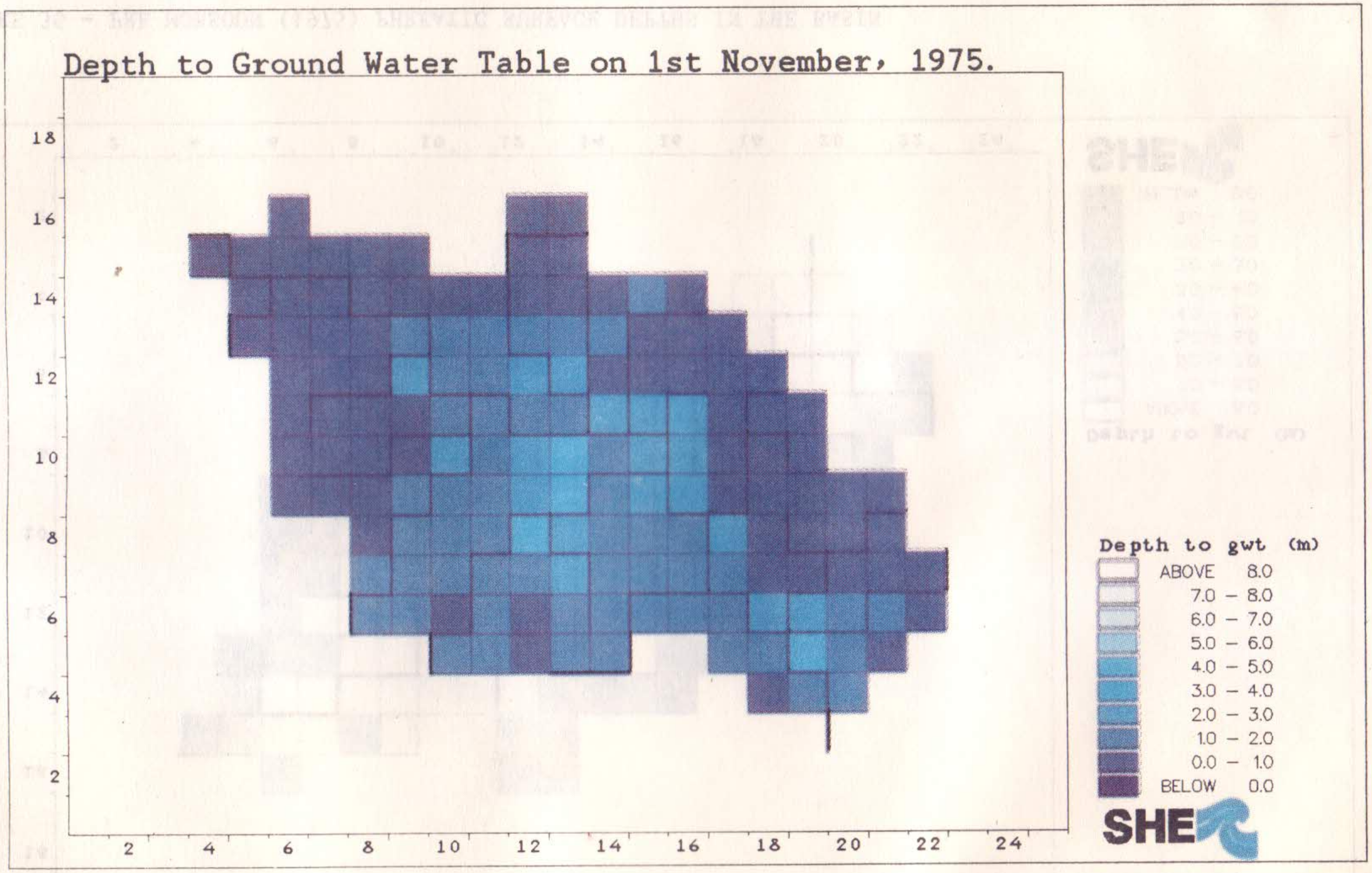

FIGURE 37 - POST MONSOON (1975) PHREATIC SURFACE DEPTHS IN THE BASIN

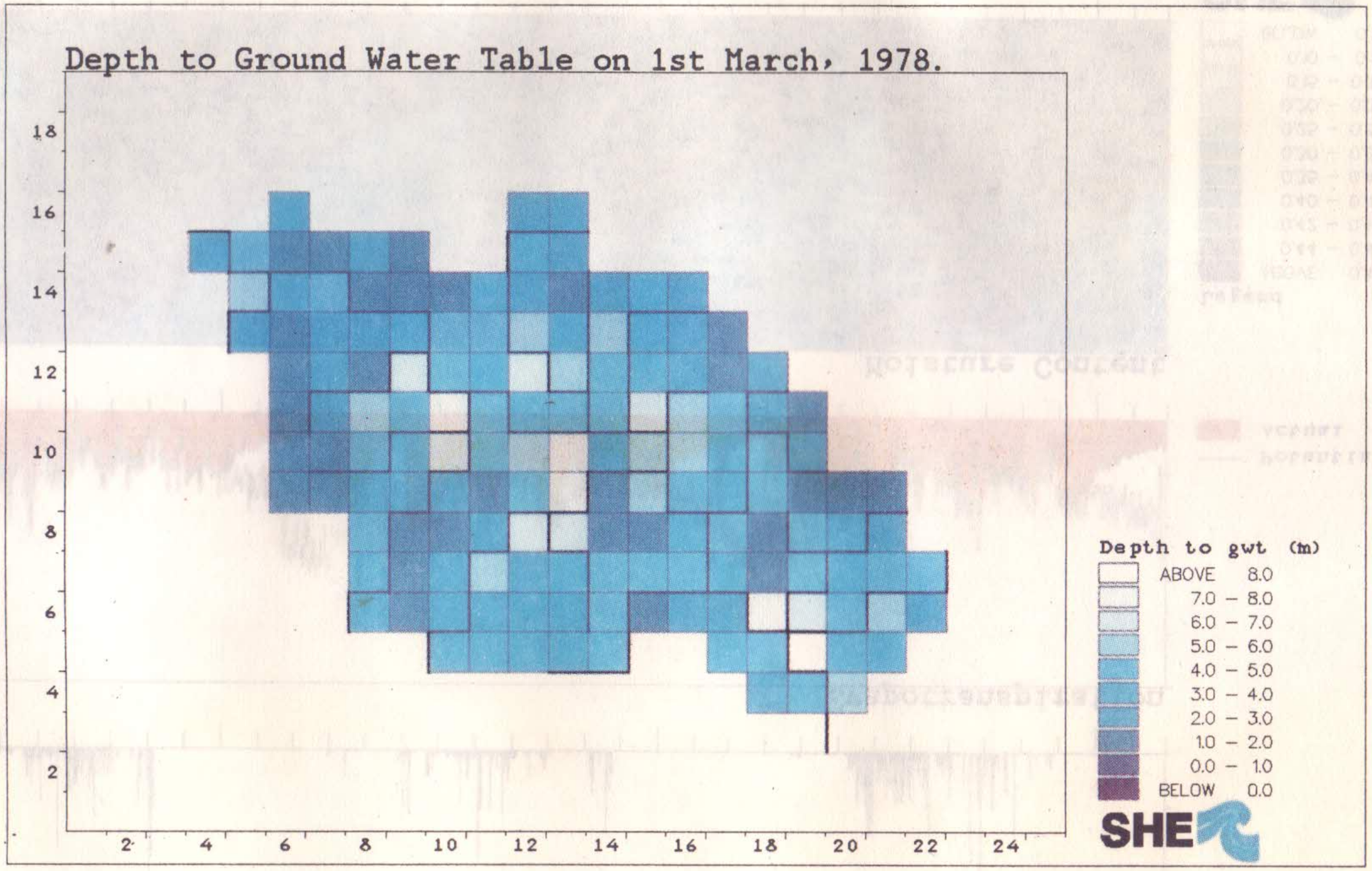
Depth to Ground Water Table on 1st March, 1978.
2
4
6
8
10
12
14
16
18
20
22
24
Depth to gwt (m)
ABOVE 8.0
7.0 – 8.0
6.0 – 7.0
5.0 – 6.0
4.0 – 5.0
3.0 – 4.0
2.0 – 3.0
1.0 – 2.0
0.0 – 1.0
BELOW 0.0
SHE

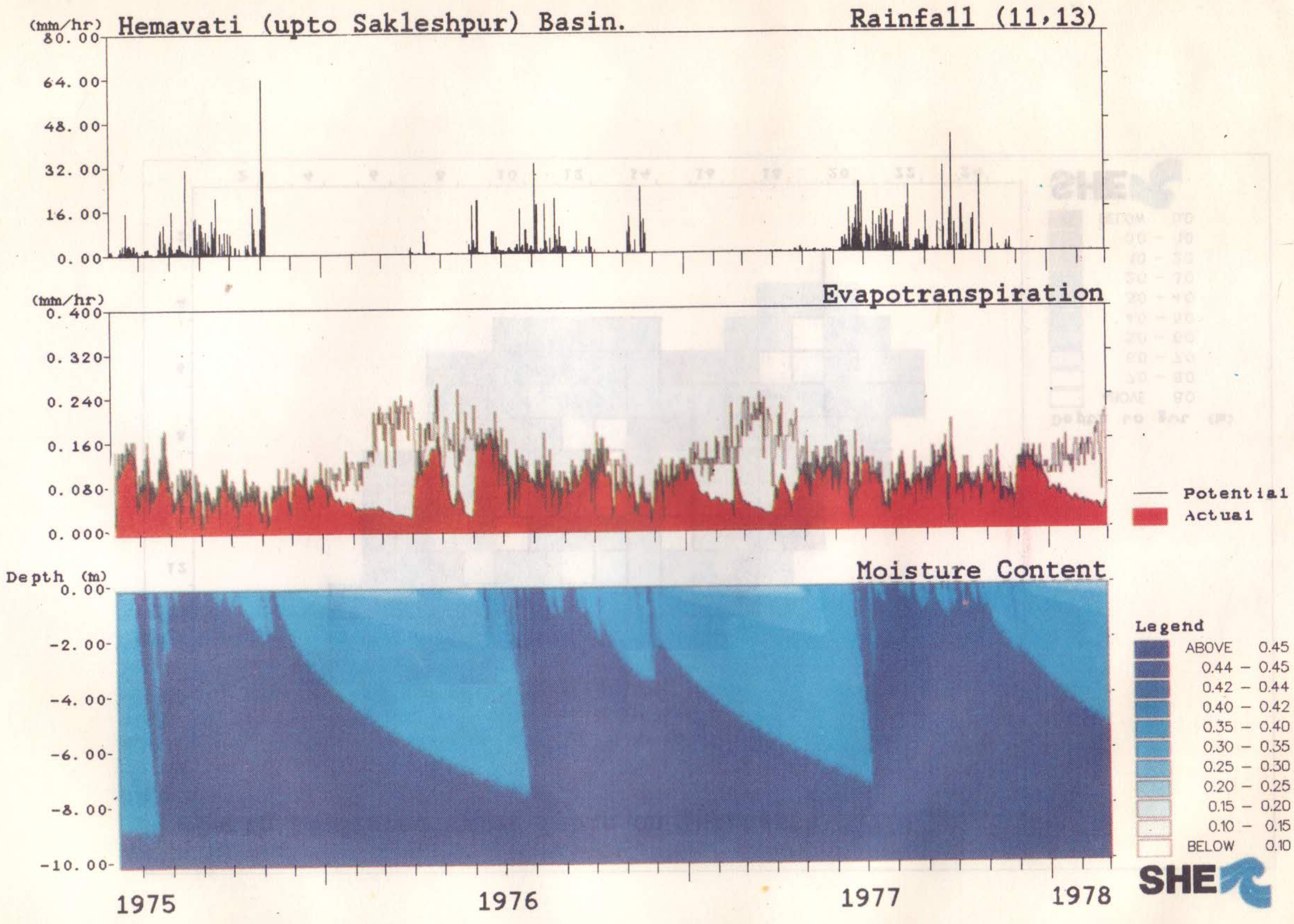

FIGURE 39 - UNSATURATED ZONE CONDITIONS (UNIRRIGATED CROPS ON LOW LAND, - CALIBRATION

evapotranspiration and actual evapotranspiration rates then fall below the potential rate.

Saturated zone

Simulated base flows were at first too slow, so with the aim of increasing them, the sensitivity of the simulated response to saturated zone conductivity was investigated. Tests encompassed values in the range 7.5 to 15.0 m/day, eventually setting on 10.0 m/day. This value contributed to a higher base flow and supported a faster drainage of the soil reservoir, so reducing the tendency to simulate unrealistically prolonged periods of water logging during the monsoon. Figure 40 presents the base flow, drainage flow and overland flow for the calibration period.

Table 19 shows the final calibrated parameter values. The calibration shows that by adjusting just few parameters and noting the effects on the simulated hydrographs for the basin and relating the responses to the characteristics of the basin, it is possible by physical reasoning to improve the simulation. Figure 41 shows patterns of simulated hydrographs for the'best-fit' run. The figure depicts the comparisons of the simulated and measured discharge time series at the basin outlet for monsoon seasons of 1975,1976 and 1977. Comparison of the monthly mass balance between the observed and simulated hydrographs are shown in table 20. Monthly water balance components for the calibration period are presented in table 21. The calibration, in general, can be considered as satisfactory when given the present uncertainty in the parameter values. The following observations were made -

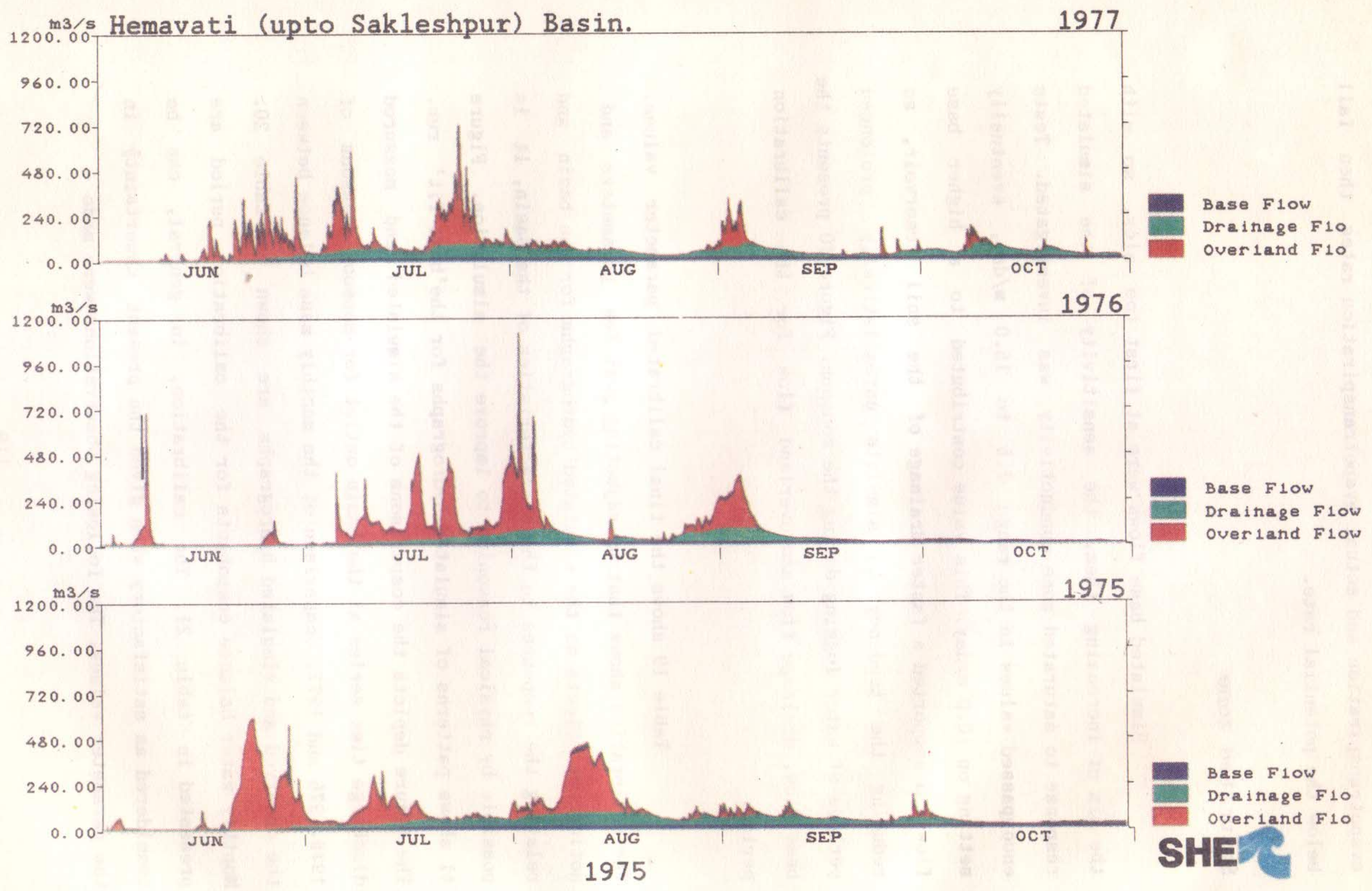

FIGURE 40 - BASE FLOW,DRAINAGE FLOW AND OVERLAND FLOW (CALIBRATION)

Table 19 : Calibrated Parameter Values

S.No.	Parameter		Value
1.	Soil depth:		
		low land	12.5 m
		semi-hilly	7.5 m
		hilly	2.5 m
2.	Strickler roughness coefficient for overland flow		1.0 $m^{1/3}/s$
3.	Strickler roughness coefficient for channel flow		20 $m^{1/3}/s$
4.	Detention storage		0.01 m
5.	Saturated conductivity (unsaturated zone)		0.1 m/day
6.	Saturated zone conductivity		10.0 m/day
7.	Initial depth to phreatic surface:		
		low land	8.0 m
		semi-hilly	5.0 m
		hilly	2.0 m
8.	Depth below surface to drainage system		1.0 m
9.	Drainage coefficient		0.01

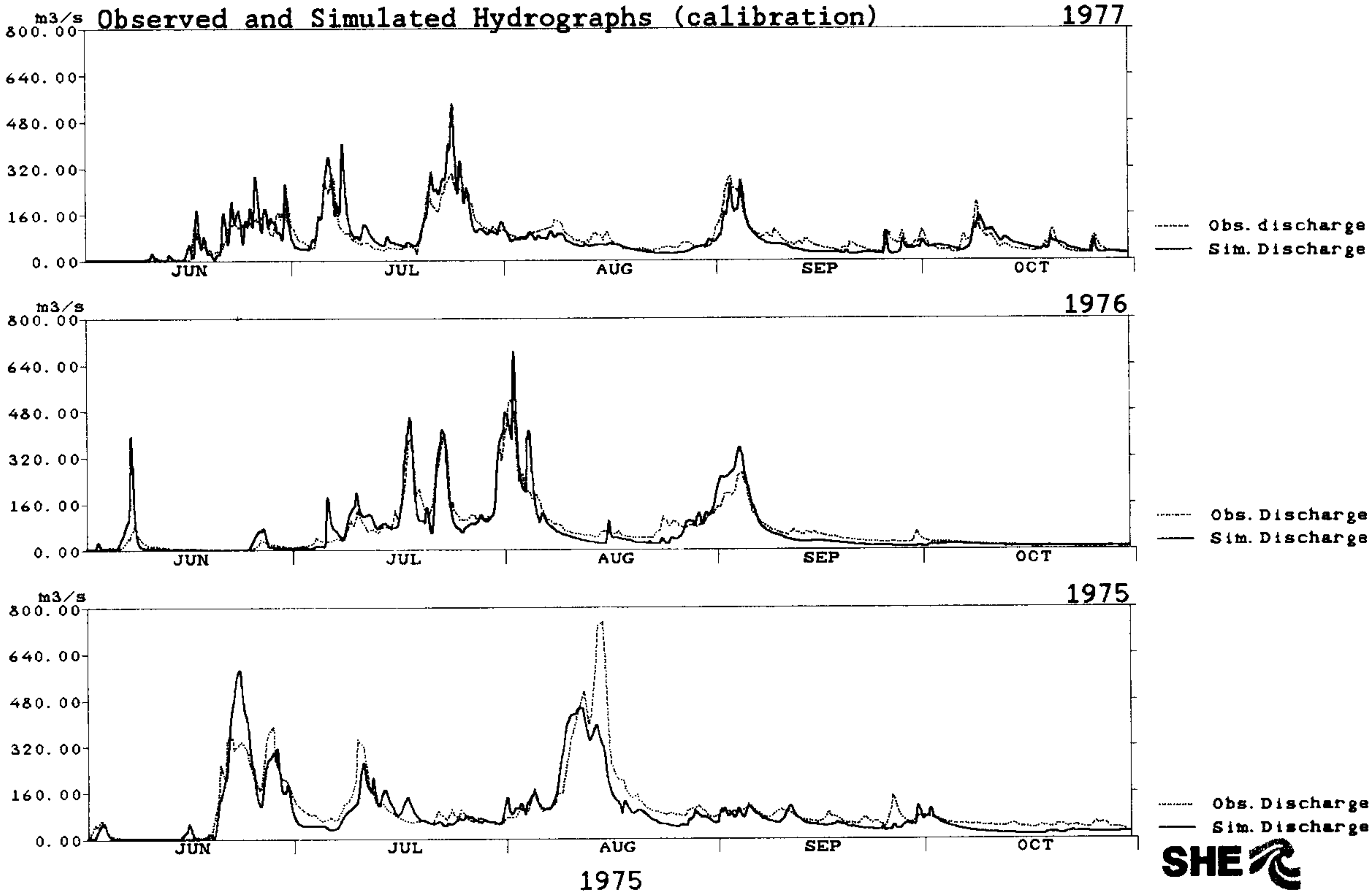

FIGURE 41 - OBSERVED AND SIMULATED HYDROGRAPHS AT THE SAKLESHPUR GAUGING SITE(CALIBRATION)

Table 20 : Comparison of Monthly Volumes for Observed and Simulated Hydrographs at the Sakleshpur Gauging Site for Calibration Period

Year	Month	Areal Mean Rainfall (mm)	Hydrograph Volumes (mm) Observed	Simulated
1975	June	978.77	467.04	476.29
	July	561.17	430.08	381.33
	August	752.34	870.22	704.76
	September	314.53	336.06	266.28
	October	116.74	208.94	125.42
	Total	2723.55	2312.34	1954.08
1976	June	373.15	58.14	92.40
	July	1041.61	584.53	589.64
	August	459.21	480.97	453.51
	September	281.46	318.50	303.88
	October	31.20	66.17	61.00
	Total	2186.63	1508.31	1500.43
1977	June	681.84	241.21	261.69
	July	706.80	560.48	657.94
	August	312.95	318.49	250.10
	September	353.76	367.64	270.06
	October	253.79	228.63	234.28
	Total	2309.14	1716.45	1674.07

Table 21 : Monthly Water Balance during Calibration Period

Note: All quantities are in mm.

Year	Month	Rainfall (p)	River Flow (q)	Evaporation (ep)	Change in Over-land Storage (h_o)	Change in River Storage (h_r)	Change in Sub-surface Storage (Δs)	Water Balance Error (p-q-ep-h_o-h_r-Δs)
1975	June	919	431	70	29	9	373	+7
	July	580	413	74	-26	-7	129	-3
	August	774	700	48	1	1	21	+3
	September	306	264	52	1	-1	-6	-4
	October	144	146	48	-2	-1	-44	-3
	November	82	102	47	-1	-1	-65	0
	December	0	45	57	0	0	-102	0
1976	January	0	40	37	0	0	-78	+1
	February	0	28	28	0	0	-55	-1
	March	11	32	17	0	0	-40	+2
	April	88	30	66	0	0	-4	-4
	May	10	29	41	0	0	-54	-6
	June	378	90	105	2	0	179	+2
	July	985	530	79	47	14	309	+6
	August	457	470	67	-36	-8	-42	+6
	September	312	345	73	-14	-5	-81	-6
	October	76	63	69	1	-1	-57	+1
	November	200	78	44	0	1	84	-7
	December	7	69	66	0	-1	-127	0
1977	January	0	46	46	0	0	-89	-3
	February	4	28	27	0	0	-56	+5
	March	6	30	21	0	0	-46	+1
	April	65	30	48	0	0	-11	-2
	May	171	32	79	1	0	66	-7
	June	676	240	72	22	13	328	+1
	July	683	651	62	-13	-9	-1	-7
	August	319	270	70	-6	-1	-17	+3
	September	357	273	78	2	-1	-2	+7
	October	274	234	60	-7	-1	-30	+18
	November	131	73	59	2	0	-3	0
	December	0	64	81	0	-1	-146	+2
1978	January	0	45	38	0	0	-80	-3
	February	0	28	27	0	0	-58	+3

i. The hydrograph volumes are underestimated in the year 1975, but agreement is good in the years 1976 and 1977 (table 20).

ii. The principal peaks are well simulated, except for the 1975 peaks which are generally low (figure 41).

iii. For the year 1975, the simulations are significantly in error. It is not clear why these errors exist, especially as the simulations for other years are reasonably good. Checks on the measured rainfall and discharge data do not show any faults which might cause the errors. It is difficult to improve one of the simulations without further increasing the error in the other.

The results were encouraging in that they reflected the observed trends in soil moisture distribution for the wet and dry seasons, and similarly the simulated discharges were of the correct overall pattern and order of magnitude. Also the simulations were obtained using parameter values which all fell within physically realistic ranges even though the degree, to which those values were representative of actual basin conditions, was unknown. On the negative side, the simulations indicated extensive periods of waterlogging which are unlikely to have occurred in reality. It is probable that all the errors could be reduced by painstakingly altering the various parameters singly or in combination and also by carrying out detailed field measurements. However, the results would be subject to the law of diminishing returns. Therefore, the calibration presented can be considered as satisfactory.

5.4 Validation

Using the calibration results, simulations were carried out for the period March 1978 to February 1981. The basin parameters were kept at the same values and the only adjustment was to the initial phreatic surface levels. Results of calibration simulation (March 1975 to February 1978) were used to develop the correct initial levels for the validation period, through the use of 'SHE Output Retrieval Routine'.

Figures 42, 43 and 44 present the post-monsoon overland flow depths in the basin for the years 1978, 1979 and 1980 respectively. Figure 45 shows time variation in simulated phreatic surface depth at four grid locations having different land uses. Figures 46 and 47 present the pre-monsoon and post-monsoon phreatic surface depths in the basin for the year 1980. Figure 48 shows the moisture content and evapotranspiration variations at a grid location (coffee plantation on semi-hilly area). Figure 49 presents the base flow, drainage flow and overland flow for the validation period. Figure 50 shows the comparisons of observed and simulated hydrographs for monsoon seasons of 1978, 1979 and 1980. Table 22 presents the comparison of monthly volumes for observed and simulated hydrographs. Monthly water balance components for the validation period are presented in table 23. The following observations were made -

i. In all the three years, observed and simulated hydrographs are reasonably well matched, although the simulated hydrographs are more fluctuating than the observed ones (figure 50).

ii. The validation results are generally good for peak discharges (figure 50).

iii. The hydrograph volumes are underestimated in the year 1978, probably due to erroneous rainfall/runoff data for

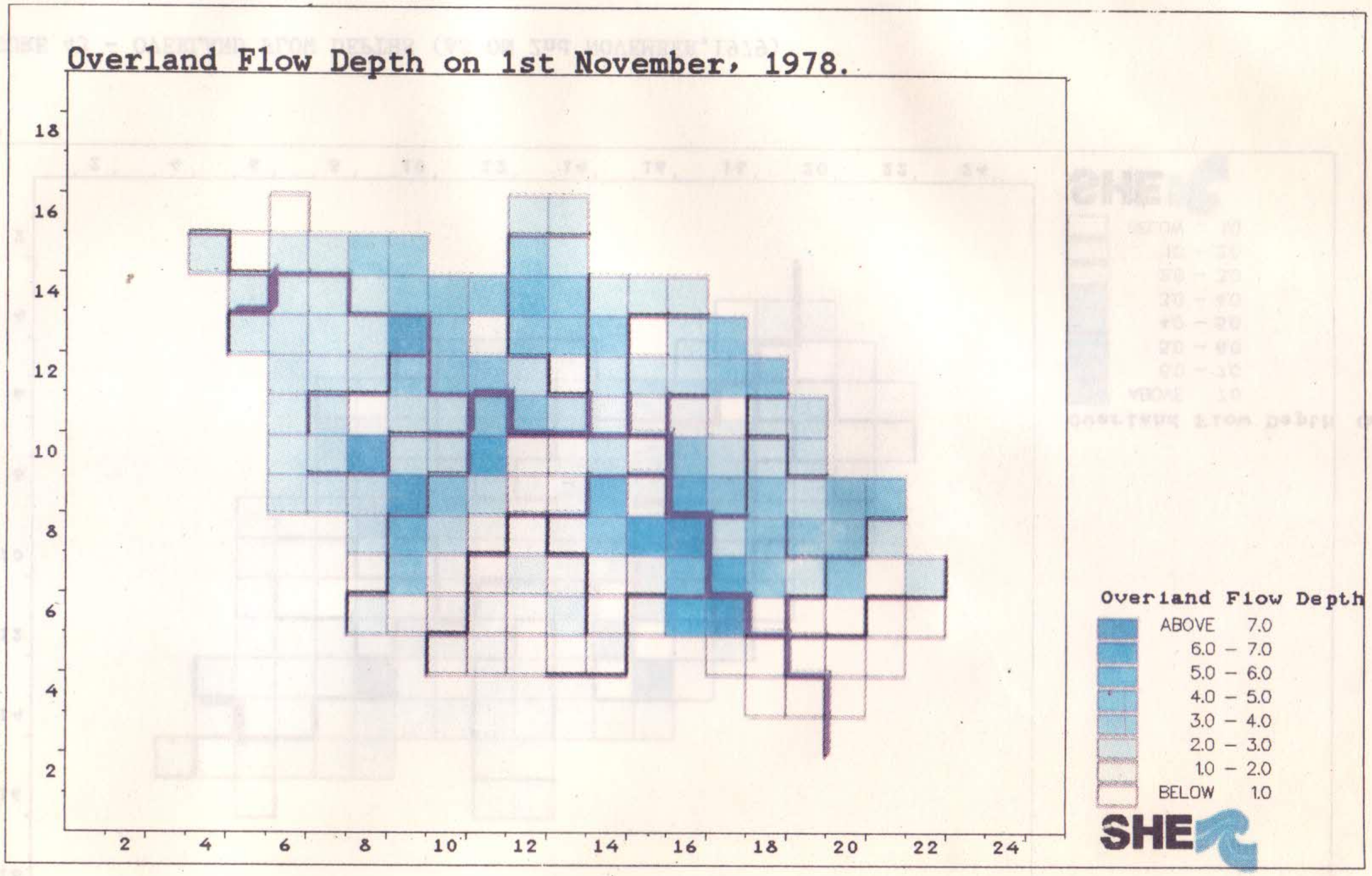

FIGURE 42 - OVERLAND FLOW DEPTHS(AS ON 1st NOVEMBER, 1978)

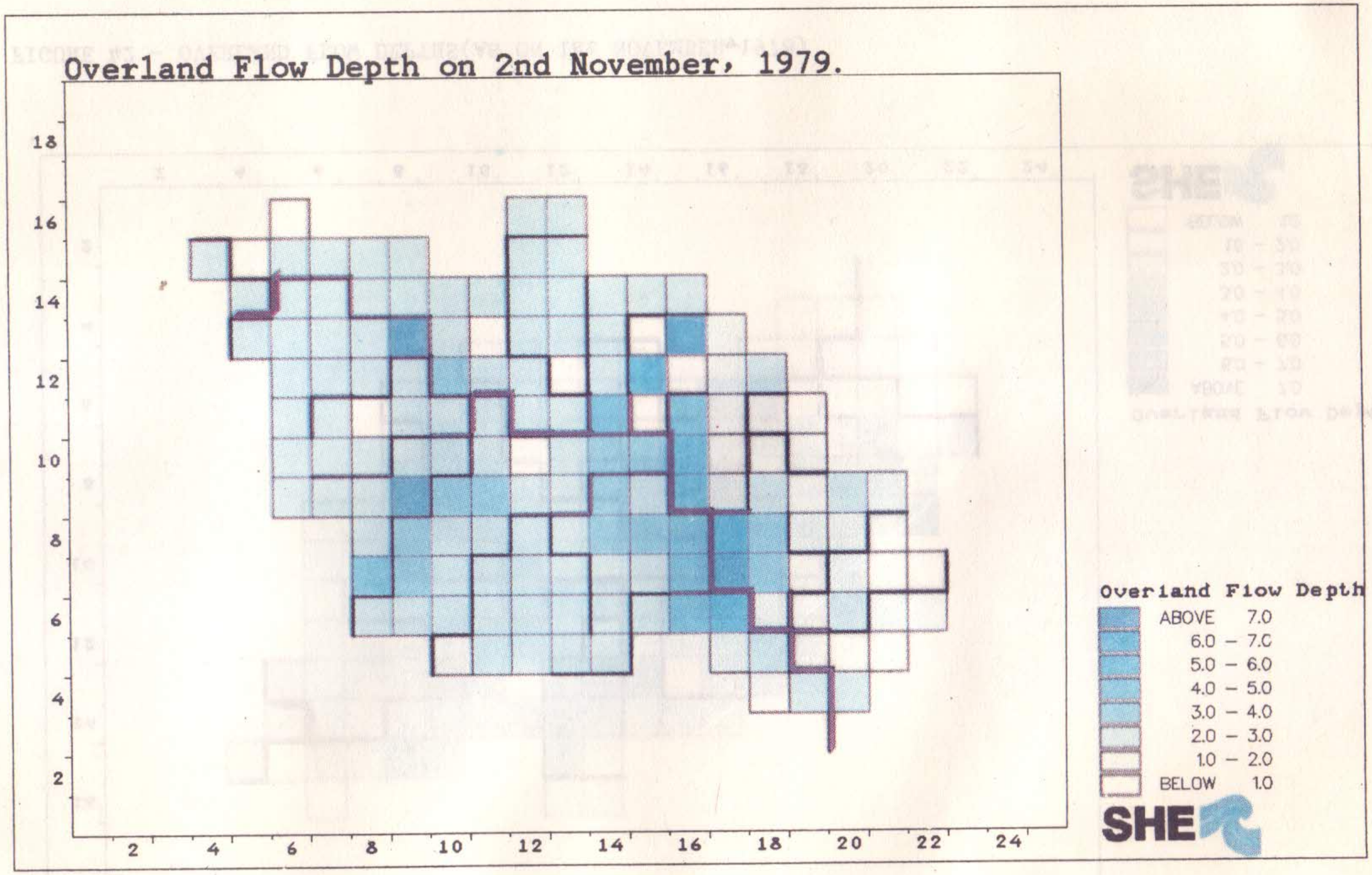

FIGURE 43 - OVERLAND FLOW DEPTHS (AS ON 2nd NOVEMBER,1979)

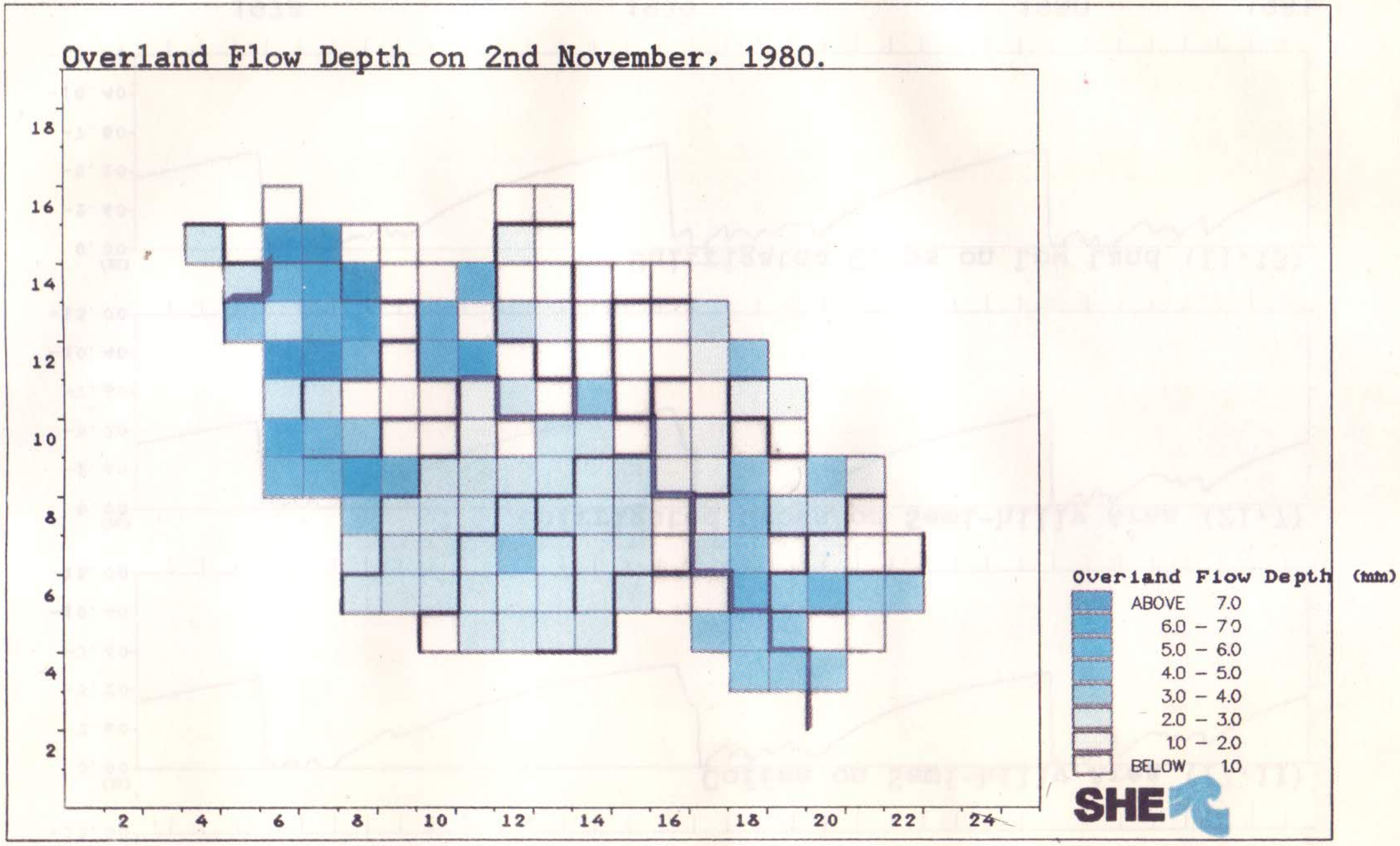

FIGURE 44 - OVERLAND FLOW DEPTHS (AS ON 2nd NOVEMBER,1980)

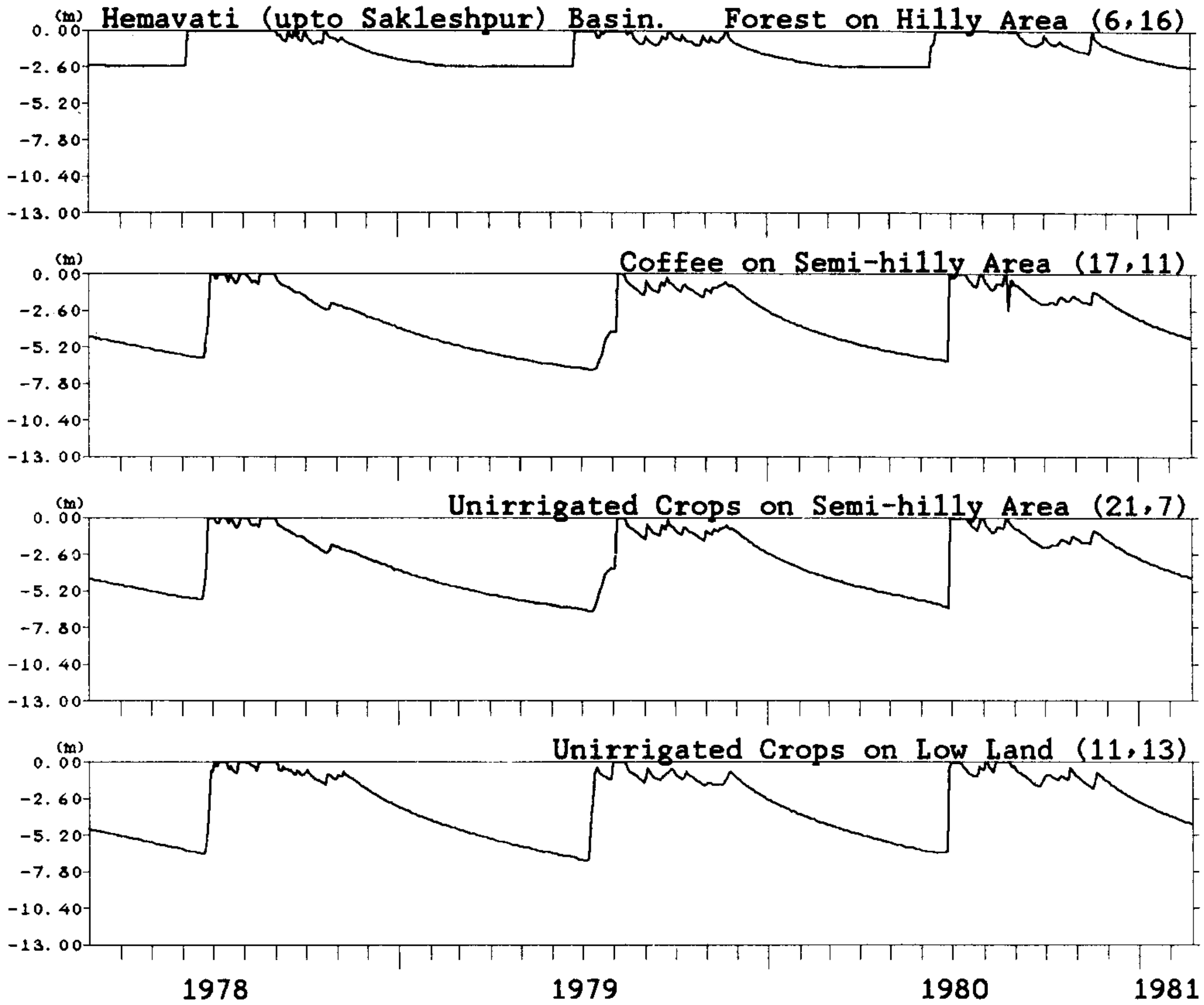

FIGURE 45 - VARIATIONS IN SIMULATED PHREATIC SURFACE DEPTH FOR DIFFERENT LAND USES (VALIDATION)

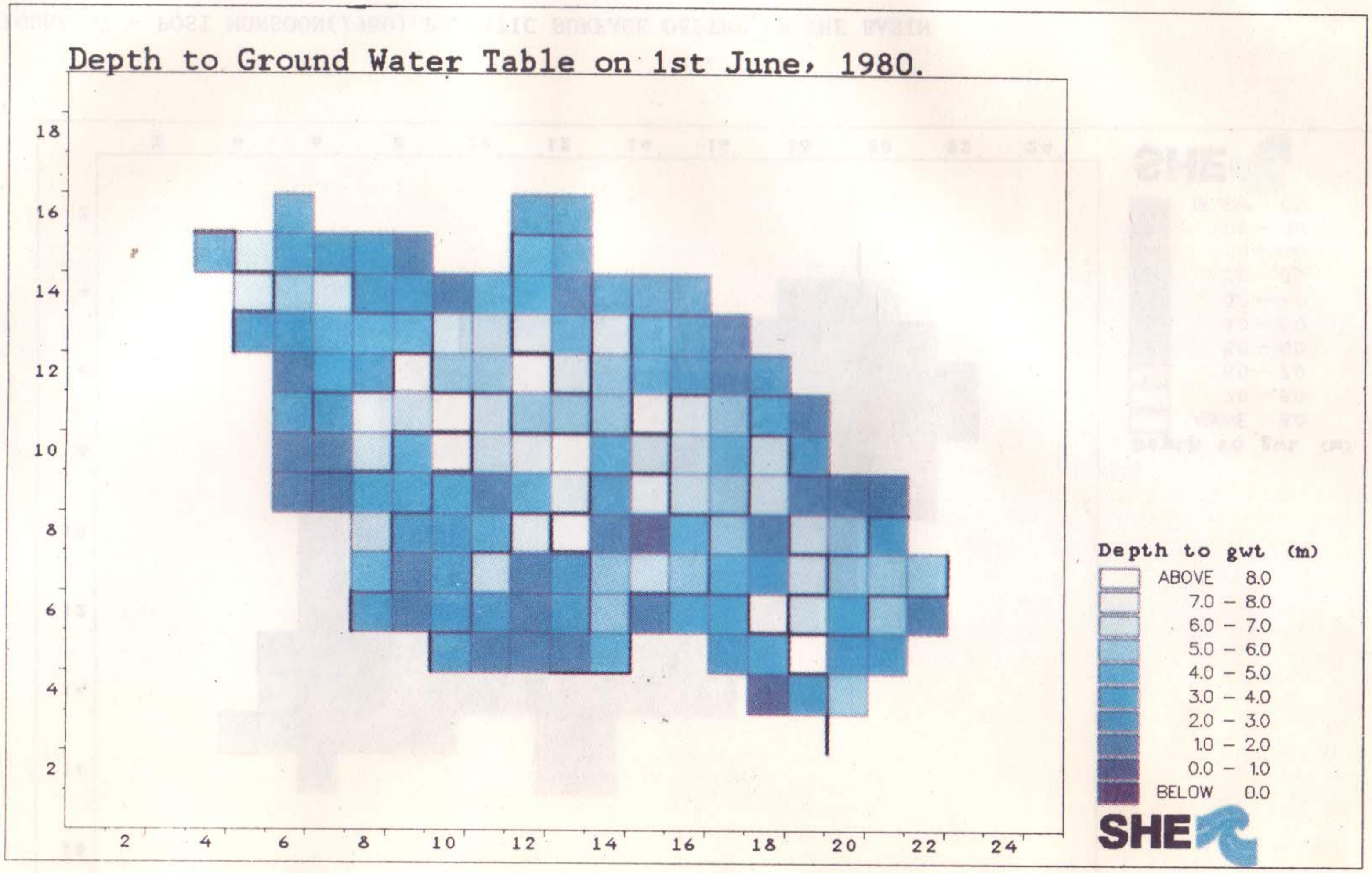

FIGURE 46 - PRE MONSOON (1980) PHREATIC SURFACE DEPTHS IN THE BASIN

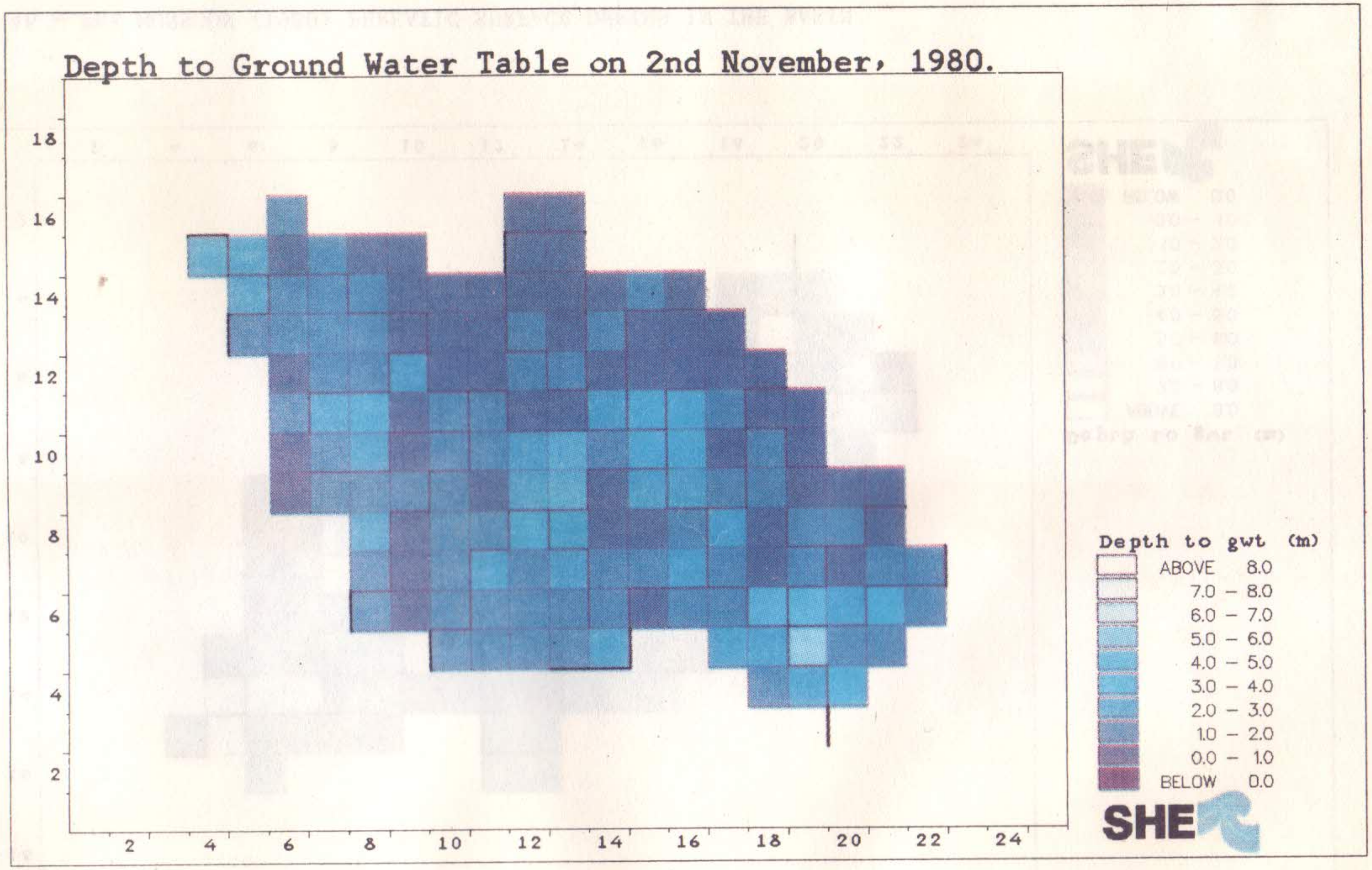

FIGURE 47 - POST MONSOON(1980) PHREATIC SURFACE DEPTHS.IN THE BASIN

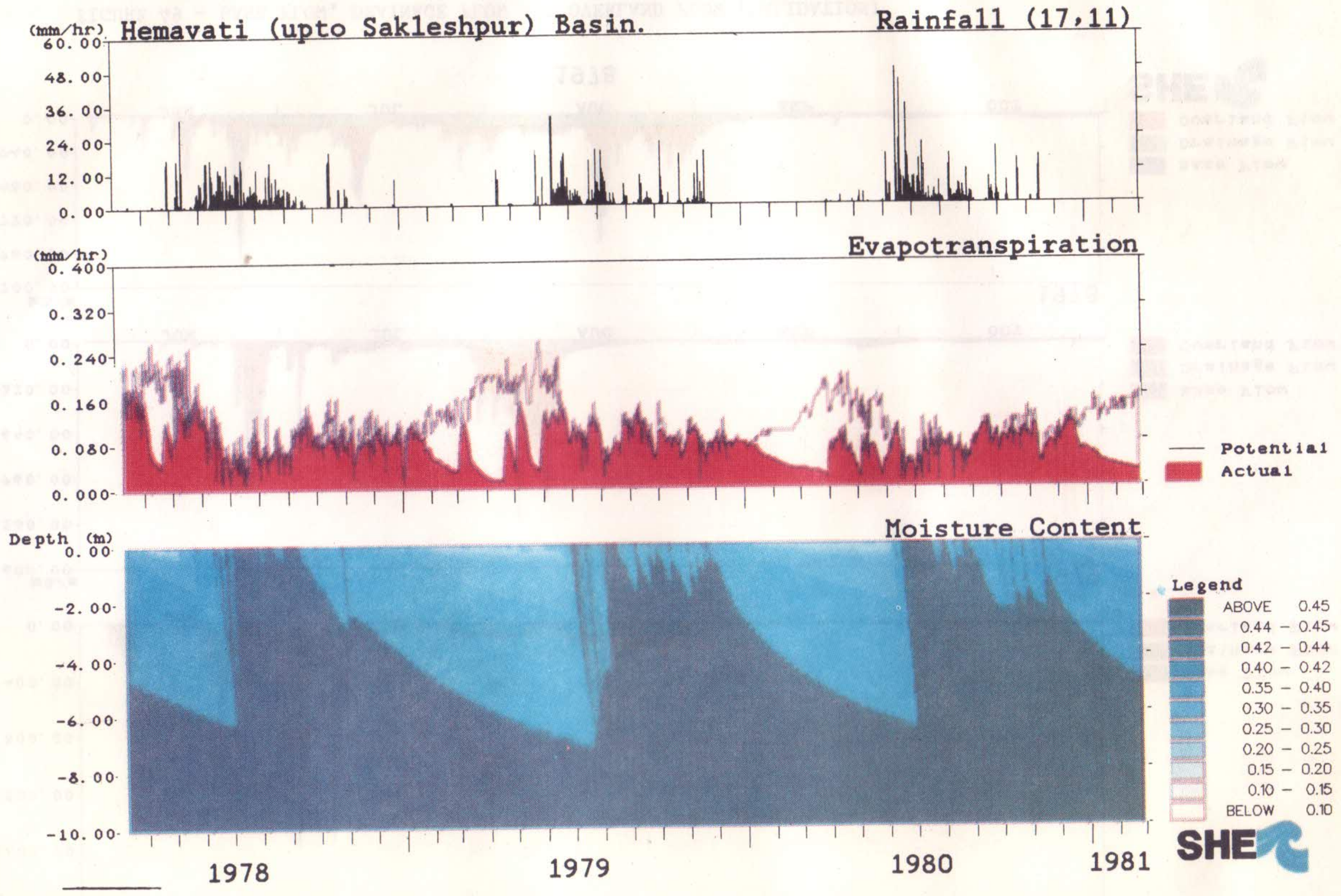

FIGURE 48 - UNSATURATED ZONE CONDITIONS (COFFEE PLANTATION ON SEMI-HILLY AREA)-VALIDATION

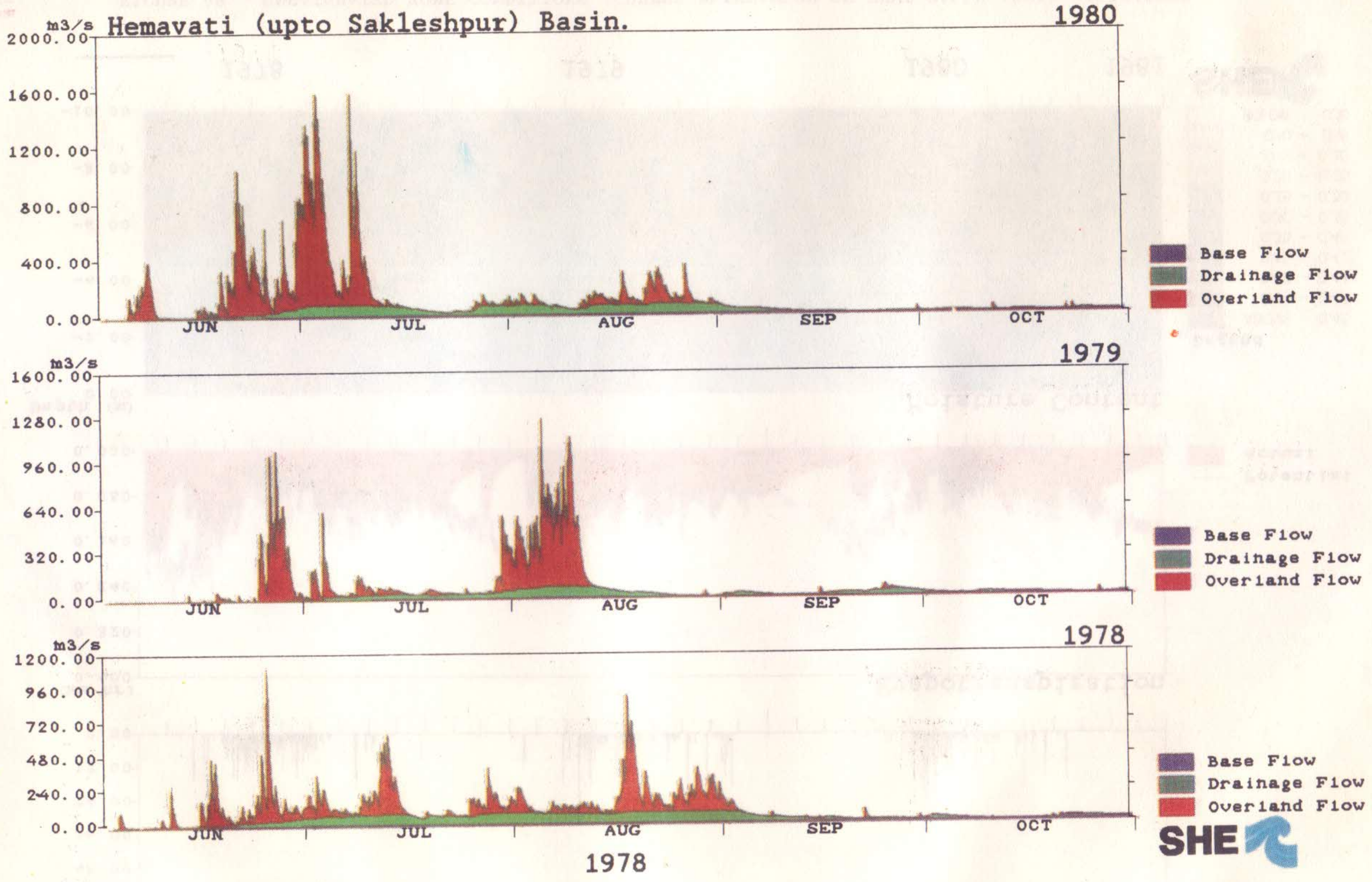

FIGURE 49 - BASE FLOW, DRAINAGE FLOW AND OVERLAND FLOW (VALIDATION)

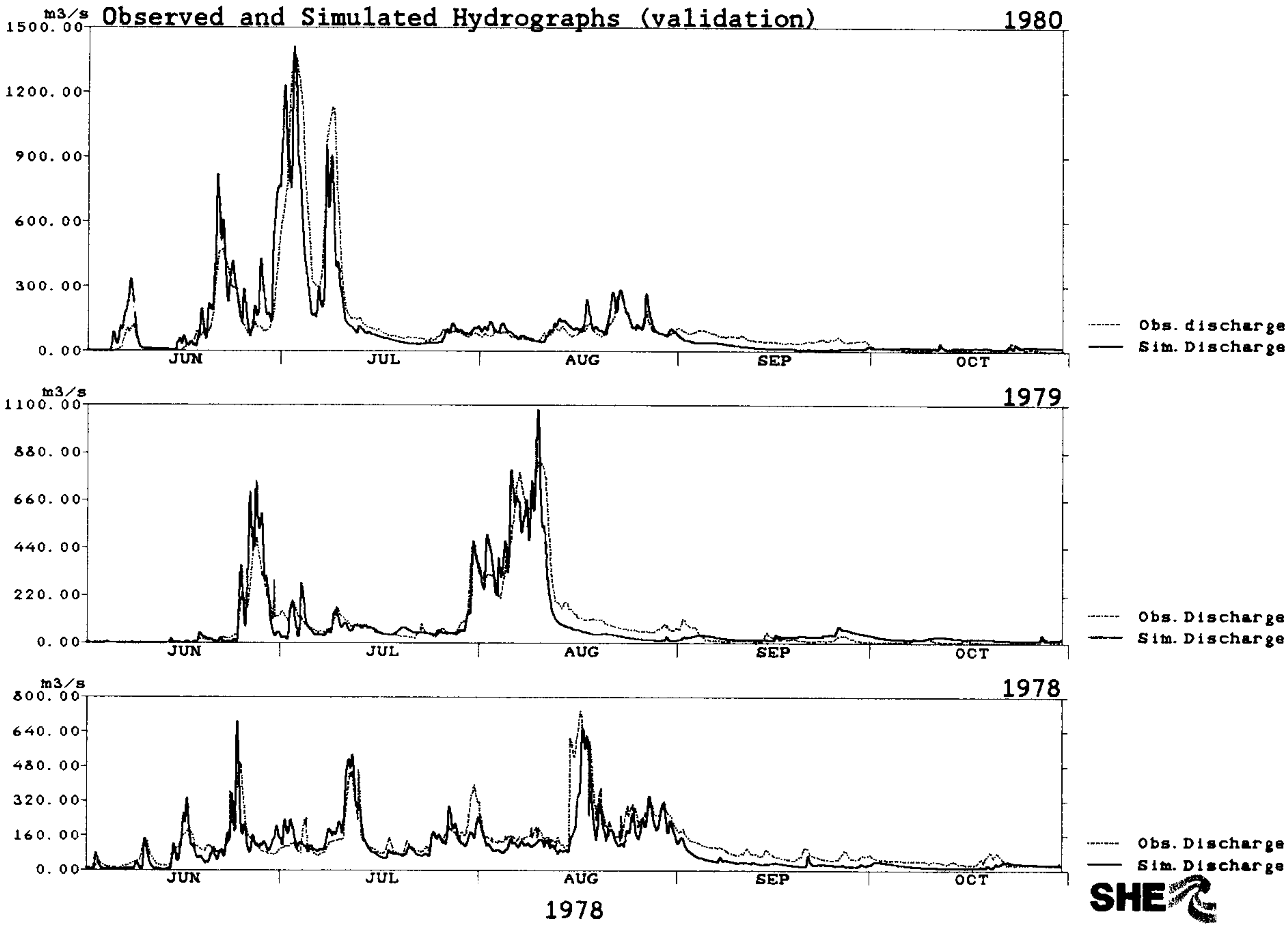

FIGURE 50 - OBSERVED AND SIMULATED HYDROGRAPHS AT THE SAKLESHPUR GAUGING SITE(VALIDATION)

the same year, as established through lumped water balance study (section 4.4). However the agreement is fair in the year 1979 and 1980 (table 22).

iv. The simulated phreatic surface levels and unsaturated zone conditions fluctuate according to the observed trends.

The results both validate the model and show that an effective calibration can be based on changes to a minimum of parameters.

Table 22 : Comparison of Monthly Volumes for Observed and Simulated Hydrographs at the Sakleshpur Gauging Site for Validation Period

Year	Month	Areal Mean Rainfall (mm)	Hydrograph Volumes (mm) Observed	Simulated
1978	June	762.02	427.33	388.14
	July	748.52	681.38	686.42
	August	847.16	1090.19	831.79
	September	202.39	365.93	178.56
	October	154.24	177.75	109.27
	Total	2714.33	2742.58	2194.18
1979	June	790.83	270.21	331.04
	July	600.22	405.10	363.92
	August	877.52	1125.09	945.80
	September	216.62	109.41	139.11
	October	150.03	42.64	95.64
	Total	2635.22	1952.45	1875.51
1980	June	1189.18	468.76	698.85
	July	1028.39	1377.23	1087.59
	August	552.66	457.26	529.14
	September	126.79	263.42	106.87
	October	107.66	53.62	88.44
	Total	3004.68	2620.29	2510.89

Table 23 : Monthly Water Balance during Validation Period

Note: All quantities are in mm.

Year	Month	Rainfall (p)	River Flow (q)	Evaporation (ep)	Change in Over-land Storage (h_o)	Change in River Storage (h_r)	Change in Sub-surface Storage (Δs)	Water Balance Error ($p-q-ep-h_o-h_r-\Delta s$)
1978	March	7	30	83	0	0	-111	+5
	April	73	30	64	0	0	-22	+1
	May	154	30	91	5	0	31	-3
	June	753	350	51	8	4	338	+2
	July	740	699	46	14	3	-23	+1
	August	849	800	44	7	5	0	-7
	September	209	228	74	-32	-11	-48	-2
	October	186	113	73	0	0	+3	-3
	November	55	77	61	0	-1	-83	+1
	December	26	45	53	1	0	-74	+1
1979	January	1	40	55	0	0	-97	+3
	February	8	28	29	0	0	-51	+2
	March	18	30	37	0	0	-50	+1
	April	37	30	39	0	0	-29	-3
	May	68	32	57	0	0	-15	-6
	June	762	325	85	9	2	339	+2
	July	474	287	70	10	4	95	+8
	August	1036	1028	61	-20	-5	-36	+8
	September	220	135	69	0	1	12	+3
	October	152	94	60	0	-1	-5	+4
	November	168	124	60	0	0	-12	-4
	December	0	61	63	0	-1	-125	+2
1980	January	0	45	45	0	0	-85	-5
	February	0	31	30	0	0	-64	+3
	March	4	30	26	0	0	-53	+1
	April	135	30	84	1	0	23	-3
	May	131	38	82	0	0	16	-5
	June	1091	592	47	74	26	349	+3
	July	1101	1165	41	-69	-23	-14	+1
	August	580	544	49	0	1	-2	-12
	September	112	119	67	-5	-3	-60	-6
	October	123	86	66	-1	0	-25	-3
	November	131	84	54	0	0	-7	0
	December	0	55	70	0	-1	-124	0
1981	January	0	39	37	0	0	-76	0
	February	0	28	23	0	0	-53	+2

5.5 Analysis of Results

Despite the problems posed by uncertainty in the parameter base, the simulation results are encouraging. Points of note are as follows:

a. In line with the observed hydrological response for the monsoon period (section 3.4), the SHE simulates, as expected, the absorption of the initial rainfall by recharge of the soil moisture reservoir, rising phreatic surface levels and eventual saturation or near saturation of the soil, decreased infiltration and increased runoff for the later rainfall and a limited ground water recharge characterised by low river base flow rates. Simulated discharges are generally of the correct order of magnitude relative to the measured values.

b. In line with the observed hydrological response for the dry period (section 3.4), the SHE simulates depletion of the soil moisture reservoir by evapotranspiration from a state of near saturation at the end of the monsoon to wilting point in the root zone by the start of the following monsoon. Potential evaporation is satisfied during the monsoon season but exceeds actual evapotranspiration during the dry season.

c. The simulations are based on parameter values which fall within physically realistic ranges even though their measured values are unknown or are surrounded by uncertainty. The final calibration values are as shown in table 19.

On the negative side, particular problem areas are as follows:

a. The simulated and measured water balances for the overall hydrograph of each monsoon season do not always match.

b. The simulations indicate extensive periods of waterlogging which are unlikely to have occurred in reality.

5.6 Remarks

Improvement in the particular problem areas will require consideration of the following:

i. The parameter values (particularly for the soils) should be evaluated more accurately, if necessary by field measurements in the basin. Sensitivity tests can show which parameters are the most important and therefore require the most attention. Similarly, improved information on basin water balance and hydrological response will indicate in what direction the simulations should be modified to produce closer agreement between the measured and simulated balances.

ii. The initial phreatic surface depth can have a significant effect on the simulations for an ensuing monsoon season. The conditions must therefore be carefully based on all available information or else obtained for a given monsoon period by running the model from the previous monsoon period.

iii. Grid size, river channel representation, the ratio of the number of channel links to grid squares, calculation time step and the intervals at which rainfall input is specified, all influence the simulation results. Sensitivity tests are needed to show what the effects are and to provide guidance on selection of these quantities for future applications.

6.0 SENSITIVITY ANALYSIS

6.1 General

The calibration and operation of physically-based distributed catchment models such as SHE requires an approach different from that associated with black box or even lumped physically-based models. In particular, physically-based distributed models, while not requiring lengthy hydrological records for their calibration, do require the evaluation of a large number of parameters describing the physical characteristics of the catchment on a spatially distributed basis. In principle, the parameters and their distributions can be measured in the field but the expense of such an effort applied to all the parameters would prohibit practical implementation of the models. Alternatives to intensive field surveys are available but, since they inevitably involve approximations, they have given rise to questions concerning the accuracy with which the parameters and their spatial distributions need to be evaluated. Further questions have arisen concerning the difficulty of calibrating parameter sets involving large number of parameters and the degree to which point field measurements can be used to represent average conditions at the large spatial scales of the grid squares used in the numerical simulations. Thus before physically-based distributed models can be used with confidence, it needs to be shown that evaluation of the parameter sets does not pose an undue problem.

Sensitivity analysis is useful for identifying the model parameters which have significant effect on the simulation results and therefore need to be evaluated most accurately. The analysis is also useful for indicating the effect on the output of a given level of uncertainty in the input and for providing information on how well the model can simulate the impacts of changes in basin characteristics.

6.2 Sensitivity Analysis

Sensitivity analysis has been carried out for the basin for studying the sensitivity of different parameter values to the simulated hydrological regime. In order to minimize the computing requirements, the sensitivity analysis was restricted to only 1976 hydrographs used in the calibration. In each of the test, just one parameter was altered from the calibrated parameter set. The simulated response (in terms of hydrograph monthly volumes and annual peak discharge) was then compared with the calibration simulation derived for the year 1976 and accounted for the differences by physical reasoning. The ability to follow this approach is a particular advantage of using physically-based distributed models, providing extra information regarding parameter sensitivity and promoting confidence in the results. It should be noted that the results are unlikely to be directly applicable to different types of basins, although the basic technique remains appropriate.

In the following, the simulated hydrographs based on the calibrated parameter set are referred to as the 'reference' simulations. The range over which the value of each parameter was varied, is based on the limits within which each parameter can reasonably be evaluated on the basis of current knowledge. The following sensitivity tests were performed:

a. Sensitivity to model ' structural' parameters

- Representation of the basin by grid squares of 1 km x 1 km.
- Representation of the basin by grid squares of 4 km x 4 km.
- Basic time step increased from 2 hours to 4 hours.

b. Sensitivity to flow resistance

- Strickler roughness coefficient for overland flow increased from 1.0 to 3.0.
- Strickler roughness coefficient for channel flow increased from 20 to 40.

c. Sensitivity to unsaturated flow parameters

- Saturated vertical conductivity increased from 0.1 m/day to 1.0 m/day.
- Exponent in Averjanov's formula reduced from 12 to 8.
- Water content at wilting point and residual water content reduced from 0.21, 0.18 to 0.12. 0.12 respectively.

d. Sensitivity to saturated flow parameter

- Saturated zone conductivity increased from 10 m/day to 20 m/day.

e. Sensitivity to spatial distribution of rainfall.

Tables 24 to 28 present the comparisons of volumes and peaks of simulated discharges for 'reference' and test hydrographs and figures 51 to 60 compare the predicted hydrographs with the measured and the 'reference' hydrographs.

6.3 Results of Sensitivity Analysis

Studies into the sensitivity of the simulation results to key parameters were carried out with the aim of developing guidelines on parameter evaluation and model setup for practical applications. The results are described in groups related to particular components of the model.

(a) Sensitivity to model 'structural' parameters

Grid spacing and time step are the most important 'structural' parameters. It is desirable to make them both as large as possible since computing requirements are then minimized. At the same time, though the larger the values assigned, the greater is the possibility of inaccurate representation of the basin and its hydrological response.

Grid spacing

Sensitivity testing to examine the effect of grid scale, for example using grid squares with sides of 1, 2 and 4 km, indicates the degree to which calibrated parameter values change with grid size and will enable the balance between computational requirements (minimized with larger squares) and basin representation (maximized with smaller squares) to be examined. It also provides an opportunity to study the effect of the ratio of the number of channel links to the number of grid squares on the results and hence the detail in which the river network should be represented.

In the reference simulations, the grid spacing was 2 km. To study the sensitivity to grid spacing, parameter sets were prepared with grid squares of 1 km x 1 km and 4 km x 4 km . This increased the number of squares representing the basin from 150 to 602 and reduced the proportion of basin per square from 0.67 % to 0.17 % in case of grid squares of 1 km x 1 km . For grid squares of 4 km x 4 km, the number of squares representing the basin were reduced from 150 to 36 and proportion of basin per square was increased from 0.67 % to 2.78 %. The result is decrease in runoff for 1 km grid spacing and increase in runoff for 4 km grid spacing (table 24). However, for individual months, the changes are more erratic in case of 4 km grid spacing. The comparisons of observed, reference and test hydrographs (figures 51 and 52) indicate that the overall pattern of hydrographs improves for 1 km grid spacing but they are more smoothened than actual for 4 km grid spacing indicating inaccurate representation of the basin.

These tests have not identified the optimum grid spacing which is small enough to support satisfactorily accurate results, yet not so small that computing costs are prohibitive. However, comparison of the tests made with spacings of 1 km, 2 km and 4 km suggests that, for the Hemavati (upto Sakleshpur) basin, the spacing should not exceed 2 km. Consequently the grid square area should not exceed 0.67 % of the total basin area and may need to be even smaller.

Basic time step

In the reference simulations, the time step was 2 hours for the unsaturated, overland and channel flow components, which have to be able to simulate relatively rapid changes. For the more slowly varying conditions simulated by the saturated flow component, a time step of 8 hours was used. To test sensitivity to the time step, an increase from 2 hours to 4 hours was made for the

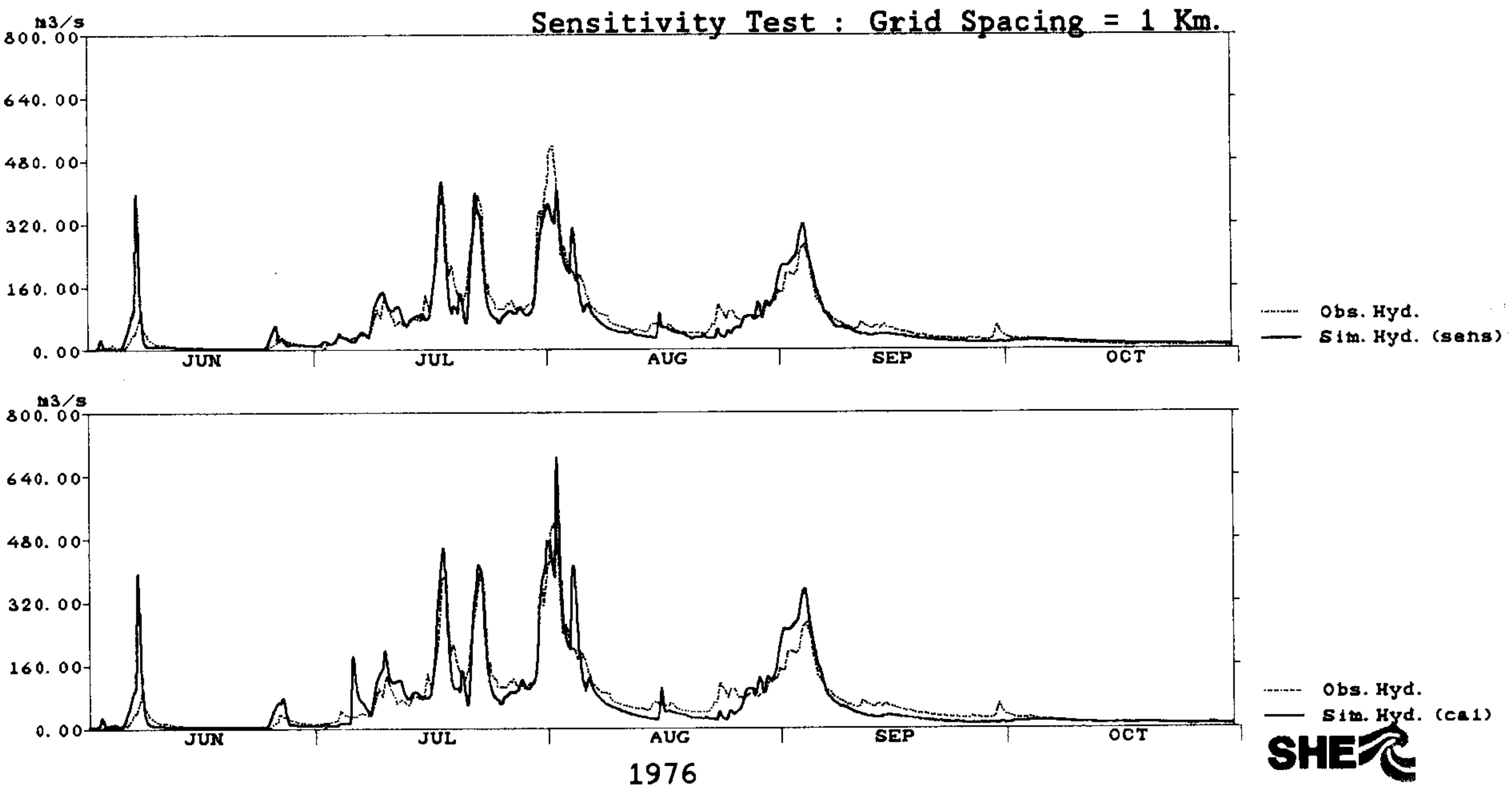

FIGURE 51 - OBSERVED AND SIMULATED HYDROGRAPHS (1976) FOR GRID SPACING = 1 km

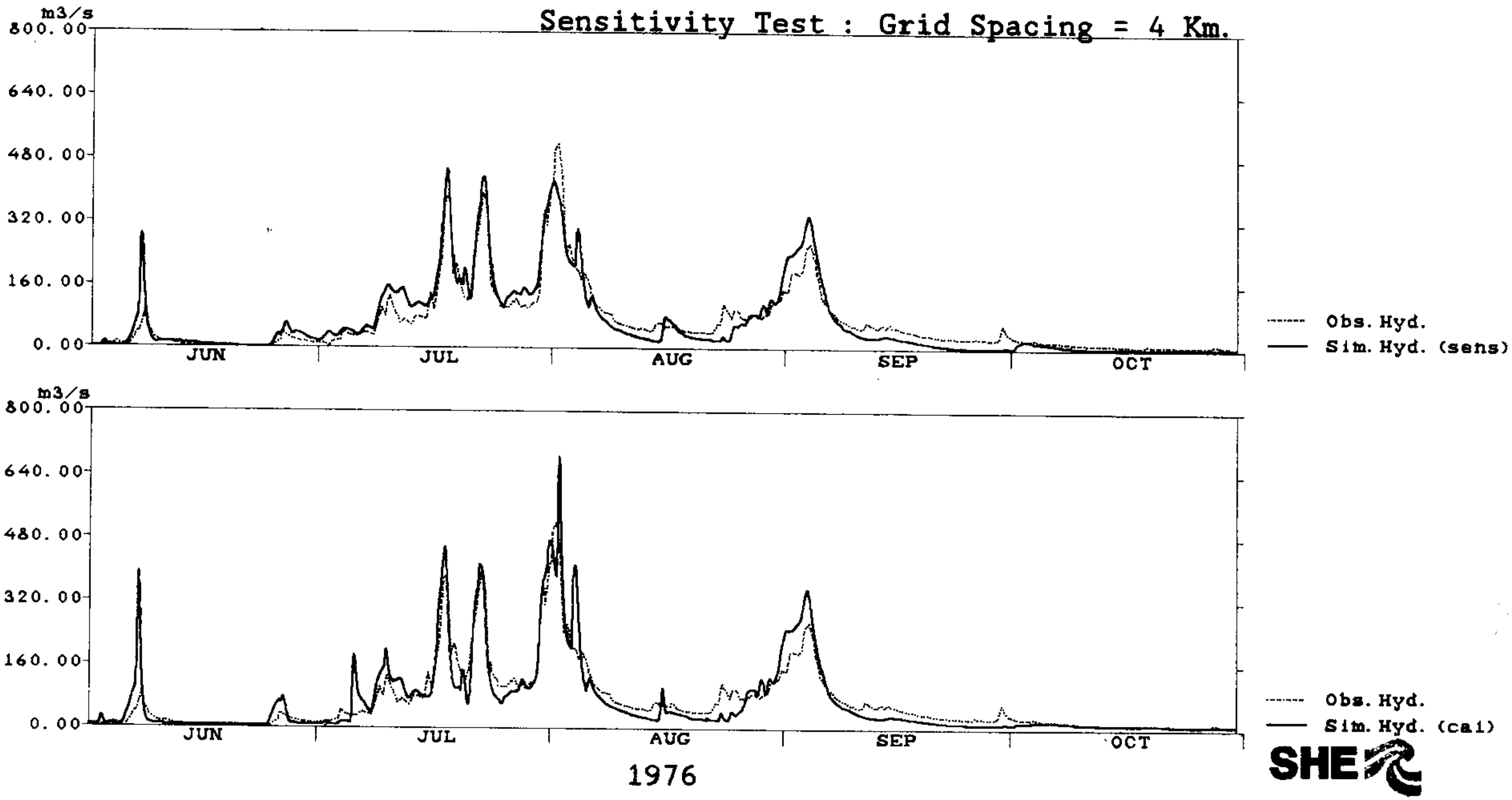

FIGURE 52 - OBSERVED AND SIMULATED HYDROGRAPHS (1976) FOR GRID SPACING = 4 km

unsaturated, overland and channel flow components. The comparison of observed, reference and test hydrographs (figure 53) indicate that there is almost no difference between reference and test simulations. Also the volume of runoff and peaks remain approximately constant (table 24). Therefore, test showed that there was no loss in accuracy through the use of a basic time step of 4 hours and also it allows adequate portrayal of the response times. Time step has a comparatively more moderate influence but clearly it should be small compared with typical hydrograph times to peak.

These results indicate that evaluation of model 'structural' parameters should be based on a careful appreciation of the hydrological processes being simulated.

Table 24 : Comparisons of Volumes and Peaks of Observed and Simulated Discharges for Sensitivity to Model 'Structural' Parameters

Year	Month	Observed Discharge (mm)	Simulated Discharge (mm) Calibration	Grid Spacing = 1 km	Grid Spacing = 4 km	Basic Time Step = 4 hours
1976	June	58.14	92.40	88.39	99.86	92.94
	July	584.53	589.64	522.03	714.57	588.78
	August	480.97	453.51	413.62	430.70	452.72
	September	318.50	303.88	304.17	298.90	306.71
	October	66.17	61.00	76.60	38.56	61.03
	Total	1508.31	1500.43	1404.81	1582.59	1502.18
Peak (cumecs)		521.20	686.69	406.40	423.69	683.03

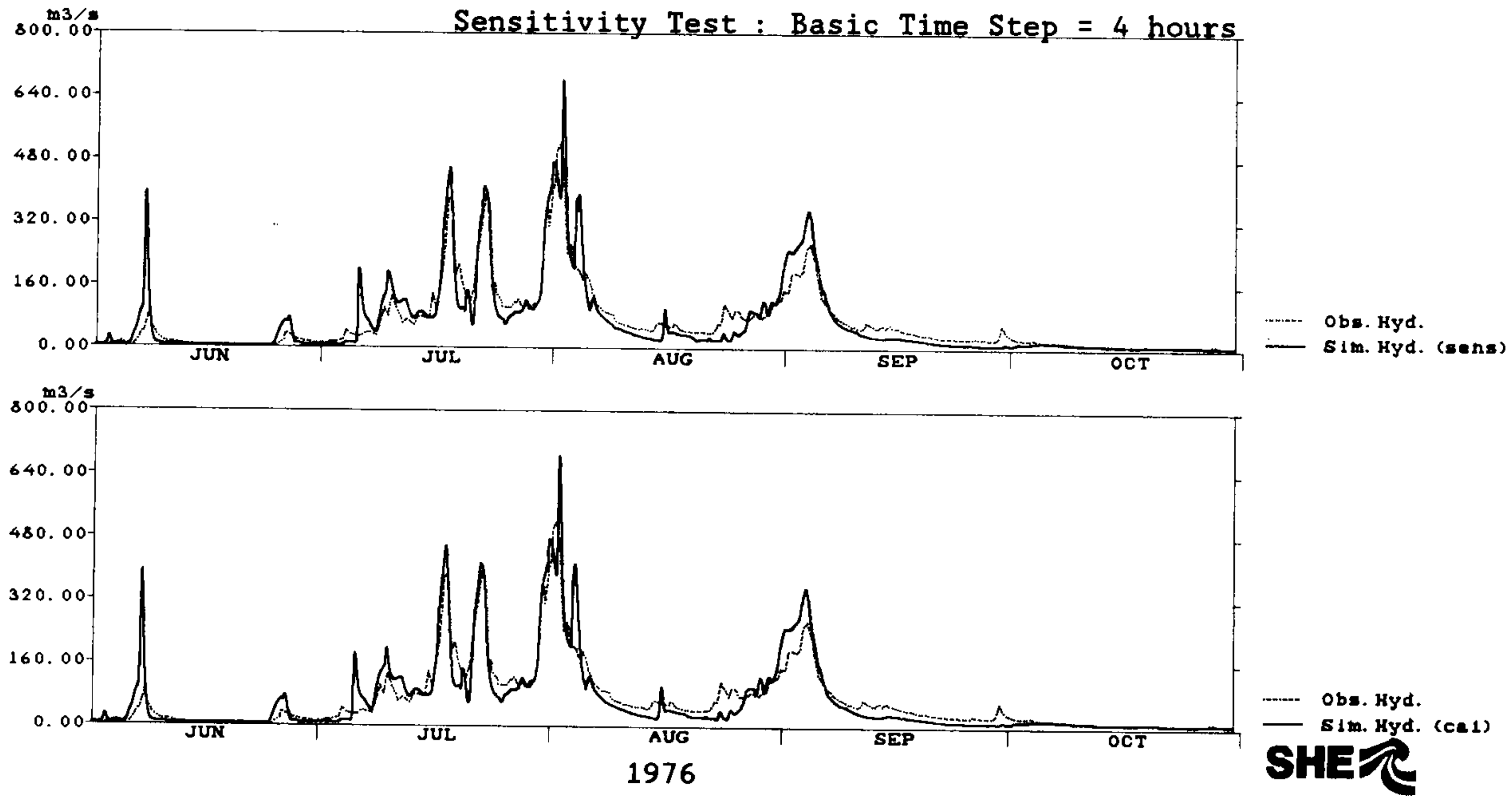

FIGURE 53 - OBSERVED AND SIMULATED HYDROGRAPHS (1976) FOR BASIC TIME STEP = 4 HOURS

(b) Sensitivity to flow resistance

The magnitude of the flow resistance coefficient included in the St. Venant equations for overland and channel flow determines the speed of response of the surface runoff. By affecting the time for which the surface runoff remains on the ground surface, the coefficient also partially determines the volume of water which can infiltrate into the soil.

Strickler coefficient for overland flow

For the reference simulations, the value of Strickler roughness coefficient for overland flow was used as 1.0 reflecting the observed occurrence of runoff. Sensitivity of the simulations was tested with value of 3.0. This increased the flashiness of the simulated response. There is a significant effect especially on the intensity of the runoff (figure 54). As expected, a reduction in resistance enables the overland flow to reach the channel system faster, so the hydrograph rise and recession are steeper and the peak discharges are higher than in the reference simulation. However, change in the total hydrograph volume was insignificant (table 25).

Strickler coefficient for channel flow

Sensitivity to the channel flow resistance was examined by increasing the Strickler roughness coefficient for channel flow from 20 to 40 (same value applied to all river links). This increased the flashiness of the simulated response (figure 55). By decreasing the flow resistance, the rate of surface runoff is increased with steeper recession. Peak discharges were increased but change in the total hydrograph volume for monsoon season was insignificant (table 25). However, the use of a constant coefficient value at a site (i.e. not changing with depth or

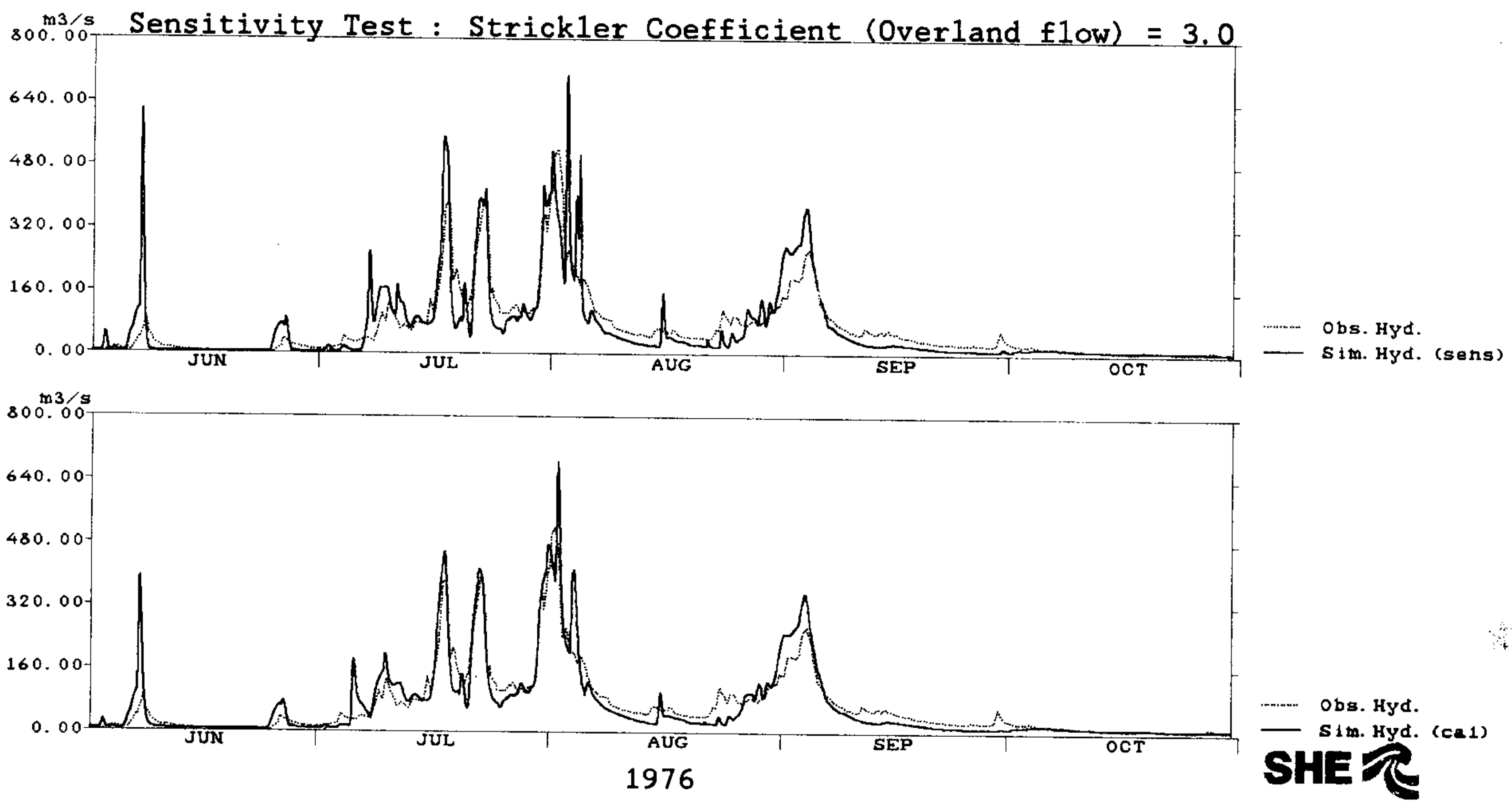

FIGURE 54 - OBSERVED AND SIMULATED HYDROGRAPHS (1976) FOR STRICKLER COEFFICIENT (OVERLAND FLOW) = 3.0

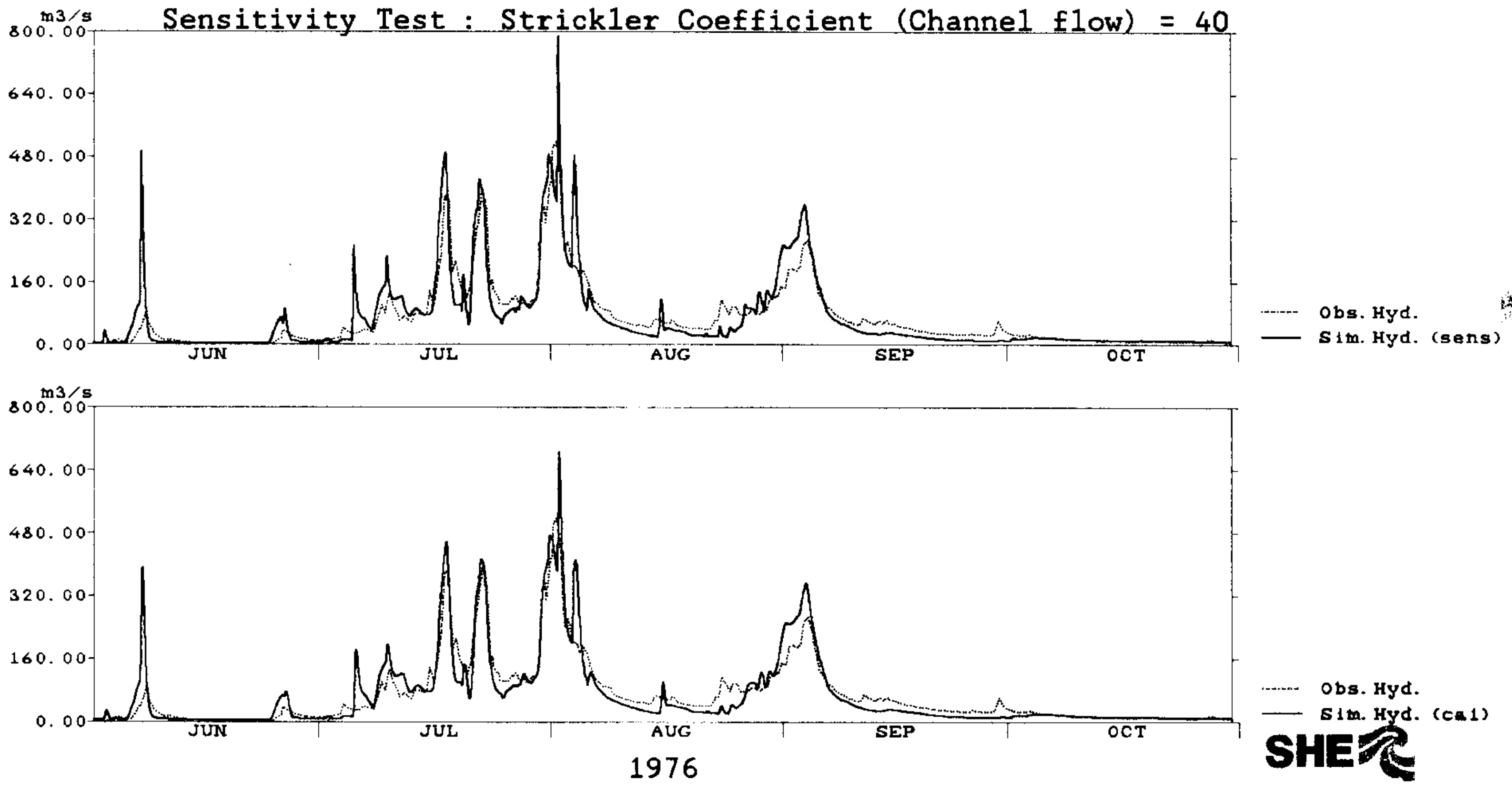

FIGURE 55 - OBSERVED AND SIMULATED HYDROGRAPHS (1976) FOR STRICKLER COEFFICIENT (CHANNEL FLOW) = 40

discharge) results in minor errors in the time to peak of the simulated hydrograph. This is because in reality the flow resistance varies at a site. Thus observed low magnitude peaks tend to occur later than predicted while observed high magnitude peaks tend to occur earlier than predicted.

Table 25 : Comparisons of Volumes and Peaks of Observed and Simulated Discharges for Sensitivity to Flow Resistance

Year	Month	Observed Discharge (mm)	Simulated Discharge (mm)		
			Calibration	Strickler Coeff.for Overland Flow = 3.0	Strickler Coeff.for Channel Flow = 40
1976	June	58.14	92.40	104.79	95.24
	July	584.53	589.64	590.06	603.84
	August	480.97	453.51	438.35	451.69
	September	318.50	303.88	297.68	300.24
	October	66.17	61.00	61.14	60.92
	Total	1508.31	1500.43	1492.02	1511.93
Peak (cumecs)		521.20	686.69	710.96	788.24

(c) Sensitivity to unsaturated flow parameters

Unsaturated subsurface flow is modelled in the vertical only, using the one-dimensional Richards equation in which the principal soil variables are conductivity and moisture content. The principal soil parameters to be furnished to the simulation therefore include the values of saturated vertical conductivity K(UZ), exponent for conductivity/moisture content relation n, water content at wilting point θ(wilt) and residual water content θ(res).

Saturated vertical conductivity

In the reference simulations, saturated vertical conductivity, K(UZ) was 0.1 m/day. The sensitivity test was made with K(UZ) = 1.0 m/day. This increases infiltration and reduces surface runoff. Thus the total hydrograph volume for monsoon season was decreased (table 26) and the peaks were lowered (figure 56) The change may also promote a more flashing subsurface saturation response.

Table 26 : Comparisons of Volumes and Peaks of Observed and Simulated Discharges for Sensitivity to Unsaturated Flow Parameters

Year	Month	Observed Discharge (mm)	Calibration	Simulated Discharge (mm) Saturated Vertical Conductivity =1.0 m/day	Exponent in Averjanov's Formula = 8	Water Content at Wilting Point = 0.12, Residual Water Content = 0.12
1976	June	58.14	92.40	66.23	67.52	76.92
	July	584.53	589.64	565.63	484.82	493.18
	August	480.97	453.51	420.29	436.98	441.28
	September	318.50	303.88	307.14	305.70	306.14
	October	66.17	61.00	62.22	61.84	62.63
	Total	1508.31	1500.43	1421.51	1356.86	1380.15
Peak (cumecs)		521.20	686.69	423.62	586.61	534.21

Exponent in Averjanov's formula

In the SHE, the hydraulic conductivity, $K(\theta)$ is described as a function of the effective saturation, Se:

$$K(\theta) = Ksat\ Se^{n} \qquad \ldots(26)$$

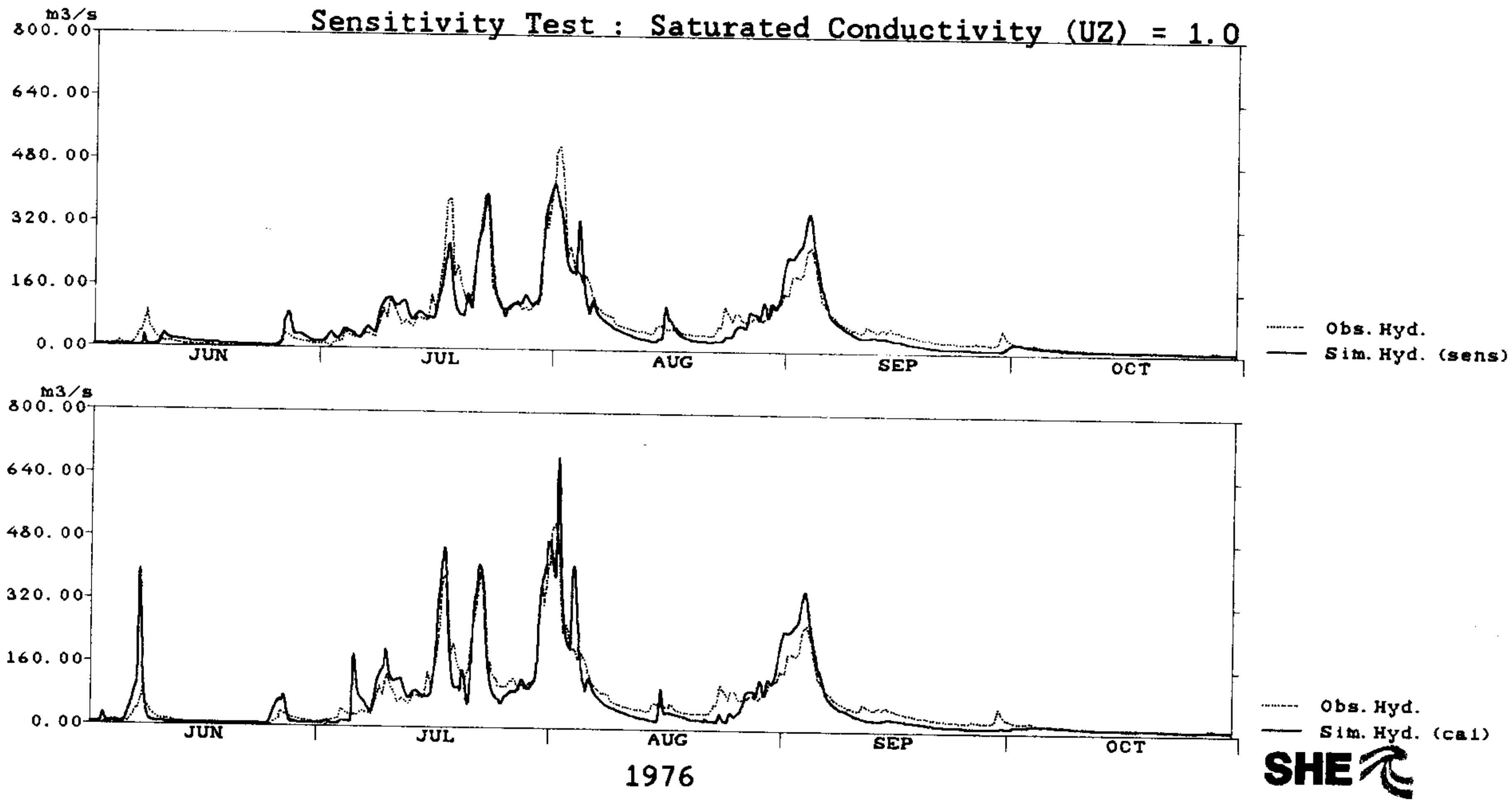

FIGURE 56 - OBSERVED AND SIMULATED HYDROGRAPHS (1976) FOR SATURATED VERTICAL CONDUCTIVITY = 1.0 m/day

where,

$$Se = \left(\frac{\theta - \theta_{res}}{\theta_s - \theta_{res}}\right) \qquad \ldots(27)$$

in which θ_s, θ and θ_{res} are saturated, actual and residual moisture contents respectively. n is the exponent appearing in Averjanov's formula (equation 26) for calculation of unsaturated conductivity as a function of θ.

In the reference simulations, exponent in Averjanov's formula was taken as 12. For the sensitivity test, the value was reduced to 8, producing a significant effect on the simulation. It can be observed from the Averjanov's formula that by reducing n, the soil conductivity at a given (unsaturated) moisture content increases. This leads to increased evapotranspiration and reduced surface runoff. Thus the total hydrograph volume for monsoon season was decreased by about 10 % (table 26) and peaks were also lowered (figure 57).

Water contents

In the reference simulations, water content at wilting point and residual water content were taken as 0.21 and 0.18 respectively. For the sensitivity test, these values were reduced to 0.12 and 0.12 respectively. This increases evapotranspiration and reduces surface runoff. Overall hydrograph total was decreased by 8 % (table 26) and peak discharges were also reduced (figure 58).

Further factors, which can affect the results, are the

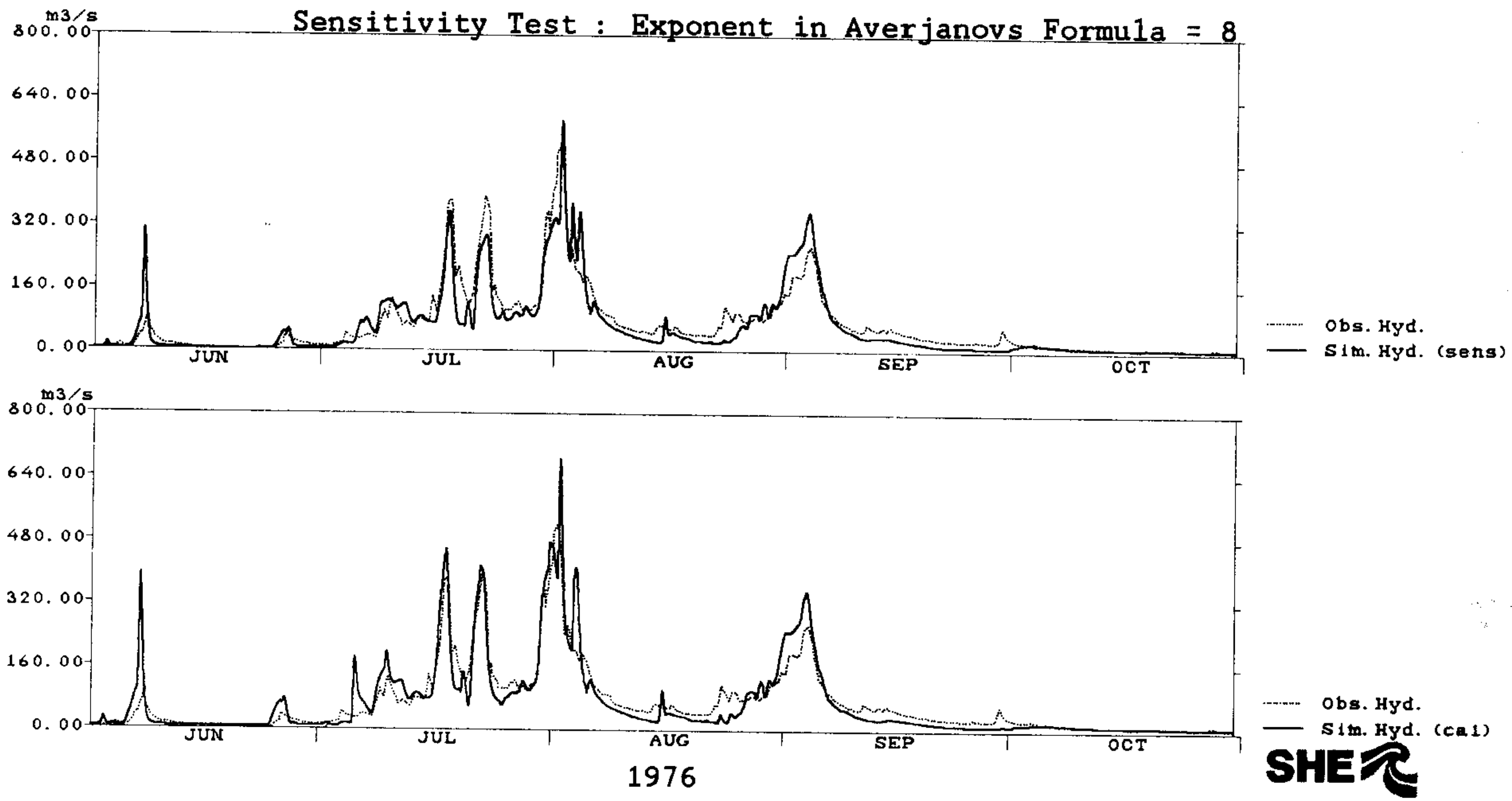

FIGURE 57 - OBSERVED AND SIMULATED HYDROGRAPHS (1976) FOR EXPONENT IN AVERJANOV'S FORMULA = 8

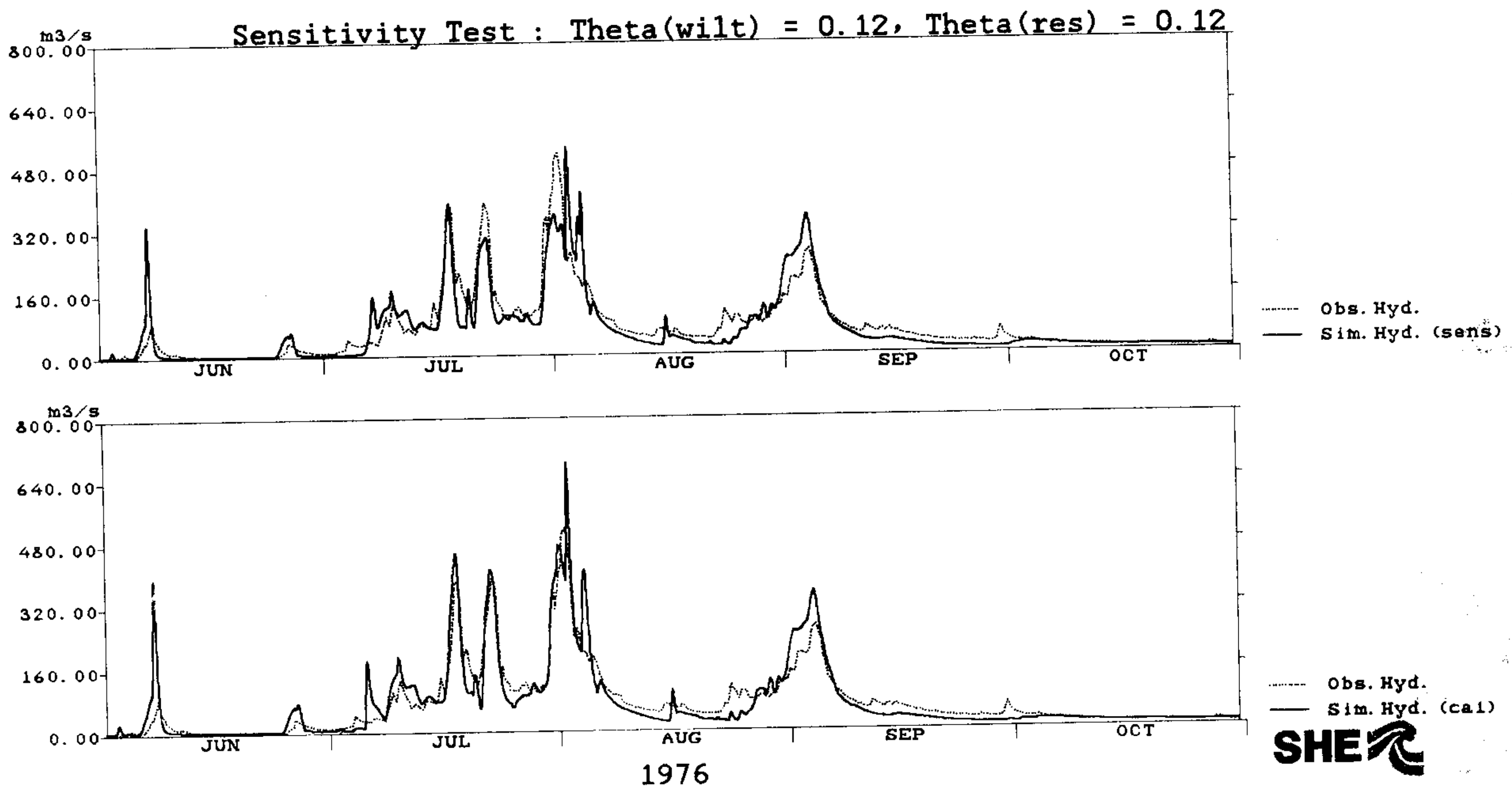

FIGURE 58 - OBSERVED AND SIMULATED HYDROGRAPHS (1976) FOR WATER CONTENT AT WILTING POINT = 0.12 AND RESIDUAL WATER CONTENT = 0.12

soil moisture tension curve, the initial soil moisture profile (dependent on the initial level of the phreatic surface) and the saturated moisture content. The soil moisture tension curve has a relatively minor effect. The initial soil moisture profile is important but can be set according to the season, i.e. a low phreatic surface level in the summer and a high phreatic surface level in the winter. Reduction in the value of saturated moisture content may be expected to decrease infiltration and therefore increase runoff, while increase has the opposite effect.

(d) Sensitivity to saturated flow parameter

Saturated subsurface flow (i.e. the base flow) is modelled in the horizontal only, using the Boussinesq equation in which the principal soil parameter is conductivity, K(SZ). An increase in the value of this parameter may be expected to reduce the runoff response because the capacity of the soil to carry away water is increased.

For the reference simulations, the conductivity values, K(SZ) = 10 m/day were applied in a spatially uniform sense. The sensitivity test was made with K(SZ) = 20 m/day, again applied in a spatially uniform sense. This accelerates the subsurface transmission of water and increases the base flow. Because of the altered base flow levels, the higher conductivity may produce an increase in peak discharge although the runoff response itself is reduced. Peak discharges were therefore boosted during the later monsoon period (figure 59) but the overall hydrograph volume varied by less than 3 %, despite large changes in the monthly volumes for some of the monsoon months (table 27).

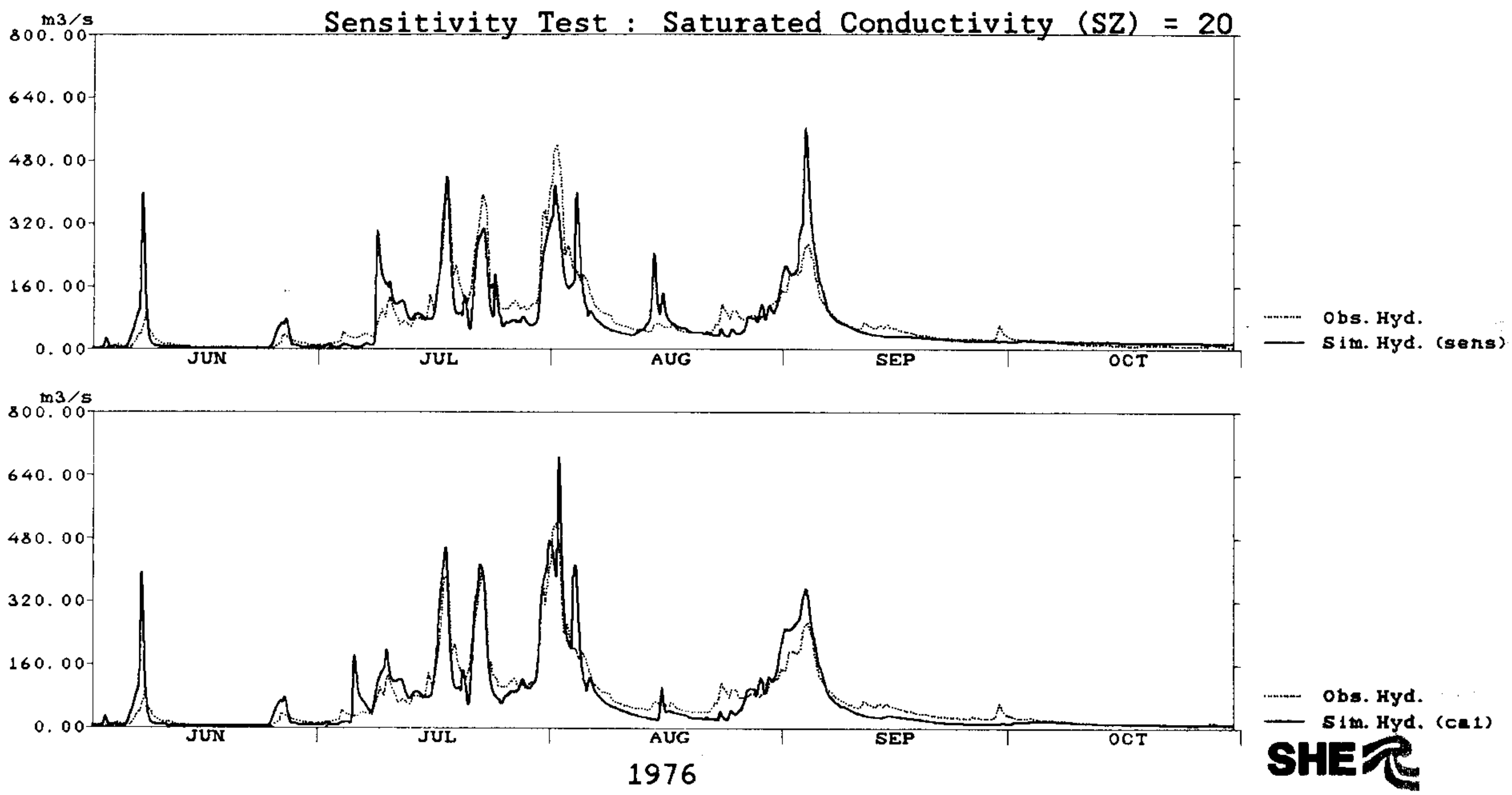

FIGURE 59 - OBSERVED AND SIMULATED HYDROGRAPHS (1976) FOR SATURATED ZONE CONDUCTIVITY = 20 m/day

Table 27 : Comparison of Volumes and Peaks of Observed and Simulated Discharges for Sensitivity to Saturated Flow Parameter

Year	Month	Observed Discharge (mm)	Simulated Discharge (mm) Calibration	Saturated Zone Conductivity =20 m/day
1976	June	58.14	92.40	94.66
	July	584.53	589.64	498.30
	August	480.97	453.51	431.14
	September	318.50	303.88	345.70
	October	66.17	61.00	90.12
	Total	1508.31	1500.43	1459.92
	Peak (cumecs)	521.20	686.69	415.80

(e) Sensitivity to spatial distribution of rainfall

Rainfall was varied spatially in the reference simulations. Test was therefore made to show the effect of applying uniform distributions. There were significant changes in hydrograph volumes during the initial monsoon months, although the total hydrograph volume was not varied significantly (table 28). Figure 60 shows that application of a uniform rainfall (equal to the average basin rainfall) produces more smoothened hydrographs than actual, probably as a result of the influence of altered intensities on runoff generation in different parts of the basin. The necessity of accounting for spatial non-uniformities is likely to increase as basin size increases (because more variability is incorporated) and where rainfall is localized.

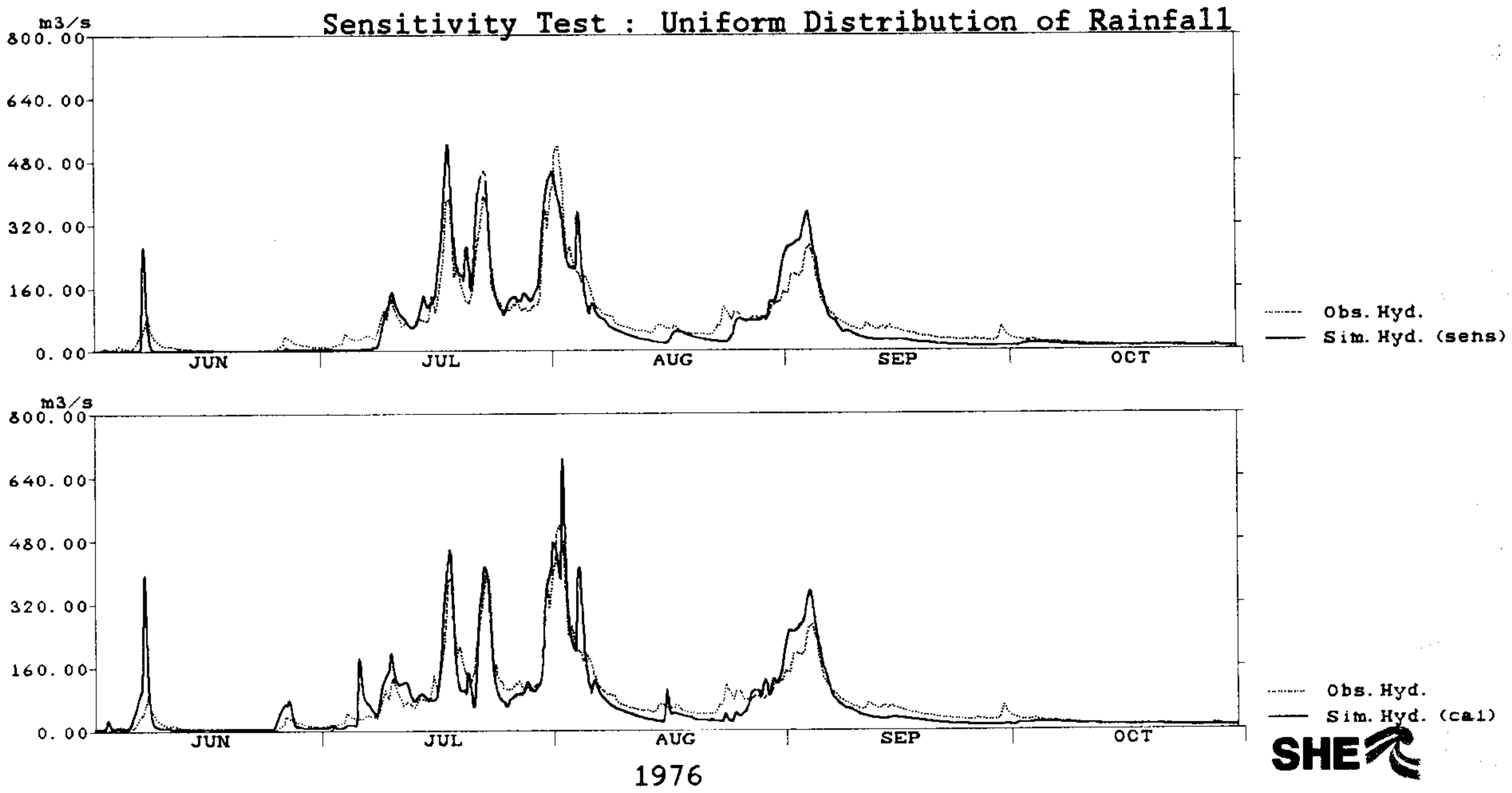

FIGURE 60 - OBSERVED AND SIMULATED HYDROGRAPHS (1976) FOR UNIFORM DISTRIBUTION OF RAINFALL

Table 28 : Comparison of Volumes and Peaks of Observed and Simulated Discharges for Sensitivity to Spatial Distribution of Rainfall

Year	Month	Observed Discharge (mm)	Simulated Discharge (mm) Calibration	Uniform Distribution of Rainfall
1976	June	58.14	92.40	41.37
	July	584.53	589.64	663.26
	August	480.97	453.51	414.21
	September	318.50	303.88	301.26
	October	66.17	61.00	57.56
	Total	1508.31	1500.43	1477.66
Peak (cumecs)		521.20	686.69	454.26

The vegetation parameters (sensitivity not examined in the present case) normally have only a minor influence on the simulations, although for periods in which transpiration is important, the results might be different. In this case, therefore, the parameters may be specified with accuracies defined only by the limiting ranges of values. To some extent this can be achieved using data available in the literature but for some parameters there is still a need for further research to define the limiting ranges for different types of vegetation.

The results of the sensitivity analysis confirm the importance of the soil parameters and the rainfall input in determining the simulated response. In particular, relatively small changes in rainfall input can significantly affect the output, implying that calibration based on erroneous rainfall data may introduce significant uncertainty into the calibrated parameters. Also the response of the basin to rainstorms is dominated by rapid surface and subsurface runoff rather than, for example, a long term ground water response. The basin parameters, to which the simulations are most sensitive, need to be specified with accuracies greater than those defined by the likely limiting ranges of values and most attention should be devoted to these parameters in similar applications. It should be possible to evaluate the critical parameters from measurements made at a few representative sites. The point worth noting is that discussion of the reactions of the simulations to parameter changes is greatly enhanced by the ability to describe those reactions in physical terms. This allows a more confident approach to parameter evaluation and to interpretation of simulation results than is possible with black box modelling.

6.4 Remarks

Before physically-based distributed catchment models can be used with confidence, it must be established that their performance is adequate and that preparation and calibration of the parameter sets do not pose overwhelming practical difficulties. These points have been addressed in the sensitivity analysis with generally encouraging results.

(a) Those basin parameters to which the simulations are most sensitive (in this case those associated with surface and subsurface runoff) need to be evaluated with relatively high accuracy. This can be provided by field measurements at a few representative sites. Point measurements are suitable for representing average conditions in a grid square. The less important parameters need to be evaluated with only moderate accuracy which can often be satisfied by data available in the literature.

(b) Grid spacing and time steps should be small in comparison with the scales of the spatial and temporal variations which they are used to represent. Errors may otherwise be comparable with those resulting from inaccurate evaluation of the more important basin parameters.

(c) The scope for achieving equally satisfactory calibrations based on different combinations of parameter values can be reduced by considering several different events.

(d) Further research is needed to delineate the likely ranges of the various basin parameters for different soils, vegetations and basins. Sensitivity tests should also be carried out for different basins in order to show how sensitivity varies with basin type.

7.0 CONCLUSIONS

The aim of the present study has been to implement a physically-based, distributed catchment model and to simulate a variety of catchment responses. The main advantage of the SHE as compared to the traditional (and simpler) hydrological rainfall-runoff models is its capability to predict the consequences of man's activities on the water resources of a basin. Application of the SHE to Hemavati (upto Sakleshpur) basin indicates generally encouraging results. Based on the above simulation study, the following conclusions are drawn:

1. The SHE has been successfully used for modelling the Hemavati (upto Sakleshpur) basin within the constraints of data availability. The patterns of catchment response, with regard to calibration and validation, accord well with the observed catchment behaviour.

2. There remain considerable uncertainties in the input data and the model parameters. Reduction of the uncertainty will depend on improved data availability.

3. Improvement of the calibrations will require a more extensive spatial and temporal coverage of rainfall input, more accurate evaluations of the model parameters (especially for the soil properties) and their spatial distribution (through field measurements), a careful consideration of the initial phreatic surface depths and careful specification of grid sizes, and river channel representation.

Model Limitations

In the SHE, a physically-based, distributed modelling system, a balance is required between adherence to the physical basis on one hand and computing requirements on the other and the system therefore incorporates a number of approximations and assumptions. The followings are some of the model limitations:

1. The channel network is represented by an orthogonal system consisting of grid squares and as such the increase in grid size leads to significant distortion in the channel representation.
2. Interception is modelled for only one vegetation in each grid square. Thus if an area is characterised by trees, the effect of secondary vegetation under the trees is neglected. In the evapotranspiration model also, only one vegetation type is considered at a point.
3. There is no allowance for the effect of erosion or deposition on hillslope topography or channel cross-section. Ground and channel bed slopes and channel cross-section do not therefore vary with time.
4. Overbank flooding and floodplain flow are not properly represented in the current version of the SHE.
5. The Strickler roughness coefficient is assumed to be constant at a site, even though large changes are observed in rivers as discharge varies at a site.
6. The Strickler coefficient is not easy to evaluate for overland flow. Often it is used (both for overland and channel flow) as a calibration coefficient, implicitly taking account of uncertainty in other parameters. The value so obtained may not then be generally applicable to events other than those similar to the calibration events.

7. At present only single-layer, unconfined aquifers can be modelled. However, the saturated zone component is so designed that it can easily be expanded to account for confined and multilayer aquifers in the future.

8. The present SHE setup does not include consideration of hydraulic structures like dams and reservoirs.

Suggestions for Further Work

The SHE requires the evaluation of a wide range of parameters and relationships with which to represent a basin, it is the soil parameters which are generally the most difficult to evaluate and to which the simulation results are most sensitive. The simulations carried out for the Hemavati (upto Sakleshpur) basin have relied on soil data taken from the literature. Many of these data are of a general nature, providing only indirect evaluations of the parameters. There is therefore some uncertainty attached to the soil parameters and relationships fed into the SHE, which in turn means that there is uncertainty in the output. It is therefore necessary that field measurements are carried out with the aim of reducing the uncertainty by providing soil parameter values determined both directly and within a simulation basin and aimed explicitly at the SHE simulations. The soil parameters and relationships which require evaluation are as follows:

(i) Unsaturated zone saturated hydraulic conductivity (for vertical flow);

(ii) Unsaturated zone moisture content/hydraulic conductivity relationship;

(iii) Unsaturated zone moisture content/tension relationship;

(iv) Saturated zone hydraulic conductivity (for horizontal flow);

(v) Soil depth and profile; and

(vi) Root zone depth.

The soil properties and functional relationships can be obtained via field, laboratory and predictive modelling techniques. The field and laboratory techniques provide the information more or less directly, the predictive modelling techniques give the information indirectly from data on soil pore and particle size distributions. The methods are not necessarily equivalent and may give significantly different results. Soil cores taken to the laboratory, for example, may suffer disturbance during sampling and transport so that the results obtained from their analysis may differ from the results which would be obtained by field measurements in undisturbed soil at the identical area of ground. Also some methods will be more convenient or practical than others, depending on local conditions. Therefore, a combination of field, laboratory and predictive modelling methods can be used.

ACKNOWLEDGEMENTS

I wish to express my deep sense of gratitude to Dr.Satish Chandra, Director for his inspiring and able guidance and Mr.K.S.Ramasastri, Scientist 'F' for his constant encouragement and direction of study at every stage of this work. The author is indebted to Dr.S.M.Seth, Scientist 'F' and Dr.G.C.Mishra, Scientist 'F' who offered motivation and inspiration throughout the course of study. The author is also thankful to the consultants from the Danish Hydraulic Institute (Denmark), the University of Newcastle upon Tyne (U.K.) and SOGREAH (France) for close interaction during author's training in Denmark.

The author gratefully acknowledges the valuable suggestions and all kinds of support by Dr.S.K.Jain, Scientist'C', Mr.R.D.Singh, Scientist 'C', Mr. V.K. Lohani, Scientist 'C', Mr. A.B.Palaniappan, Scientist 'C' and Mr. Rakesh Kumar, Scientist 'C'. The author is also grateful to the staff of N.I.H. Hard Rock Regional Centre, Belgaum for collection of some of the required data for the basin. The help provided by the officers of Water Resources Development Organisation, Bangalore, Department of Mines and Geology, Bangalore, Gauging Sub-Division, Hassan and other organisations in collection of the required data is gratefully acknowledged.

Thanks are due to Mr. Sanjay Mittal, Mr. S.L.Srivastava, Mr. U.V.N. Rao and Mr. Naresh Saini for computerisation of meteorological and hydrological data. The author is also thankful to Mr. S.S.Kanwar for extending documentation facilities and Mr.Rajneesh Kumar Goel for carefully typing the manuscript. In the last, but not the least, the author is greatly indebted to all those who have provided assistance directly or indirectly for successfully carrying out the present study.

Chandra Prakash Kumar
Scientist 'C'

REFERENCES

1. Abbott, M.B., J.C. Bathurst, J.A. Cunge, P.E. O'Connell, and J. Rasmussen (1986), "An Introduction to the European Hydrological System - Systeme Hydrologique Europeen, "SHE", 1: History and Philosophy of a Physically-based, Distributed Modelling System", Journal of Hydrology, Vol.87, pp.45-59.

2. Abbott, M.B., J.C. Bathurst, J.A. Cunge, P.E. O'Connell, and J.Rasmussen (1986), "An Introduction to the European Hydrological System - Systeme Hydrologique Europeen, "SHE", 2: Structure of a Physically-based, Distributed Modelling System", Journal of Hydrology, Vol.87, pp.61-77.

3. Anderson, E.A. (1968), "Development and Testing of Snowpack Energy Balance Equations", Water Resources Research, Vol.4, pp.19-37.

4. Bathurst, James C. (1986), "Physically-based Distributed Modelling of an Upland Catchment using the Systeme Hydrologique Europeen", Journal of Hydrology, Vol.87, pp.79-102.

5. Bathurst, James C. (1986), "Sensitivity Analysis of the Systeme Hydrologique Europeen for an Upland Catchment", Journal of Hydrology, Vol.87, pp.103-123.

6. Engman, E.T. (1986), "Roughness Coefficients for Routing Surface Runoff", Proceedings, American Society of Civil Engineers, Journal of the Irrigation and Drainage Engineering, Vol.112, No.1, pp.39-53.

7. Feddes, R.A., P.Kowalik, S.P. Neuman, and E. Bresler (1976), "Finite Difference and Finite Element Simulation of Field Water Uptake by Plants", Hydrol. Sci. Bull., Vol.21, pp.81-98.

8. Hydrological Computerized Modelling System (SHE), Project ALA 86/19, Inception Report, February 1988, Danish Hydraulic Institute, Denmark.

9. Hydrological Computerized Modelling System (SHE), Project ALA 86/19, Progress Report, July 1988, Danish Hydraulic Institute, Denmark.

10. Hydrological Computerized Modelling System (SHE), Project ALA 86/19, Interim Report, December 1988, Danish Hydraulic Institute, Denmark.

11. Hydrological Computerized Modelling System (SHE), Project ALA 86/19, Progress Report, May 1989, Danish Hydraulic Institute, Denmark.

12. Hydrological Computerized Modelling System (SHE), Project ALA 86/19, Bi-Annual Report, November 1989, Danish Hydraulic Institute, Denmark.

13. Hydrological Computerized Modelling System (SHE), Lecture Notes and Exercises, Training Course 1989, Danish Hydraulic Institute, Denmark.

14. Hydrological Computerized Modelling System (SHE), User's Guide and Documentation, 1989, Danish Hydraulic Institute, Denmark.

15. Jensen, Karsten Hogh and Torkil Jonch-Clausen (1981), "Unsaturated Flow and Evapotranspiration Modeling as a Component of the European Hydrologic System (SHE)", Proceedings of the International Symposium on Rainfall Runoff Modeling held May 18-21, 1981 at Mississippi State University, Mississippi State, Mississippi, U.S.A., pp.235-252.

16. Kristensen, K.J. and S.E. Jensen (1975), "A Model for Estimating Actual Evapotranspiration from Potential Evapotranspiration", Nordic Hydrology, Vol.6, pp.70-88.

17. Kumar, Chandra Prakash (1990), "Application of SHE Model to Narmada (upto Manot) Basin", Case Study Report No.29, National Institute of Hydrology, Roorkee.

18. Lecture Notes, Workshop on "Application of SHE Model to Sub-basins of River Narmada", Bhopal (M.P.), 13-16 December, 1989, Organised by National Institute of Hydrology, Roorkee with cooperation of Madhya Pradesh Irrigation Department.

19. Lecture Notes, Workshop on "European Hydrological System Model Applications", CBIP Secretariate, New Delhi, 10-11 September, 1990, Organised by National Institute of Hydrology, Roorkee with cooperation of Central Board of Irrigation and Power, New Delhi.

20. Mahesha, V., A.N. Seetharam, Nazeer Ahmed, and L.G. Jaganathachar (1980), "Assessment of Groundwater Resources of Hassan Taluk, Hassan District", Groundwater Studies No.207, Department of Mines and Geology, Government of Karnataka, Bangalore.

21. Monteith, J.L. (1965), "Evaporation and Environment. In: The State and Movement of Water in Living Organisms", Proc. 15th Symposium Society for Experimental Biology, Swansea, Cambridge University Press, London, pp.205-234.

22. Palaniappan, A.B. and Vibha Jain (1989), "Hydrological Year Book, Hemavathy Subbasin, Year 1985-86", Technical Report No. 53, National Institute of Hydrology, Roorkee.

23. Preissmann, A. and J. Zaoui (1979), "Le module - ecoulement de surface - du Systeme Hydrologique Europeen (SHE)", Proc. 18th Congress, International Association for Hydraulic Research, Cagliari, Vol.5, pp.193-199.

24. Report of the Irrigation Commission (1972), Volume III (Part 2), Ministry of Irrigation and Power, New Delhi, pp.297-338.

25. Rutter, A.J., K.A. Kershaw, P.C. Robins, and A.J. Morton (1971/72), "A Predictive Model of Rainfall Interception in Forests, 1. Derivation of the Model from Observations in a Plantation of Corsican Pine", Agricultural Meteorology, Volume 9, pp.367-384.

26. Soil Survey Report No.74, Pertaining to the Hemavathy Project Right Bank Canal, State Soil Survey Organisation, Department of Agriculture, Bangalore, 1979.

27. Soil Survey Report No. 95, Pertaining to Hemavathy Left Bank Canal Command Area, State Soil Survey Organisation, Department of Agriculture, Karnataka State, 1981.

28. The Soils of Hassan District (Karnataka) for Land Use Planning (1987), Soils Bulletin 12, National Bureau of Soil Survey and Land Use Planning, Nagpur.

29. Thippeswamy, T. and V.S. Bidi (1973), "Groundwater Resources of Mudigere Taluk, Chikmagalur District", Groundwater Studies No.90, Department of Mines and Geology, Government of Mysore, Bangalore.

30. Water Year Book for 1970-71 to 1974-75, Volume 1 - General Description of Discharge Sites, Public Works Department, Water Resources Development Organisation, Government of Karnataka, Bangalore, 1975.

DIRECTOR : SATISH CHANDRA

PROJECT JOINT COORDINATOR : K.S. RAMASASTRI

SCIENTIST : CHANDRA PRAKASH KUMAR

SCIENTIFIC STAFF : SANJAY MITTAL
S.L. SRIVASTAVA
U.V.N. RAO
NARESH SAINI

DOCUMENTATION STAFF : S.S. KANWAR
RAJNEESH KUMAR GOEL